



UNIVERSITY OF TRENTO
DEPARTMENT OF INDUSTRIAL ENGINEERING
MASTER'S DEGREE IN MECHATRONICS ENGINEERING

~ · ~

ACADEMIC YEAR 2023–2024

A New Model to Capture the Impact of Behaviours on the Spread of Infectious Diseases

Supervisor
Prof. Giulia GIORDANO

Co-Supervisor
Dr. Daniele PROVERBIO

Graduate Student
Riccardo TESSARIN
222819

FINAL EXAMINATION DATE: December 12, 2024

*To my source of
inspiration, Montgomery
Scott*

Summary

The thesis develops and presents a novel multi-system model (i.e., a model that simultaneously captures different coexisting and coupled dynamic phenomena) that couples behavioral and epidemic phenomena by combining a SIR-like epidemiological model with a behavioral model. This behavioral model partitions the population into three compartments:

H: Heedless, people careless of the risk associated with the infection;

C: Compliant, people that want to avoid becoming infected or infecting others;

A: Against, people who not see the epidemic as a risk and do not use protections or change their behavior during the epidemic.

The model's features are not only based on theoretical principal, but also developed considering real empirical datasets regarding both disease and behavior evolution during the recent COVID-19 pandemic. This approach overcomes the limitations of previous works that implement similar models, but use proxies for individual behaviors or rely on the assumption of a direct correlation between opinion and behavior. The key contributions of the work include:

- **Coupling between behaviors and contagion:** The developed model considers phenomena such as peer pressure, fatigue, non-pharmaceutical interventions (NPIs), self-isolation, and mean-field parameters representing government policies to mitigate the spread of the disease. These elements contribute to modeling the behavioral transitions of the population and realizing the coupling with the epidemic model.
- **Analysis:** An extensive analysis of the model components is conducted, focusing first on the new behavioral model alone and then on the full model. This allows the development of a foundational framework for the full multi-system model.
- **Epidemic-reproduction number and simulations:** The epi-behavioral model's reproduction number is computed using the Next-Generation Matrix method. A full set of simulations to test the system behavior for different conditions and parameter sets is also performed.

The flexibility of the developed model and its ability to capture the interplay between individual behaviors and disease spread offer a foundational tool to explore future scenarios in which the dynamics of social behaviors, such as wearing face masks or self-isolating, significantly alter the epidemic evolution.

Contents

List of Figures	9
I Introduction	11
1 Introduction epidemics and social dynamics	13
1.1 Presentation of the thesis work	17
2 Main objectives and thesis structure	19
3 Theoretical background	21
3.1 Epidemiological theory: foundations	21
3.1.1 Epidemiological research: historical background	21
3.1.2 Epidemiological glossary	22
3.2 Opinion/behaviour glossary	25
3.3 Epidemiological models categorization	26
3.3.1 Mean field models	27
3.3.2 Other modeling techniques	34
4 Review of epidemiological behavioural and opinion models in literature	37
4.1 Information sources	38
4.2 Classification of different types of information	39
4.3 How to integrate behavior in epidemiology	39
4.3.1 Individuals-based models	40
4.3.2 Homogeneous population models	47
4.4 Perspective review of the literature	48
4.4.1 Individual state models	49
4.4.2 Well-mixed population models	49
4.4.3 Final remarks	50
II Behavioral-Epidemiological Model	51
5 Model development and justification	53

6 Epidemic model and Behavioral model alone	55
6.1 SIRS model	55
6.2 Behavioural model	56
6.2.1 Model simulation	60
6.2.2 Equilibrium and stability analysis	61
6.2.3 Equilibrium simulations	64
6.2.4 Behavioural model: numerical experiments	66
7 Behavioral-epidemic model	73
7.1 Model description	73
7.2 Basic reproduction number calculation	75
7.2.1 DFE calculation	77
7.3 Model simulations	78
7.3.1 I case: $\mathcal{B}_1, \mathcal{B}_2 < 1$, $\mathcal{B}_1 > \mathcal{B}_2$, and $\lambda_1 > \lambda_2$	80
7.3.2 II case: $\mathcal{B}_1, \mathcal{B}_2 > 1$, $\mathcal{B}_1 = \mathcal{B}_2$, and $\lambda_1 < \lambda_2$	80
7.3.3 III case: $\mathcal{B}_1, \mathcal{B}_2 > 1$, $\mathcal{B}_1 < \mathcal{B}_2$, and $\lambda_1 = \lambda_2$	81
7.3.4 IV case: $\mathcal{B}_1, \mathcal{B}_2 > 1$ and $\mathcal{B}_1 > \mathcal{B}_2$, and $\lambda_1 < \lambda_2$	82
7.3.5 V case: $\mathcal{B}_1, \mathcal{B}_2 > 1$ and $\mathcal{B}_1 < \mathcal{B}_2$	83
7.3.6 Influence of the ψ parameter	83
8 Conclusions	87
8.1 Limitations	87
8.2 Future perspective	88
Bibliography	89

List of Figures

1.1	Smallpox on native Americans	14
1.2	Epidemic distribution in time	15
3.1	SIRS example	28
3.2	SIR dynamic example	34
3.3	Agent-based network representation	35
3.4	Multi-layer network	36
4.1	Metacritical effect	41
4.2	Multiplex networks	42
4.3	Stability analysis of epi-behavior model	43
4.4	Game theory	43
4.5	Simulation of disease spreading within a city	45
4.6	Rules in opinion disease model	46
4.7	Mean field models literature review	48
5.1	Mask wearing evolution	53
6.1	SIRS simulation	56
6.2	Behavior model	58
6.3	Behavioural model simulation first	60
6.4	Behavioral model simulation second	61
6.5	Nullclines first figure	66
6.6	Nullclines second figure	67
6.7	Nullcline fourth case	67
6.8	Final Behavioural variables	69
6.9	Final Behavioural variables varying \mathcal{B}_1	70
6.10	Maximum Against	71
6.11	Max against first case	71
7.1	Epidemic behavior model	76
7.2	E_0 simulation results	80
7.3	Full model simulation figure first	81
7.4	Full model simulation figure second	82
7.5	Full model simulation figure third	84
7.6	Simulation varying ψ	85

Part I

Introduction

Chapter 1

Introduction epidemics and social dynamics

One of the main dangers humanity has faced throughout its history, a great threat that has severely affected the lives of almost all human populations over time, is caused by diseases and epidemics. There were no periods - not in the past, nor nowadays - when illnesses did not influence human lives.

In the past, the consequences of epidemics for the population were worse than today, mostly because of the lack of knowledge about medical science and the poor hygienic conditions. During the bubonic plague of the 14th century, for example, 25 million deaths were reported in Europe out of a population of 100 million. The pandemic also triggered social unrest and the spread of fake news: Jews were considered responsible for the disease spread and persecuted: There were several attacks and massacres to the Jewish communities in different European cities, such as Toulon, Barcelona, Erfurt, Basel, Frankfurt, Strasbourg. The persecution was mainly due to the false belief that Jews were less affected by the disease, and responsible of the poisoning of wells. This is an important example of the connection between epidemics and social dynamics including false beliefs and ensuing behaviors. Analogously, the Irish were accused of spreading cholera in New York and Italians were blamed for importing poliomyelitis to Brooklyn [1].

Moreover a well-known example of the impact of infectious disease on civilizations is the following: during the colonization of the Americas, the diseases imported by the Europeans cause a huge death toll in the local populations, largely contributing to their defeat against the Spanish conquistadors. In fact, diseases such as smallpox and measles were unknown in these countries and native Americans had no antibodies to contrast them. For example, epidemic outbreaks are considered by some historians to be the primary cause of death in the Taíno genocide during the conquest of Hispaniola [2], surpassing fatalities caused by warfare or direct attacks. On the other hand, syphilis was likely imported in Europe from the Americas, leading to the first outbreak in Naples in 1495. Other important epidemics, famous for their consequences, were the Spanish flu, smallpox, typhus, HIV/AIDS, and the recent COVID-19. Diseases have a huge effect on our lives.

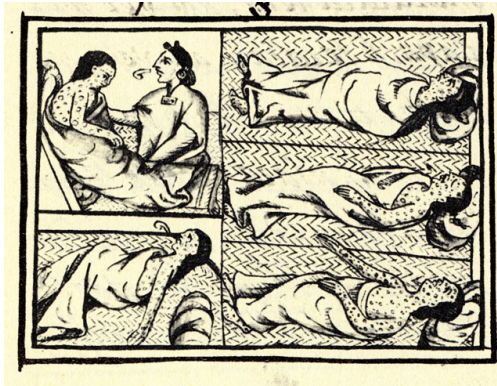


Figure 1.1: Representation of smallpox disease affecting the Mexican population in the *XIV* century. Figure from the Florentine Codex [3].

The development of modern medicine and hygiene contributed to enhancing the quality of life. Only in the last three centuries and especially in the most economically developed countries, a significant increase in life expectancy has been observed [4]. This increase is also observed in poorer regions, such as Sub-Saharan Africa: although current life expectancy there is lower than in wealthier countries, recent research [5] predicts a significant rise over the next 30 years. This study also forecasts that this trend will lead to a global convergence in life expectancy between now and 2050. The most plausible explanation for this future prediction is that improvements in healthcare levels lead to changes in the main causes of mortality as nations' wealth increases. In poorer regions, the primary causes of death are communicable, maternal, neonatal, and nutritional diseases, whereas in more developed and wealthier countries, non-communicable diseases such as cancer and cardiovascular conditions are the main causes of death [6].

Despite rising life expectancy, epidemics continue to be one of the most significant threats to populations. In fact, there was a notable increase in the frequency and magnitude of reported epidemics during the 19th and 20th centuries [4] also because travels became easier and more affordable for more people and the world became increasingly connected. Figure 1.2 highlights this trend.

This makes it essential to develop effective policies to control and mitigate the impact of epidemics, requiring coordinated implementation by countries within the same macro-region. Although it becomes increasingly difficult to obtain reliable information about disease outbreaks the further back in time one goes, epidemics remain a tangible and present threat. This underscores the need for attention and action in shaping health policies that effectively address these dangers. However, health status is not the only factor impacted by diseases. Illness can profoundly alter relationships, work, and social life, leading to a deterioration in overall social well-being as well [9]. There is also an economic cost associated with treatment. Only in a few nations worldwide, treatment is covered free of charge by the state. In most countries, being ill can result in having to sustain high costs, causing people to go into debt or not receive healthcare [10, 11]. All these effects sum together and influence how populations behave when facing an epidemic.

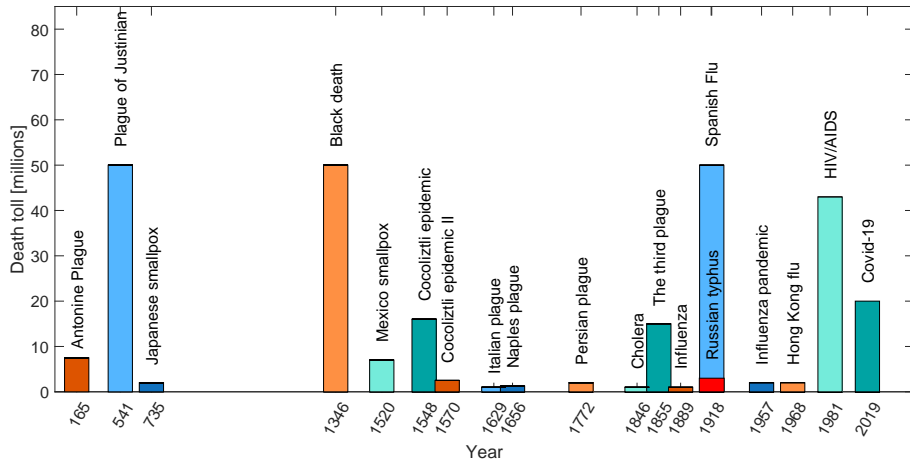


Figure 1.2: A graphical representation of the distribution of most well-known epidemics over the years and of their associated death toll. It is observable how there is an increment in the number of these events in the last three centuries. Data extracted from [7, 8].

What are the consequences of adopting a certain behavior during a disease outbreak? It is a crucial question and the answer can help us understand how to develop more efficient policies for contrasting epidemics. Answering the following question is the main objective of the present thesis: How can a multidisciplinary model be developed that integrates both social and epidemiological phenomena to provide insight into their mutual influence during the spread of a disease?

Taking a step back, it is important to understand why epidemic models are crucial. When a new disease emerges, the primary objective is to develop a defense against it. This begins with an epidemiological investigation to understand the disease's origin, the biological mechanisms behind its spread, and its resistance to existing drugs. The goal of this investigation is to gather all available information and understand the unfolding situation. The next crucial step involves studying the dynamics of the disease and developing a predictive model for its evolution. This process requires understanding and estimating various parameters associated with the disease, including the transmission mechanisms within the population, the reproductive rate of the infectious agent, the acquisition and persistence of immunity, and the contagion mechanism. Creating a reliable model is not only scientifically valuable but also provides as a powerful tool for stakeholders, helping to formulate effective policies during a pandemic emergency. Theoretical epidemiology aims to provide insights and policy recommendations in this context. Furthermore, data acquisition and analysis are essential for statistically modeling epidemic coefficients. Ultimately, a model that can address stakeholders' questions and make predictions—whether or not safety regulations are implemented—has significant implications for society. Beyond the economic costs associated with illnesses, there are also substantial social costs. Developing tools to better understand disease transmission can help mitigate its impact

and alleviate the social burden, potentially saving numerous lives.

A clear example of the potential benefits of having an epidemic model is the ability to generate synthetic insights that are easy to understand and can be expressed numerically. Such models can provide answers to critical questions such as:

- Is the disease so infective that can cause a pandemic?
- What are the threshold conditions that can cause an outbreak?
- What is the expected number of infections over time?

At first glance, the problem may appear straightforward. However, the creation of a model that faithfully captures the evolution of every disease remains an unsolved challenge. Research in epidemic modeling requires balance between simplification and accuracy. A good model effectively reproduces key phenomena with reasonable sophistication. While creating an overly complex model that attempts to incorporate every detail of a disease might be tempting, it often requires significant effort and data. In many cases, such models do not outperform simpler ones that focus on capturing the most important aspects of disease spread. By prioritizing essential characteristics, simpler models can provide more practical insights while remaining computationally efficient.

Over the past century, various aspects of epidemics have been extensively studied. Notable achievements by scientists include:

- Development of epidemiological models using different mathematical tools, such as differential equations, networks or agent-based models [12, 13].
- Predictions about the progression of epidemics or reconstructions of their dynamics [14–16].
- Insights into epidemics, explaining phenomena such as the periodicity of re-infection for certain diseases or the seasonal patterns observed in cases such as influenza [17].
- Understanding the effectiveness of specific strategies against outbreaks, such as vaccines or quarantine [18].

Furthermore, by using multilayer networks or systems, more complex analyses can be performed. The objective is to create models capable of simulating the evolution of multiple phenomena simultaneously, and thus develop a more accurate representation of the real world by constructing more intricate scenarios. Examples of such models include:

- The simultaneous evolution of two different diseases [19].
- The formation of public opinions during an outbreak [20].
- The progression of a disease for which a vaccine exists, but where there is public fear of both the disease and potential vaccine side effects [21].

1.1 Presentation of the thesis work

The work presented in this thesis is part of the multidisciplinary field of research in multi-systems, namely models that simultaneously capture different coexisting and coupled dynamic phenomena. Its focus is on understanding the mutual influence between human behavior and epidemic spreading. On the one hand, it examines how the presence of an epidemic affects the behavior of individuals; on the other hand, it explores how behavioral changes influence the progression and dynamics of the epidemic.

To this aim, a new model is developed, drawing from existing multi-system models and from empirical data that integrate both epidemiological and behavioral aspects.

The framework involves coupling a SIR-like epidemic model with a new behavioral model consisting of three compartments: Heedless, Against, and Compliant individuals. These categories are designed to represent different courses of action taken during an epidemic.

- Heedless individuals represent the segment of the population that is either unaware of the disease's spread, particularly in its early stages, or indifferent to the risks, continuing with regular routines that may increase their likelihood of infection.
- Against individuals are skeptics who reject precautionary measures and refuse to follow established guidelines.
- Compliant individuals are those who actively seek to avoid infection by adhering to health policies and precautions.

The model incorporates mechanisms to account for changes in behavior among social groups, primarily driven by peer pressure, but also considers the intervention of a central global actor. Additionally, it accounts for fatigue associated with adhering to a particular behavioral spectrum (either complying with or opposing rules). The epidemiological model we developed can track both the initial phase of an epidemic and further waves of contagion, including the possibility of reinfection.

A distinguishing aspect of this work is its reliance on empirical data. Unlike other studies that use ad-hoc assumptions or data from sources not directly related to behavior (such as opinions), this thesis leverages research conducted during the COVID-19 pandemic that provides insights into people's behavior, including not only opinions about the disease and trust or distrust in doctors or governments, but also actions such as mask-wearing and hand washing. For a novel multi-system model such as the one developed here, an analysis of its dynamics is performed. The two components alone are studied, and the social one, which represents a novelty, has been thoroughly analyzed and simulated. Furthermore, an epidemic reproduction number, defined as E_0 in the thesis, is calculated and used to understand which model-free disease scenarios can evolve into an epidemic if perturbed by the entry of infected individuals.

A powerful feature of multi-system models is their ability to reveal phenomena that would not be apparent when examining individual components in isolation. This comprehensive approach enables a deeper understanding of complex interactions and dynamics. Moreover, the developed model is designed as a flexible framework, capable of adapting to a wide range of scenarios, reflecting the multiplicity of reality.

Chapter 2

Main objectives and thesis structure

In this chapter, we present the main objectives of the thesis and describe its structure. Starting from an analysis of the theoretical contributions already developed for epidemiology, and in particular focusing on multilayer systems and mean-field models, the following questions are studied:

- How can population behaviors be effectively included in epidemiological models? What are the characteristics that must be considered?
- Can individual behavior influence the evolution of an epidemic?
- Can an outbreak be stopped just by relying on the natural subdivision of the population into compliant and non-compliant groups regarding safety measures, or is the intervention of a central "controller" necessary to enforce new behavior rules?

Starting from these questions, the following objectives have been identified:

- Create an original epidemic-behavioral multi-system model that captures the evolution of a disease and represents behavioral changes using a peer pressure mechanism within the same population.
- Add a control mechanism within the model, represented by government rules that can modify individual behaviors in a centralized way.
- Develop a comprehensive analysis of the epidemiological and behavioral model to understand its mechanisms and correctly interpret the mutual effects arising from the coupling of the social and epidemic phenomena.

The thesis is structured as follows.

The introductory Chapter 3 presents the main concepts of social science and epidemiology and provides all the necessary information to understand the presented research, including a glossary of the most important terms and an overview of the mathematical

tools used in epidemiology. Additionally, different models implemented to simulate an epidemic are shown in Section 3.3, with a focus on the properties of mean fields model, used in the thesis. Furthermore, a historical background of the research field is provided to give a perspective on the principal milestones.

Chapter 4 offers a review of the literature analyzed for the thesis. The articles are categorized into different main topics: epidemiology theories, opinion models, behavior models, and multi-agent and multi-system models. This subdivision highlights the most interesting aspects of each work and identifies the elements that have been considered for inclusion in the thesis.

The second part of the thesis is composed of four main chapters.

In Chapter 5 the reasons that led to the development of a new model are presented.

In Chapter 6, the developed epidemiological and behavioral models are simulated. The SIRS epidemic model is introduced, and its main features are described. The behavioral model developed for the thesis is also introduced, the assumptions made for its dynamics are explained, and a set of simulations and analyses is performed. This analysis is conducted to gain a clear understanding of how the hypothesized social dynamics can evolve and to develop initial insights to better understand the behavior of the fully coupled final model.

Chapter 7 presents the model resulting from the integration of the two layers, forming part of a more complex multi-system model. The implementation of this coupling is explained, detailing how the mutual influence between the two components operates. The main features of this model are analyzed using both simulations and insights gained from calculating the epidemic reproduction number. In fact, the threshold effect, which explains whether a disease-free equilibrium can evolve into an epidemic, is determined, and its value is calculated under varying model scenarios.

Finally, the last chapter 8 contains the conclusions of the thesis.

Chapter 3

Theoretical background

3.1 Epidemiological theory: foundations

A clear description of the main concepts in social science and epidemiology is essential for understanding the rest of the work. In this chapter, the theoretical basis and main concepts that will be used in the present work are defined.

First, a brief historical review of the emergence of epidemiology as a discipline is provided, focusing on the explanation of its genesis. Indeed, these key findings laid the foundation of modern epidemiology. The following section presents a glossary of the key terms used throughout this thesis to ensure clear communication of the core concepts that will be used later. Initially, terms related to epidemiology are explained, followed by definitions of behavior-related concepts.

Subsequently, the most commonly used mathematical tools are introduced, including an overview of various modeling techniques. Special attention is given to the theoretical background of mean-field models, the category to which the model developed in the thesis belongs.

3.1.1 Epidemiological research: historical background

The research field regarding the development of techniques to understand how epidemics can evolve over time has a history dating back to the 20th century. The first important discovery in this field must be attributed to the scientists that found the mechanism used by diseases to spread. A first innovative work was the one by John Snow, who during an epidemic of Cholera in London in 1854 successfully determined the source of the infection, even without knowing its etiological agent. Further advances in the microbiological research were due to Pasteur and Koch. They found the etiological agent of disease, enabling the possibility to treat and prevent people from being infected. Then, Hamer's work in 1906 added a first major theoretical contribution. He formulated a theory about the correlation between the course of an epidemic and the interaction, or contact ratio, between susceptible and infectious individuals. It was the so called "mass action" principle. The number of contacts between these two groups determines the spread rate of the disease. This law, originally written in discrete time, was then updated in 1908 by Ross,

who wrote it in continuous time. For the first time the problem could be studied using a clearly, well defined mathematical theory. Then the contributions of Kermack and McKendrick in 1927 added another fundamental principle to the modern epidemiology. They formulated a threshold theory explaining which conditions can generate the development of an epidemic. Their theorem states that a certain value – called reproduction number – must be exceed, depending on the proportion of susceptible and infectious individual. Monitoring this value allows us to understand if the number of infections will increase, until a peak is reached, or if the epidemic is in a descendent phase [4, 22]. Their contribution based on the mass action principle represents the fundation for the mean field model theory, presented and analyzed in Section 3.3.1.

3.1.2 Epidemiological glossary

For a better comprehension of the subject analyzed in the present work, a list of principal concepts and terms is presented.

CFR, IFR and mortality excess

The case fatality rate, CFR, is the ratio between the number of deaths due to a specific disease and the total number of confirmed positive cases detected by testing. The infection fatality rate, IFR, is instead the percentage of people infected with the disease that are expected to die. The two quantities can have a similar value: if every person who contracts the disease and every death attributable to the disease is known and recorded, then the CFR will equal the IFR. The excess in mortality can be calculated by observing the difference between the total death rate (due to any reason) before and during an epidemic.

Disease transmission

A disease can spread in different ways:

- Person to person: involving direct (e.g. sexual transmission or skin diseases) or indirect (e.g. respiratory) contact.
- Airborne: through inhalation of infected air.
- Food or water borne: ingesting contaminated food or water.
- Vector born: the contagion is mediated by infected animals.

Furthermore, when the spread is within the same generation, the transmission is called horizontal, while vertical transmission is the one between different generations, from parents to children. Zoonosis is the phenomenon in which a disease that starts in an animal species mutates and infects humans. The opposite can also happen and it is called inverse-zoonosis.

Endemic disease

It is a disease that lasts for a long time and requires consideration of its impact on population renewal and in the number of susceptible individuals.

Epidemic disease

An increase in disease prevalence typically manifests as a rapid outbreak. This type of illness is confined to a limited geographical region, unlike a pandemic that affects a much larger area.

Immunity and herd immunity

Immunity refers to the protection from a disease gained after contracting it (or after vaccination). This immunity can be lifelong or diminish over time. When a person is immune, re-exposure to the virus does not result in infection, or there is only a reduced chance of being infected, known as partial immunity.

Herd immunity is a phenomenon where a large portion of the population becomes immune, either through vaccination or surviving the disease. This majority limits the spread of the illness, indirectly protecting those who are not immune by slowing or halting disease transmission.

Incidence and prevalence

The first term refers to the number of new cases within a certain period (daily or weekly for example), while prevalence is the portion of the population affected by a disease in a specific time.

Incubation, Symptoms, Infected and Infectious

When a person comes into contact with an infectious individual, they may or may not become infected. The incubation period refers to the time after infection when the disease grows within the host without producing symptoms.

Symptoms refer to the physical signs of illness caused by a disease in the affected individual.

A person is described as infectious when they carry the disease and can transmit it to others, while infected refers to someone who has been exposed to the infection and has become ill.

Incubation period and serial interval

The incubation is the time after exposure in which the infection develops in the host and ends when the infected start to show symptoms. The serial interval is instead the time that exists between two transmissions in a chain of infections.

Micro and Macro parasite

An etiological organism responsible for a disease can be either a microparasite or a macroparasite. The former lives and reproduces within the host, generating an immune response and causing an infection that usually has two possible outcomes: death or immunity. Infections due to microparasites are shorter than the life span of an individual, and

have a transient nature. Most viral and bacterial parasites belongs to the microparasitic category.

Instead, macroparasites have no direct reproduction within their host. Arthropods and helminths are in this category. They are larger and have a much longer generation times than microparasites, with a life span that can be a considerable fraction of the host life span.

Outbreak

The rapid raise in the number of infected during an epidemic.

Overdispersion and Superspreading

Overdispersion is a term that refers to observing a larger variance than expected from a normal distribution. It is used in statistics to measure superspreading, a circumstance in which there is an abnormal (higher) number of secondary infections brought about by low numbers of spreaders.

Pandemic disease

It is an epidemic that spreads across multiple regions, on a global scale. The severity of the disease also makes a distinction in calling a disease a pandemic. For example, the common cold is spread in the whole world but is not defined as a pandemic by the WHO (World Health Organization).

Reproduction number \mathcal{R}_0

It is the fundamental measure of the infectiousness of a disease. It is the average number of secondary infections caused by one infected person in a fully susceptible population. If it is recalculated during the epidemic progression it is called $\mathcal{R}(t)$, a time-varying reproduction number, also called the effective reproduction number: it is obtained by rescaling the Reproduction number value with the true number of susceptible individuals.

Types of infectious diseases

An infectious disease is an illness resulting from the presence of pathogenic microbial agents such as bacteria, viruses, parasites or other microorganisms.

It is possible to distinguish between *transmittable* and *communicable* disease. A transmittable disease can be transmitted between persons through close contact (e.g. blood borne transmitted sexually or through bodily fluids). A communicable disease is one that easily spreads from one person or animal to another by casual contact or from a surface to a person.

Virulence and Contagiousness

Virulence is used to describe how aggressive, harmful, and pathogenic is a biological agent in attacking cells. Contagiousness is the capability to transmit a disease.

3.2 Opinion/behaviour glossary

To establish a framework suitable for developing and understanding behavioral models, the following key concepts from social science are outlined.

Awareness

It is the knowledge and alert level that an individual has on a certain subject or situation. It changes with time and it is developed with information or experience.

Behaviour

It is how one acts or conducts oneself. It can depend on the response to external stimuli and have effects, especially on others.

Belief

It is the conviction of the truth of a statement or the reality of a being or phenomenon, especially when based on the examination of evidence, but also on matters for which there is no proof.

Group decision-making

It is a phenomenon at the intersection of psychology, management, biology, and applied mathematics studying how people in groups interact, exchange information, and realize decisions. The decision made by the group is no longer attributable to any single individual but to the whole group.

Homophily

The tendency to bond and associate preferentially with others that are similar.

Information

The term "information" is commonly understood as "knowledge communicated." However, given its crucial role in modern society, there is considerable debate about its various meanings [23]. Today's world is often described as an "information society," where the advancement of information technology has impacted nearly every aspect of life.

Currently, the term "information" carries two key meanings. The first, more general, definition refers to anything that is valuable in answering a question. The second definition pertains to Information Science, the discipline that manages information in all its forms. In this context, information is something with the capacity to inform. On a fundamental level, anything that is not entirely random can be considered to convey some degree of information.

Perception

It is the mechanism through which something is regarded, understood, or interpreted.

Polarization and Consensus

Polarization refers to the divergence of beliefs within a population. There are several mathematical methods available to measure the degree of polarization. For instance, one can collect data on opinions, beliefs, or behaviors within a group and then measure the distance between the most extreme views, or analyze their distribution across a defined range.

This contrasts with the concept of "consensus," where the exchange of opinions, information, or resources among individuals leads to widespread agreement. Both polarization and consensus can be studied and modeled using network theory [24].

Threshold theory

It is a theory formulated by Granovetter in [25] regarding collective behavior. The theory posits that in a society where individuals face two possible alternatives, and their choices involve certain costs and benefits depending on how many others choose each alternative, an individual will decide based on the number of others who have already chosen a particular option when this number exceeds a certain threshold.

Trust

It is the sentiment of confidence associated with the ability, strength, and truth of someone or something.

3.3 Epidemiological models categorization

Starting from the observation of the real world, the desire to better understand a certain phenomenon is the fundation of mathematical model development. A perfect model does not exist, because each model is based on data or on assumptions that are incomplete with respect to reality. However, a useful model allows us to provide general predictions and can be a powerful instrument for researchers and policymakers. For example, an application is the estimation of the effects of certain policies on the population during an epidemic: in this case, the aim is to obtain meaningful prediction, under a given set of real-world circumstances. When working on a model, the importance of the uncertainty related to the obtained predictions and forecasts must always be remembered. This concept is remarked also in the definition of mathematical model present in [16].

"A Mathematical model is a self-contained collection of one or more variables together with a set of rules (usually formulas and equations) that prescribe the values of those variables. Models serve as an approximate quantitative description of some actual or hypothetical real-world scenario. They are created

in the hope that the behavior they predict will capture enough of the features of that scenario to be useful."

There are several different types of mathematical models. A first classification can be done considering the method used to obtain them: we thus have mechanistic, empirical, phenomenological or conceptual models. Mechanistic models are based on assumptions about reality, or theoretical principles, modeled using a collection of one or more variables together with a self-contained set of rules. These models have an explanatory value on the reality they represent. Empirical models are realized by fitting set of data. They are a powerful instrument, because data can be fitted quite well, but they lack the explanatory value of mechanistic models. A phenomenological model describes the empirical relationships between phenomena in a way that aligns with fundamental theory, but it is not directly derived from first principles. These models define the relationships between variables and provide insights into the phenomenon under study. Finally, a conceptual model is a verbal description of a real-world phenomenon.

In the thesis, we consider mechanistic/phenomenological models. In fact, in epidemiology, the objectives for which a model is developed go beyond just fitting data. Examples of possible objectives are:

- monitor the epidemic evolution;
- realize a framework capable of understanding the information related to the disease, as incidence and prevalence for example;
- obtain general insight about epidemic control strategies;
- realize predictions.

Several different types of mechanistic models have been developed or are adapted to be used in epidemiology modeling. In this section, the principal typologies are now introduced.

In particular, mean-field models are discussed in depth in section 3.3.1, because the multi-system model developed in the thesis belongs to this class.

We introduce the logic underlying their structure, their main mechanisms, and the important conclusions that can be derived from them because it is a useful introduction to the approach that will later be employed in the rest of the thesis.

3.3.1 Mean field models

Mean field model, also known as compartmental model, is the first developed and most studied type of mathematical model used in epidemiology [4, 15, 26, 27]. A mean field model assumes that a well-mixed population is divided into several subgroups (i.e. compartments). Each compartment is associated with a different stage of the disease under consideration. Some possible states are susceptibles, asymptomatic (infected), symptomatic (infected), infected (if in the model no distinction between symptomatic or asymptomatic is done), exposed, vaccinated, quarantined, dead, recovered, and hospitalized.

The classes considered in a given model determine its base structure. The choice to include a certain compartment depends on the disease that is modeled and on the considered assumptions. Different models can be suitable to analyze the same disease but can be used with different aims. A more complex model can emphasize some aspects or effects of the disease, that are not highlighted by a simpler one.

For example, both a SIR (Susceptible- Infectious-Recovered) [28] and a SPQEIR (Susceptible -Protected-Quarantined- Exposed- Infectious- Removed) [29] can be used to model COVID-19, but the second model considers explicitly quarantine, exposed and use of protections to avoid infection - elements that cannot be observed or considered with a simpler model like a SIR.

In mean-field class of models, the primary focus is to describe the spread of the disease rather than its biological impact on the health of each infected individual. The transitions between compartments (such as Susceptible, Infected, and Recovered) are governed by differential equations. The parameters that control these transitions are coefficients whose interpretation depends on the underlying assumptions of the model. For example the γ parameter is usually interpreted as the inverse of the time an individual spend in the infectious compartment. Mathematically, these parameters determine the rate of flow between compartments.

The most critical metric in this model category is the "Basic Reproduction Number" (often denoted as \mathcal{R}_0), which represents the average number of secondary infections caused by a single infected individual in a fully susceptible population. It is a fundamental threshold in epidemiology, indicating the potential severity of an outbreak [12]. By observing the value of \mathcal{R}_0 , it is possible to immediately determine whether a newly developed disease can spread within the susceptible population and cause an outbreak leading to an epidemic. In fact, if $\mathcal{R}_0 > 1$, the disease can generate an epidemic, whereas if $\mathcal{R}_0 < 1$, the disease dies out.

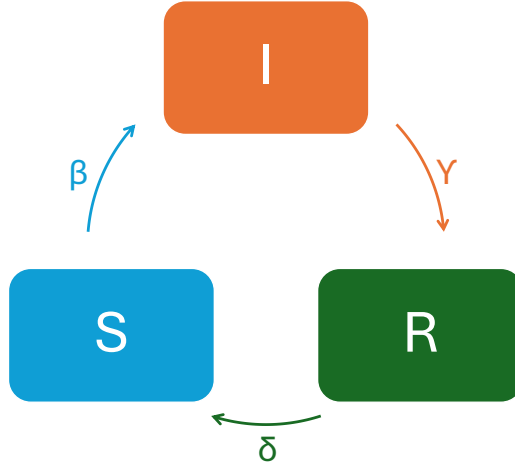


Figure 3.1: An example of the graph structure of a mean field SIRS model. There are three compartments and the flow rate between them is ruled by the coefficients β (transmission rate), γ (recovery rate) and δ (immunity waning rate).

SIR model

The foundational model for studying epidemics mathematically is the SI model. In this model, the population is divided into two compartments: Susceptible (S) and Infected (I). Individuals transition from being susceptible to infected, but there is no recovery, meaning that individuals can remain infectious indefinitely. Alternatively, in the SIS model class, once individuals are healed, they become again susceptible, so no immunity is acquired. The SIR model adds a third compartment, Recovered or Removed (R). This additional compartment represents individuals who have either gained immunity or have died, and are thus removed them from the cycle of infection. After spending a certain period in the infected state, individuals transition to the recovered state, making them no longer susceptible to the disease, so in the SIR model the population or density of individuals is sub-divided into three groups: Susceptible, Infectious, and Recovered. At time t the three groups are identified with the symbols: $S(t)$, $I(t)$, and $R(t)$. The symbols used to indicate the fractions of population in each group are instead s , i , and r , while the capital letters are used to specify both the name of the groups or the absolute number of individuals in each one. Like for the SI model, waning of immunity can be captured also in the SIR model, turning it into a SIRS by introducing an additional parameter driving the transition from R to S (see Figure 3.1).

The SIR model, which will be described in the following sections, is built upon several assumptions that shape the mathematical framework. These guiding principles are introduced in the following paragraphs. Furthermore, the main properties of the model will also be introduced.

Mean-field approximation

The approximation that gives the name to this model class is based on a method that permits the analytical analysis of complex systems. With mean-field, individual-level interactions are averaged, focusing not on individual behavior but on the collective behavior of the population. Using this method, equations can be derived that describe disease evolution in terms of average rates rather than tracking individual agents.

Homogeneous mixing

It is the assumption that all individuals in the population mix homogeneously, meaning that the probability of interacting with any individual is the same. It is a strong assumption because it implies ignoring any spatial or social heterogeneity.

Average rates of changes

In the model, differential equations are used to represent the transition of individuals between different compartments. These transitions can depend on the state of the system but, in the simplest form, are based on average rates. The three rates used in the SIRS mean-field model are:

- β : transmission rate;

- γ : recovery rate;
- δ : waning immunity rate.

The flow of individuals in the system is shown in Figure 3.1.

Population conservation

The total population size, represented by the letter N , is the sum of the numbers of individuals in the compartments (e.g., Susceptible, Infected, and Recovered). It is often assumed to remain constant during the course of an epidemic. This assumption is based on the idea that epidemics typically last much shorter than the average human lifespan, making the effects of births and deaths negligible. In more complex models, where demographic effects are considered, such as in models of longer-lasting epidemics, the population size can still be assumed constant by balancing the number of births (modeled as an influx into the Susceptible compartment) with the number of deaths (modeled as an outflux). This approach assumes that births and deaths occur at approximately the same rate, keeping the total population size constant over time. The result of this assumption implies that:

- The population densities in the compartments sum up to one.

$$s(t) + i(t) + r(t) = 1$$

- The sum of their time derivatives is equal to zero.

$$\dot{s}(t) + \dot{i}(t) + \dot{r}(t) = 0$$

Recover transition

The first fundamental dynamic process of the model assumes that the infected compartment decreases in size with a rate of decrease proportional solely to the current number of infected individuals. This gives the following relation:

$$\frac{di}{dt} = -\gamma i, \quad i(0) = i_0,$$

which models a continuous process. Specifically, it assumes that individuals transition from the infectious state to the recovered state at a constant rate, denoted by γ . The physiological meaning of this parameter is that it represents the inverse of the infection duration, i.e. that the average infection lasts $1/\gamma$ days. Thus, γ is the recovery rate, reflecting the speed at which the population recovers from the disease.

Person-to-person disease transmission

Assuming a population composed of susceptible and infected individuals, each infectious individual encounters a fraction c of the population per day. If all encounters are equally likely, a fraction s of these encounters will be with susceptibles. Therefore, each infectious individual has $c \cdot s$ encounters with susceptibles. The probability that an encounter leads to transmission is p , hence the average number of transmissions per day is $p \cdot c \cdot s$. Considering

the fraction of infected individuals i , and combining p and c into a single parameter β , the transmission rate becomes:

$$\text{transmission rate} = \beta s i.$$

Here, β represents the transmission coefficient.

Immunity

In SIR model, once individuals recover from the disease, there are no further transitions. Two possible model scenarios can cause this:

- Lifelong immunity acquired after recovery.
- Death of infected individuals.

Both cases assume that, once the illness period ends, the disease can no longer be transmitted. If immunity acquired from an infection wanes after a certain period, individuals can become susceptible again, leading to an SIRS model. The δ rate is used to express the outflow from the Recovered compartment, and it corresponds to the inverse of the average duration of immunity.

Threshold value

Although the SIR model is simple, it plays a fundamental role in predicting a key aspect of epidemics: the threshold value, a concept first introduced by Kermack and McKendrick in their pioneering work [26]. They showed that, in a fully susceptible population, an epidemic will only start if the basic reproduction number \mathcal{R}_0 is greater than 1, marking the birth of the term "threshold value" in epidemiology. In the SIR model the reproduction number value is equal to the ratio between the transmission and recovery rate:

$$\mathcal{R}_0 = \frac{\beta}{\gamma}. \quad (3.1)$$

Over the years, the dynamics of this system have been extensively studied and analyzed [16, 30–36]. The threshold effect highlights two distinct scenarios:

- **Disease-Free Equilibrium ($\mathcal{R}_0 < 1$):** When \mathcal{R}_0 is less than one, the disease does not spread within the population. Although infected individuals make contact with susceptibles, the rate of disease transmission is slower than the recovery rate. Mathematically, this means $\beta/\gamma < 1$, or $\beta < \gamma$, where β represents the transmission rate and γ the recovery rate. Consequently, the healing process is faster than the spread of infection, and the number of infected individuals quickly drops to zero. The majority of the population remains susceptible, and the Disease Free Equilibrium is globally asymptotically stable, as demonstrated by [12].
- **Epidemic spread ($\mathcal{R}_0 > 1$):** When the threshold is greater than one, the number of infected individuals grows until it reaches a peak and then declines toward zero. The peak number of infected people, as well as the final number of susceptibles, can be calculated using the system initial conditions and the values of β and γ , as described by [37]. As reported in this work:

Let $s_s(t), i_s(t)$ be a solution of the system

$$\begin{aligned} ds/dt &= -\beta is \\ di/dt &= \beta is - \gamma i \end{aligned} \tag{3.2}$$

with $s(0) = s_0 \geq 0$, and $i(0) \geq 0$. The mass conservation assumption holds so $r(t) = 1 - s(t) - i(t)$. The triangle in the si phase plane given by

$$T = \{(s, i) | s \geq 0, i \geq 0, s + i \leq 1\}$$

is positively invariant and unique solutions exist in T for all positive time, so that the model is mathematically and epidemiologically well posed. If parameter \mathcal{R}_0 is defined as $\mathcal{R}_0 = \beta/\gamma$ it holds that if $\mathcal{R}_0 s_0 > 1$, the $i(t)$ first increase up to a maximum value $i_{max} = i_0 + s_0 - 1/\mathcal{R}_0 - [\log(s_\infty/s_0)]/\mathcal{R}_0$ and then decrease to zero as $t \rightarrow \infty$. The susceptible fraction $s(t)$ is a decreasing function and the limiting value s_∞ is the unique root in $(0, 1/\mathcal{R}_0)$ of the equation

$$i_0 + s_0 - s_\infty - \log(s_\infty/s_0)/\mathcal{R}_0 = 0.$$

This scenario illustrates how a highly aggressive infection can spread widely within a population. If no countermeasures are taken, it can lead to significant social and economic consequences. A typical epidemic outbreak has an infective curve that first increases from an initial i_0 near zero, reaches a peak, and then decreases toward zero as a function of time. The susceptible fraction $s(t)$ instead always decreases, but the final susceptible fraction s_∞ is positive. The epidemic dies out because, when the susceptible fraction $s(t)$ goes below $1/\mathcal{R}_0$, the effective reproduction number $\mathcal{R}_0 s(t)$ goes below 1.

Thus, even with its simplicity, the SIR model provides critical insights into the potential severity of an epidemic and highlights the importance of timely interventions to prevent widespread harm.

The SIR mean-field model equations

After introducing the basic framework of the model, the set of differential equations that describe the rates of change in the system states is presented. The equations, along with initial conditions, are necessary to fully define the model. The class sizes are expressed as fractions of the total, constant population.

The model is then

$$\begin{cases} ds(t)/dt = -\beta s(t)i(t), & s(0) = s_0 \gg 0; \\ di(t)/dt = \beta s(t)i(t) - \gamma i(t), & i(0) = i_0 > 0; \\ dr(t)/dt = \gamma i(t), & r(0) = r_0 = 0; \end{cases} \tag{3.3}$$

where

$$s_0 + i_0 + r_0 = 1. \tag{3.4}$$

Several works analyze this model and provide a detailed mathematical derivation of its solution [14, 31, 36]. However, this is not the focus of the present work. Instead, we provide an overview of the main results and a summary of the dynamics that emerge from the model.

Model behavior

To present the evolution of the model, a simple numerical simulation is carried out. The removal rate is set to $\gamma = 0.1$, meaning the infection lasts, on average, 10 days. The transmission rate is $\beta = 0.5$. At the start of the simulation, the majority of the population is in the susceptible class, with only a small portion of individuals already infected.

The initial reproduction number is $\mathcal{R}_0 = \frac{\beta}{\gamma} = 5$, which is greater than 1. As discussed in Section 3.3.1, this indicates that the disease will evolve into an epidemic.

The key features that emerge from the model simulation are:

- **Slow initial phase:** The early stages of the epidemic are marked by a slow start, as seen in the first part of the curves in Figure 3.2a. The curves remain nearly flat because only a few individuals are initially infected, and it takes time for the infection to spread and reach a larger portion of the population.
- **Exponential growth:** In the second stage, the number of infections increases exponentially.
- **Peak infection:** Eventually, the number of infections reaches a peak.
- **Residual susceptible population:** By the end of the epidemic, a portion of the population remains susceptible, though this amount depends on the model parameters.

An additional detail emerging from the model, as analyzed in [33] and visible in Figure 3.2, is the evolution of the reproductive ratio over time. The reproductive ratio is given by the formula $\mathcal{R}(t) = \frac{\beta}{\gamma} \cdot s(t)$. Initially, assuming $s(0) \approx 1$, we can simplify this to obtain the value of \mathcal{R}_0 . However, as the susceptible fraction decreases exponentially alongside the growth in infections, the reproductive ratio also decreases, and the infection peak occurs when $\mathcal{R}(t) = 1$.

Two key metrics to consider during the emergence of a new disease are the rate of increase of infections and the final size of the remaining susceptible population by the end of the epidemic. The course an epidemic takes can vary dramatically depending on whether it spreads rapidly, overwhelming healthcare systems, or whether interventions succeed in "flattening the curve." The rate of infection growth depends on how quickly the disease spreads through the population. If an epidemic grows rapidly, a large number of people fall ill in a short period, potentially overwhelming healthcare resources. On the other hand, the final size of the susceptible population indicates how many individuals remain uninfected once the epidemic has run its course. This is influenced by factors such as herd immunity or interventions like vaccination. "Flattening the curve" refers to strategies aimed at slowing the spread of the disease, thereby reducing the peak number of infections and spreading cases over a longer period. This reduces the strain on healthcare systems without necessarily reducing the total number of infections.

Some strategies for flattening the curve include:

- Social distancing and quarantine to reduce contact between susceptible and infected individuals. This decreases the transmission rate β .

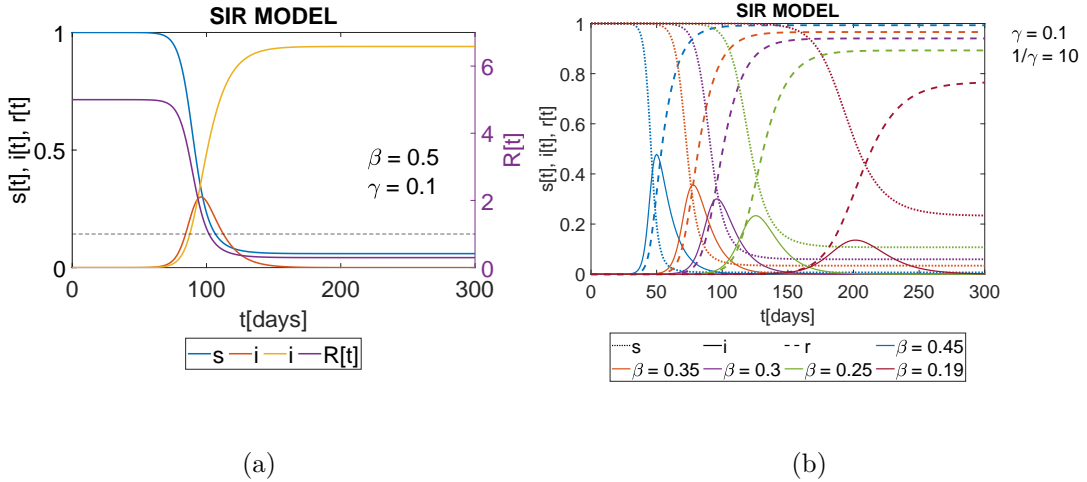


Figure 3.2: SIR system: numerical solutions. Panel a) shows the evolution of the model variables in the case of an epidemic. The violet line represents the time-dependent $R_0(t)$. When this parameter is equal to 1, the number of infected reaches its maximum value. Panel b) presents different evolutions of the disease obtained by varying only the β coefficient. The smaller its value, the more flat and delayed the infected curve is.

- Vaccination, which immediately reduces the number of susceptible individuals, thus preventing the disease from spreading widely.

While flattening the curve may not lower the total number of infections (i.e., the cumulative number may remain the same), it reduces the number of active cases at any given time, which is crucial for ensuring that healthcare systems are not overwhelmed.

3.3.2 Other modeling techniques

There are several other ways to model an epidemic, and the main types of models are now introduced. Many of the articles that will be reviewed in Chapter 4 make use of one or more of these model types.

Stochastic models

This group of models, which originate from the mean-field approach, utilizes a different mathematical framework. In these models, the transition between states is governed by stochastic functions. Conceptually, they share the same foundation as ordinary differential equation (ODE) models but differ in application. These stochastic models are particularly useful when studying diseases with a lower number of infected individuals or when the epidemic outcome is influenced by changes in individual dynamics, a phenomenon known as demographic variability. Demographic variability includes changes in transmission rates, birth rates, recovery rates, or mortality within the population. An approach to

model such variability is through stochastic models paired with Monte Carlo simulations [38].

Networked models

In this class of models, disease dynamics are considered over complex and realistic networks, with a focus on understanding how the network structure impacts the epidemic spread by analyzing parameters such as the rate of infection. The model represents individuals as nodes in a graph, with edges illustrating interactions between them. Nodes can also represent subgroups, and the relationships between individuals or groups can be weighted, representing varying strengths of interactions [39, 40]. The larger the number of nodes and the more accurately the connections reflect real-world interactions, the better the model is at faithfully reproducing the spread of the disease.

Agent-based models

Agent-based models (ABMs) simulate the progression of a disease by focusing on the behavior and interaction of autonomous agents, which could be individuals or collective entities like organizations. This modeling approach is built on observing spontaneous interactions between individuals [41], creating a dynamic system where each person acts according to certain rules. The goal is to understand how these individual behaviors influence the overall evolution of the system.

One key advantage of ABMs is that they provide an intuitive way to interpret epidemic modeling by focusing on individual perspectives, making the model results easier to understand. Additionally, because agents act according to individual behavior, ABMs can deliver highly detailed simulations and offer insights into specific countermeasures that might help mitigate the spread of a disease.

However, ABMs require a large amount of detailed, reliable data to be effective, as their accuracy depends on the precision of the information integrated into the model. Collecting and incorporating this data can be a challenging task, which is a potential limitation of this modeling approach [12].



Figure 3.3: Agent-based network representation.

Multilayer systems and networks: multi-system models

The complex dynamic of interactions existing in the real world, evolves in multiple patterns, with complicated relationships, that can change over time. Using the theory of multilayer systems can improve the comprehension of such complexity. Additional information can be added to the model, for example, different types of interactions, like physical contact or information sharing, time dependency coefficients, or reliance between different parameters in nature, creating cause-effect relationships.

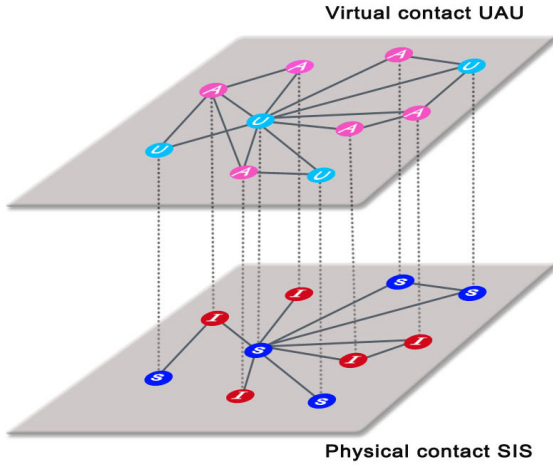


Figure 3.4: Representation of a multilayer structure. The figure is taken from [42] and shows a network implemented with two coupled layers: one representing awareness and the other the epidemic state. Nodes connected by interlayer connections represent the same individual. The model thus describes people with two attributes: awareness of a disease and health state. The mechanisms of infection and becoming aware are distinct, but both influence the evolution of an agent's state. For instance, if an agent is aware of the disease, they may act more cautiously, reducing their probability of becoming infected.

Recent research developments revisits the traditional network theory to create a framework including multiple networks, that evolve and influence each other [19, 43] and can be helpful to describe complex systems like human relationships. For instance, the onset of one disease may depend on the onset of another. There can be regimes in which the criticality of the two dynamics is interdependent and others in which the critical effect is only one-directional [19]. One possible way to develop models with this structure is to imagine that each layer represents a different type of interaction. For instance a model that considers, for each agent, both its physical contacts with others, where the disease can be transmitted, and its network of relations, representing the social dynamics in which everyone is involved. An example of this network is shown in Figure 3.4. This instrument provides a natural representation of coupled structure and dynamical processes. It has been used in multiple works in the past years, for example in [44]. Multiple systems have a coupled dynamic and, with their structure, describe phenomena in each layer that evolve under the mutual influence of events occurring in other layers.

Chapter 4

Review of epidemiological behavioural and opinion models in literature

The scientific community's interest in epi-behavior (coupled epidemiological and behavioral) models has grown over the years. Initially, as noted by [45], the behavioral aspect in epidemiology was not given significant attention. Its development has been a gradual process, resulting from years of evolution in research.

In fact, in initial epidemiological works, the focus of scientists was primarily on presenting the evolution of diseases. The resulting models did not account for the effect of behavior; the population was considered homogeneously mixed, leading to random contact between susceptibles and infectious [12, 22]. It was only later, as epidemiological models proved to be effective and reliable in describing and predicting disease spread, that interest in their beneficial impact on population safety and well-being grew. Tools that integrate real data with epidemiological models emerged, helping inform decisions on matters such as school closures or travel restrictions, as described in [45].

Furthermore, new categories of models have emerged, such as agent-based models, networked models, and multi-layer/multi-system models. Despite their differing approaches, they aim to integrate various population characteristics, for example contact structure, age distribution, and movement patterns, to go beyond the original homogeneity assumption [15]. This focus on societal composition and behavior naturally stems from the desire to use modeling tools as a reference for decision-making in safety and health.

To integrate behavioral ad epidemiological models, one possible approach is to incorporate changes in the structure of models that describe aspects of behavior or population composition. In these models, the behavior of the population is implicitly considered by integrating time-varying parameters that capture changes in societal behavior. This approach represents the classical modeling technique used in the formulation of epidemiological models. Examples of studies that use this methodology for analyzing COVID-19 include [28, 29, 46].

Although these models developed in this way have proven to be powerful tools for generating insights about disease dynamics and providing recommendations to policymakers, they fall short in their ability to accurately reconstruct how populations behave during an epidemic outbreak. The desire to explore this aspect and develop a framework capable of simultaneously capturing both behavior effects and disease diffusion—where each mutually influences the other—has driven the development of a specific research field dedicated to behavioral epidemics.

But how can behaviors be integrated into pre-existing epidemiological theory? To better address this question, we follow the classification proposed in [47], which offers a possible subdivision of the behavioral literature based on the different approaches that most articles focus on. Three major categories emerge:

- The source of information used to make decisions;
- The type of information used to make decisions;
- The effect of behavioral change on the dynamic described by the model.

The first two points focus on distinguishing between the various strategies implemented to model and integrate information dynamics, which play a crucial role in behavioral models. In this context, information acts as an infectious agent within the social layer. Models incorporate this effect in different ways, highlighting how messages are communicated—whether through media or conversation—and the type of information researchers choose to emphasize (e.g., fear of the disease or data about infection numbers). The last categorization is dedicated to the different strategies used to integrate human behavior into epidemiological models.

4.1 Information sources

When analyzing the source of information, there is a clear distinction between works assuming that governments and populations base their decisions on precise data, such as the number of infected individuals (prevalence) [48–50], and those that consider more informal sources, such as conversations between people, public opinion, or media [51, 52]. Media sources include both traditional outlets like television and newspapers, as well as newer platforms like social networks. This distinction highlights the diversity in how behavioral factors are integrated into models, reflecting the varying degrees of reliability and influence these sources have on decision-making processes during an epidemic.

Regarding information quality and the negative effect of misinformation spreading within the population, an example is fear of vaccination [53]. Several works analyze its effects on the spread of infection [21, 54]. An example of how this phenomenon can occur is the case of an article originally published by a prestigious source. Although the thesis presented in this work [55], which claimed a correlation between measles, mumps, and rubella (MMR) vaccine and autism (as well as with gastrointestinal disorders), was later debunked by the scientific community and the article retracted, the negative impact in terms of spreading fear about vaccines has persisted. In many cases, this fear has become

deeply ingrained, leading to a reduction in herd immunity and a resurgence of measles [45].

4.2 Classification of different types of information

Another interesting aspect relates to the different types of information used as a basis for developing a new model. Choosing a specific type of information leads to the creation of distinct models that focus on different aspects of behavior. Some studies focus on the influence of media on behavior [49, 56], while others examine peer-to-peer conversations, information exchange, and individual beliefs [50]. These are completely different approaches, even though they aim to achieve the same effect: simulating the evolution of people's opinions and behavior. Incorporating media involves hypothesizing that the population is influenced by a few "central" information nodes, so the same news, data, or future predictions are shared with everyone. In contrast, models that use personal information exchanges can depict a scenario where many different ideas about the disease situation circulate simultaneously. Another concept used in models that simulate a sort of "collective consciousness" is referred to as "awareness" [57]. To model how awareness spreads in the population, that is often treated as a spreading disease [42, 44, 58–61]. Although there are many differences between the two, the main idea is that theories and concepts about a certain topic can spread among people, which can be considered at a higher level as a unified opinion. For example, there may be many different personal positions on how to respond to a health emergency like COVID-19, but it is possible to abstract the various opinions and reconstruct what the majority of people, or macro-groups, ultimately feel. They may either be more cooperative and in favor of following guidelines issued by authorities, or more focused on their well-being and inclined to act independently. This process can be related to opinion formation studies, which aim to understand how people build their ideas [24, 62] and also analyze the possible formation of opinion distributions, such as perfect consensus, consensus, polarization, clustering, or dissension.

4.3 How to integrate behavior in epidemiology

While the type and source of information are crucial for understanding the basic framework and synthesizing key concepts, the final criterion used to categorize works related to epidemiological behavior is *how* the influence of people behavior on the model is integrated. This aspect is the key focus of the literature reviewed for this thesis, as it plays a significant role in comparing and selecting relevant works to be used as basis for the present research.

There are various ways to describe behavior in response to an epidemic and integrate this aspect into epidemic models [18, 44, 63].

The first approach involves observing and simulating how the states of connected individuals are linked to specific behaviors and how this influences the epidemic. This category includes agent-based models. Additionally, the reverse relationship, where disease spread alters individual behavior, has also been considered, as discussed in [59].

There is also a broad class of mean-field models that explicitly consider the effects of behavior. In these cases, time-varying or state-varying parameters are used, resulting in a non-linear system of equations where the parameters are not constant but change based on information such as disease prevalence. Refer to Section 4.3.2 for further details on this topic.

Another possibility involves modifying the structure or connections in the network used to simulate disease evolution [64]. In network-based models, data extracted from social network structures [65] or small-world models [66] are often used to simulate connections between people more realistically.

In the following paragraphs, several articles are presented using this classification to simplify their categorization. Each article is then discussed in more detail, highlighting its original contribution.

4.3.1 Individuals-based models

Multiple networks simulated with Markovian process

To begin the presentation of individual-based models, the first category discussed is network simulations using Markovian processes. A notable example is the article by Granell et al. [59]. In this work, a multiplex model is implemented with two distinct connectivity layers: the physical layer, where the disease spreads, and the virtual contact layer, through which "awareness" about the disease diffuses. Awareness is in the knowledge about how to reduce the risk of infection, and diffuses through conversation or is due to becoming infected. The article then uses the Microscopic Markov Chain approach to simulate the interaction resulting from the coupling of the two layers. Interestingly, the authors observe the existence of a metacritical point for the onset of the epidemic, which depends on awareness dynamic and topology of the virtual network. There is, in fact, a parameter related to the ability to influence through communication and it impacts the onset of the epidemic only when it exceeds a certain threshold. A subsequent work by the same authors [42], considers also the effect of a global communication agent. In this case, the metacritical point disappears.

In the article by [67], there is a complete description of the stochastic process at the agent level, which is useful for understanding how agent interactions are modeled across different layers using a Markovian approach. Other works using this method include [58, 61, 64]. Here, a similar double-layer structure, composed of an SIR model coupled with an unaware-aware-unaware (UAU) process, is presented. To simulate the evolution of the complex structure resulting from the coupling of the two models, these works develop transition trees for all possible state changes and their respective transition probabilities. An example can be seen in Figure 4.2.

In [64], a slightly more complex situation is described, where two possible opinions – pro-physical distancing (P) and anti-physical distancing (A) – are considered. In contrast, [68] studies a simpler structure, where a SIS model is coupled with either adopting or not adopting self-protective measures.

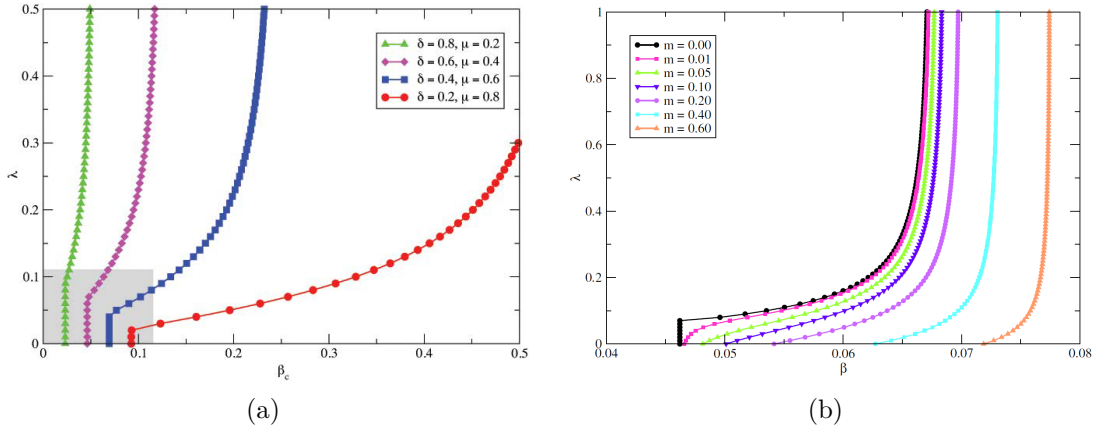


Figure 4.1: The effect of awareness communication on the onset of an epidemic is depicted in the studies by Granell et al. [42, 59]. In the first plot (a), the x-axis represents the minimum value of the transmission rate β that is necessary to trigger an outbreak, while the y-axis measures the level of awareness in the population, denoted by the parameter λ . The shaded region shows that below a critical threshold of λ , awareness has little to no impact on controlling the epidemic. However, once awareness exceeds this threshold, the value of β required for an outbreak increases significantly, indicating that the spread of awareness can effectively delay or prevent the epidemic. In contrast, in the second plot (b), a global communication agent, represented by the media parameter m , continuously influences the population. This parameter ensures that the awareness layer consistently impacts the epidemic dynamics, regardless of the value of λ , making it evident that a strong media presence can amplify the protective effects of awareness.

Interesting results derived from these works include:

- The observation of the influence of opinions on transmission speed and the final epidemic size [64].
- The effect on epidemic spreading of authoritative information, publicizing epidemic prevention processes, and encouraging reasonable behavior, such as isolating when infected [61].
- The importance of self-awareness as a mechanism to reduce disease prevalence [58].

The investigation conducted in [68] provide a stability analysis of a two-layer model that links the decision to use or not use self-protection measures with the disease state. The equilibria of the system are explicitly calculated, including the epidemic threshold. Figure 4.3 illustrates their simulations, where a parameter representing risk perception is varied. The study shows how this parameter influences the emergence of periodic oscillations and identifies the conditions that lead to global convergence towards such periodic solutions. This is a significant result, indicating that, during an epidemic, there is a collective behavioral response, and it specifies under what conditions the system stabilizes or further evolves.

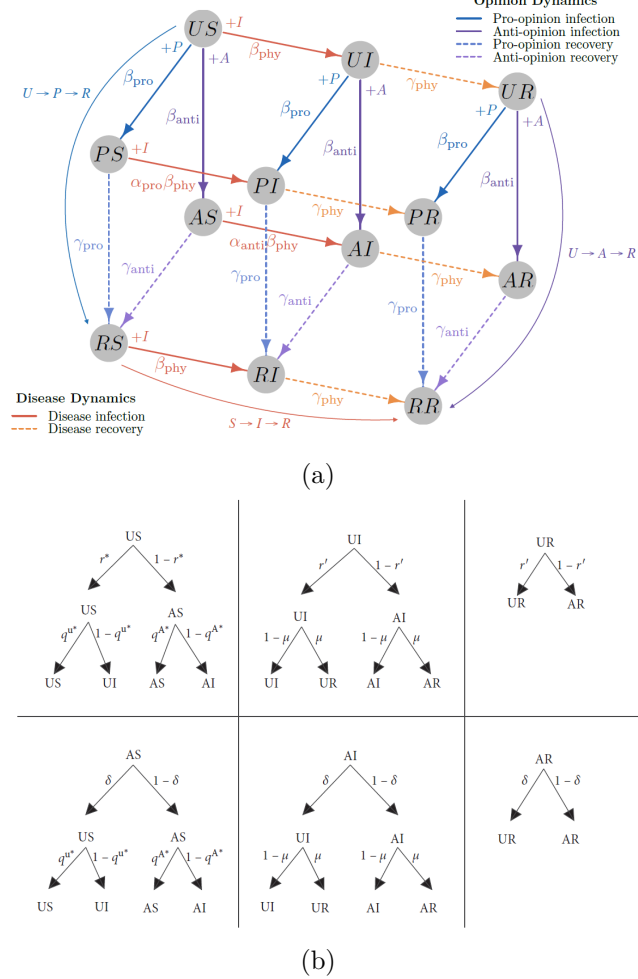


Figure 4.2: a) An example of a multi-layer network structure resulting from the coupling of a SIR and a uninformed-pro/anti physical distance-recovered (U-P/A-R) model. b) The transition trees realized to describe the system of a SIR coupled with a UAU model using a Markovian process. Figures taken from articles [58, 64].

Game theoretical models

In the probabilistic framework, another area involves the use of game theory principles. These are used to explore strategic interactions between individuals, where participants act to maximize their utility, potentially influencing the actions of others. The concept of Nash Equilibrium is also important in this context. It is defined as "a set of strategies such that no player has an incentive to unilaterally deviate from the present strategy" [18]. That is, the Nash Equilibrium leads individuals to adopt strategies consistent with their goal of maximizing their benefit or utility in a perfectly rational way, forming the best responses to one another.

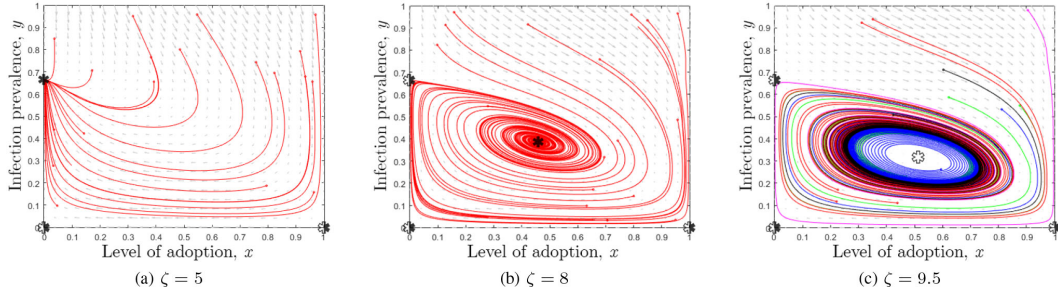


Figure 4.3: Simulations from the article [68] demonstrate the evolution of their model across various values of the risk perception parameter. In the visual representation, the x-axis shows the adoption level of precautionary measures, while the y-axis indicates the prevalence reached by the infection. The diagram highlights stable equilibria, saddle points, and unstable equilibria, which are marked with black, black-white, and white asterisks, respectively.

Many articles use this idea to model how populations adjust their behavior during an epidemic. One such example is [69], which focuses on the behavior of a population deciding between their sexual habits and the risk of HIV infection. The main result is derived by observing how population behavior changes as information about a possible vaccine spreads. Optimistic news lead to a decrease in the number of contacts, while pessimistic forecasts cause an increase in risky behavior, even at the same level of risk, as shown in Figure 4.4. A particularly interesting conclusion is that focusing public health messaging on dire forecasts may unintentionally lead to an increase in risky behavior.

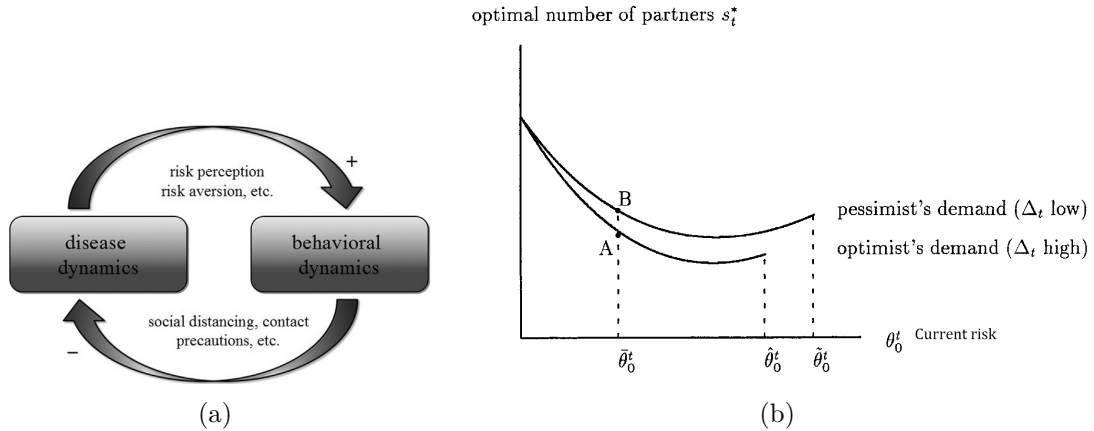


Figure 4.4: a) A representation of the feedback loop, taken from the article of [70], representing the trade-off between: advantages related to avoiding the disease and social cost of using precautions. b) The effect on people behavior due to optimistic or pessimistic forecasts is described in the illustration presented in [69]. The population tends to act more cautiously if there is hope that the situation will improve in the future.

A different focus is adopted in [71] which studies the behavioral change related to contact rates and especially social distancing, in the context of a pandemic like COVID-19, to understand the efficacy of policies for partial or full voluntarily contact reduction. The authors aim to obtain more insight into the percentage of adoption from the population of social distancing policies because increasing the quality of these estimations matters in the planning of strategies to handle a pandemic from a government point of view.

Another case study is [72], which defines different utility functions to model the trade-off between social well-being from maintaining connections, the fatigue of doing so, and the potential physical harm those connections may cause. The main results outlined in [72] confirm that a higher number of connections between individuals leads to greater disease transmission, resulting in more infections and a shorter epidemic duration. It also highlights that "the higher the (perceived) risks of a disease, the lower the net benefit of a tie, the stronger the social distancing, and consequently the smaller the epidemic size." Using this co-evolutionary approach, a highly correlated dynamics between the two layers emerges: a feedback loop between the spread of infection and behavioral adaptation, with structural modifications in the network occurring in the simulated scenarios. The introduction of network-based modeling further develops this work and leads to several key findings. First, including the benefit of social connection creates multiple transmission routes for the disease. Second, a reduction in the final epidemic size only occurs when the indirect benefits are relatively low and the costs of maintaining ties are high. Finally, small changes in social behavior can have large impacts on the epidemic. In the next paragraph, other similar studies that incorporate network models will be discussed. However, before that, a final case where the game-theoretical approach is often applied will be presented: vaccination. Many models examine the decision-making process behind vaccination, highlighting the trade-off between the benefits of getting vaccinated and the risks associated with it. In terms of modeling, the link between behavior and epidemic spread in this case is that individuals who choose vaccination are removed from the susceptible group, with a percentage reflecting the vaccine efficacy, thereby reducing the potential for disease transmission. In the study developed in [54], a feedback loop is established between disease prevalence and individual strategic vaccination behavior. Their model successfully fits vaccine coverage data from both pertussis and MMR vaccine fear and can also predict future trends in disease prevalence and vaccine coverage. Moreover, the article highlights the phenomenon for which the vaccine fear becomes more frequent as eradication goals for more vaccine-preventable diseases are approached.

Network based models

The inclusion of networks in the modeling process has gained popularity as a tool for scientists to enhance the accuracy of their models by simulating real-world connections between people. The main goal behind developing network-based models is to create a representation of society and then use it to simulate the spread of disease. A comprehensive example of this approach is presented in [40], where a method is introduced to simulate scenarios such as quarantine or regional barriers that limit population movement. By adjusting network connections—reducing contacts between nodes or cutting

ties between specific regions—these models effectively demonstrate the impact of interventions like lockdowns or travel restrictions on disease transmission. They also enable analysis of how containment measures affect the trajectory of an epidemic. Works such as [41] also fall into this category, utilizing urban mobility patterns as a proxy for modeling epidemics. Similarly, in [65], social networks are used as a proxy for connections, hypothesizing that people’s behavior in maintaining social contacts is analogous to how they might behave in the context of disease transmission. Another innovative approach involves the development of multilayer networks, such as in [66], where the social structure of a town is recreated. Each layer represents a different environment—ranging from homes to workplaces, distinguishing between various job types, and even considering a layer for friendships. Each individual exists across multiple layers and interacts with different groups depending on their social environment. This model found that the layer associated with friendship poses the highest risk for outbreak development, due to closer interactions and lower security measures.

Consequently, even on the friendship layer, a lower transmission rate (β) compared to other layers can result in a significant epidemic involving many susceptible individuals.

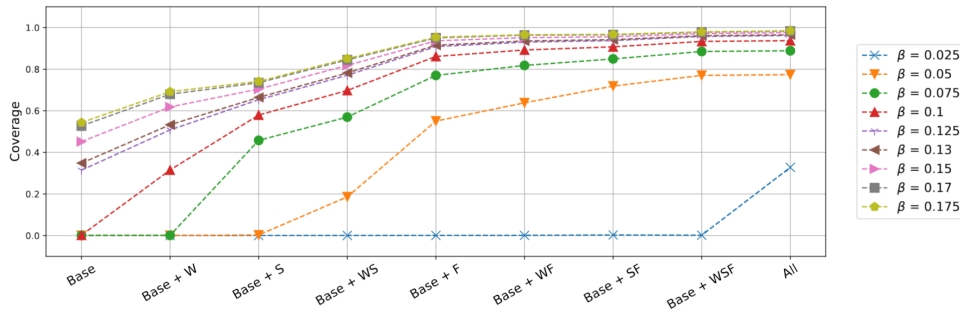


Figure 4.5: In the simulation presented in [66], a city is modeled with people divided into several social groups. The layer associated with friendships is where the disease outbreak occurs with the lowest value of the infectivity parameter, β .

Threshold models

Another possible mechanism for modeling how individuals change their actions is by observing the behaviors and opinions of their neighbors [25, 73]. A well-known theoretical tool for this context is the Watts threshold model [74], which is foundational for studying such transitions. In [44], various threshold models are discussed, including the Watts threshold, which is linear. In their model, each node is assigned a random threshold value based on a given distribution. The threshold represents the point at which a node changes its opinion when a certain number of its neighbors adopt a different behavior. The structure of the network is crucial for determining how opinions spread: opinion propagation is most favorable in networks with low randomness and a regular structure. Additionally, the authors analyzed the effects of network clusters, noting that well-connected clusters can act as opinion hubs, reinforcing the spread of opinions.

Ad-hoc rule-based models

The last category of individual-based models focuses on individuals acting according to specific rules designed to simulate particular situations. A clear example of this is found in [75], where disease propagation is modeled based on opinions for or against vaccination. The evolution of these opinions is determined by the interaction and exchange of ideas between agents and co-evolves alongside their health condition. A comprehensive set of rules is established to model all possible situations that lead to changes in both opinion and disease states. An example is visible in Figure 4.6.

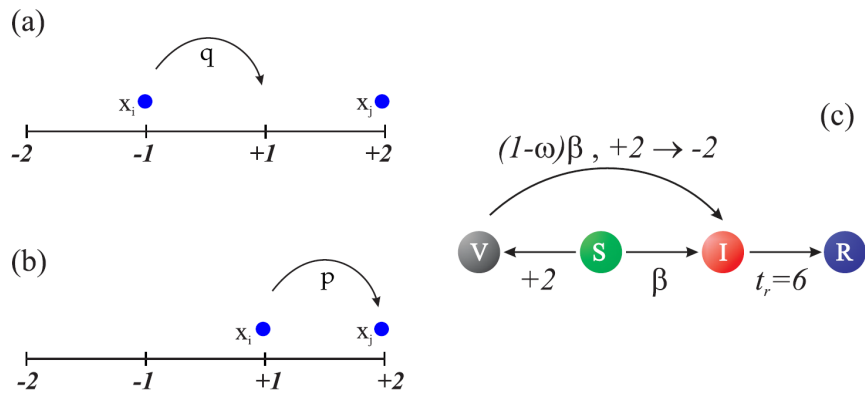


Figure 4.6: The Figure, taken from the article [75], illustrates the mechanisms underlying the model's dynamics. The figures on the left depict opinion dynamics: when two nodes have opposing opinions, one adjusts its state to match the other's opinion with a probability $q(a)$. If both nodes share the same opinion, the opinion is reinforced with a probability $p(b)$. The figure on the right represents contagion dynamics: a susceptible individual S (green) becomes infected (red) with a probability β and recovers (blue) after a time t_r . A susceptible individual can also become vaccinated V (grey) upon acquiring an opinion state of $+2$. However, they can still become infected with a probability $(1 - \omega)\beta$ - with ω the efficiency of the vaccine- which causes their opinion to shift to -2 .

A similar approach is developed in [20], where an explicit mechanism is implemented to govern the competition between different health opinions. Individuals with a positive + opinion may switch to the opposing - opinion after interacting with others, following a switch rate function. By varying the parameters of this function, its behavior can become linear, saturating, or sigmoidal similar to established functions used to describe predator responses to prey population density.

Finally, [49] extends the SEIR model by incorporating the effect of mass media on disease spread, using a specific set of functions. These functions account for disease prevalence, recovery rate, and media impact. The goal is to conduct a sensitivity analysis on the parameters influencing the epidemic peak magnitude, timing, and ending.

4.3.2 Homogeneous population models

This section presents the works that have most contributed to shaping the development of the thesis: mean-field models. The assumption that the population is homogeneously mixed results in models capable of describing phenomena nationwide, which is difficult to achieve when modeling individual behavior.

However, the effectiveness of this class of models relies heavily on the modeling principles applied. Models are powerful tools, but they represent the aspects the modeler chooses to emphasize. Therefore, selecting and integrating the most promising features is crucial for creating a useful instrument. By analyzing prior works, we gain insights into what has been previously explored and the outcomes achieved. The most interesting characteristics of various models are now presented, followed by an explanation of how they have contributed to the development of the model in this thesis.

The article [50] was one of the first studied for its interesting modeling approach. It integrates two dynamics: the epidemic evolution influences the parameters governing people behavior, and, conversely, the population behavior affects the spread of the disease. This bidirectional interaction allows for a more realistic simulation of how behavioral changes and disease dynamics influence each other. A SIR model is associated with an opinion dynamics that occurs only within the S compartment. This compartment is divided into four subgroups, representing different attitudes toward prophylactic behavior. In this way, more cautious individuals have a lower probability of becoming infected. The opinion dynamic focuses on the phenomenon of influence, modeled by a specific parameter, and on opinion amplification, a cognitive bias where confronting someone with the same belief strengthens that belief. The most interesting aspect of this work is the concept that opinion spreads through conversation, not through a utilitarian or contagion process like fear diffusion.

A similar hypothesis of social learning is explored in [76]. In this model, both risky and cautious behaviors coexist in the population and can be transmitted. The model also incorporates the effects of clustering and the phenomenon of "cultural bias." This bias suggests that the risky trait is more likely to be adopted by cautious individuals than the reverse. Additionally, the authors introduce the concept of uncertainty regarding the infection causes, meaning that people are unsure of the best way to behave to avoid contracting the disease.

In [77], compliance with the use of NPIs (Non-Pharmaceutical Interventions) is the central focus of the behavioral component of the model. In this case, non-compliance is modeled as a social contagion: the population is divided into two groups, compliant (c) and non-compliant (nc). Using the mass-action mixing property, compliant individuals become non-compliant, but there is no recovery once their status changes. The primary goal is to understand the interplay between the stringency of lockdown measures, non-compliant behavior, and the spread of the disease. Vaccine adoption and awareness diffusion are the main aspects considered in [78]. Awareness is present only in the Susceptible compartment, and there is a term, $M(t)$, that represents the accumulated density of awareness programs driven by various information sources. This term is influenced by several factors: awareness generated by neighboring individuals, the intensity of awareness

programs in response to the prevalence of the disease, and a waning effect due to the decreasing quality or effectiveness of the information over time. Their complete model and the interplay between disease and behavior is shown in Figure 4.7. An interesting aspect of this article is that the authors evaluate their model using data from the COVID-19 vaccination campaign in China. They observe how their model effectively reproduces the population behavior and government policies during different phases of the epidemic.

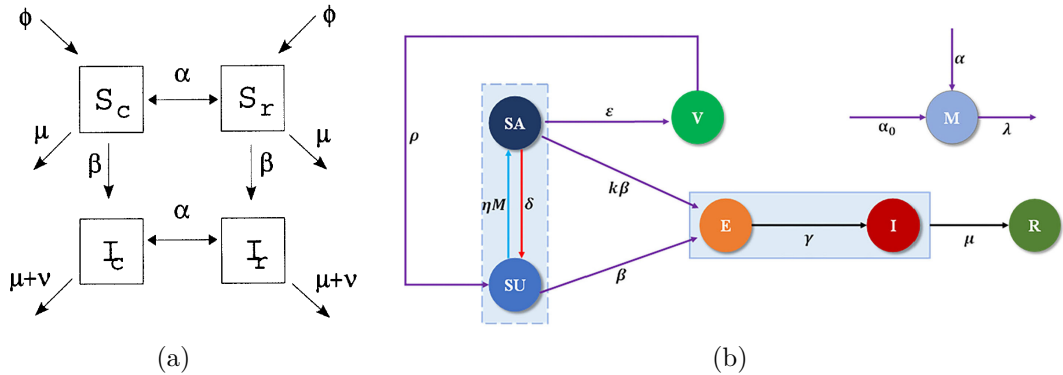


Figure 4.7: a) The model presented in [76] shows horizontal layers representing behavioral diffusion, while vertical layers represent disease spread. Behavior diffuses between both infected and susceptible individuals, but this is not depicted for visual clarity. b) The model developed in [78] incorporates behavior dynamics only in the susceptible (S) layer, influencing both contagion rates and the probability of vaccination. The M compartment, which is the accumulated density of awareness programs, follows its own dynamics, observing the state of the disease and the distribution of public opinion, and it influences the diffusion of awareness.

An interesting article about behavior and vaccines is [21]. In the proposed model, an initially susceptible population can split into two opposing compartments, depending on what they fear more: the disease or vaccination. The model includes six compartments, with the fear dynamics occurring only in the susceptible (S) compartment.

In this scenario, fear of vaccination can undermine outbreak control. Initially, people may get vaccinated, but they stop too early as their fears reverse. The study also conducts a sensitivity analysis on the contact rates for the two fears, showing that transmission speed significantly affects the model outcomes. The results range from multiple infection waves to complete disease extinction without an outbreak, depending on the conditions.

4.4 Perspective review of the literature

To conclude this chapter on the literature review, an evaluation of the models discussed is presented, with a focus on how they relate to the scope and aim of this thesis. This evaluation aims to explain the key insights gained from the literature and highlight also what are the differences and novelty introduced in this work.

4.4.1 Individual state models

Referring to the individual-based models presented in the Section 4.3.1, most of them face the challenge of developing complex simulations to model the evolution of disease and individual behavior, but struggle to scale these simulations to the nationwide level. In many cases, small groups of agents are used, such as the 50 nodes mentioned in [72], and even in works where a larger number of nodes is implemented, they typically are thousands [42], not millions, as would be necessary for national-scale modeling. To overcome this difficulty, some articles use mean-field approximations, considering the limit of an infinite population size and employing statistical approaches [68].

Another critical issue these models face is the need for large amounts of data to accurately represent how populations behave during unusual situations such as epidemic outbreaks. Without this data, it becomes difficult to draw precise conclusions from the models. While these models can still provide useful insights, their application for precise, real-world predictions remains limited. They are better suited as scientific tools for exploring theoretical scenarios rather than for offering actionable advice on a larger scale. An article that demonstrates the volume of data required to test a model with real-world scenarios is [79]. In this study, data from three different countries—Luxembourg, Austria, and Sweden—was collected, including information on total detected cases, hospitalized individuals, people in intensive care units (ICUs), and deaths. This comprehensive dataset was used to fit the model.

In the case of behavioral-epidemic models, even fewer data were available until the recent COVID-19 pandemic. As explained in [80], this lack of data was a significant challenge. However, it was partially addressed by implementing models based on population behavior with respect to influence. Despite these improvements, the availability of data today is certainly better, offering more robust insights. As written in [80] : *"The issue is that research has not yet provided empirical benchmarks for endogenous contact rates in disease scenarios, so it is unclear how such policies can be evaluated scientifically: ideally a policy is benchmarked against a set of counterfactuals given the disease, not compared with what was before the disease"*.

4.4.2 Well-mixed population models

As stated earlier in Section 4.3.2, a major critique of developing complex mean-field models is that, if they are not supported by consistent observation of the phenomena they aim to reproduce, their capacity to generate meaningful insights can be significantly limited. For this reason, developing a model using empirical data as reference, is one of the main objectives pursued in this thesis work. Comparing a model's emerging dynamics with real-world data can help assess the model's validity and its predictive capacity. Reading through works in this field, a common approach emerges for modeling systems that aim to incorporate two distinct dynamics, such as behavior and disease spread. Most of these models introduce additional compartments, which represent subgroups of homogeneously mixed individuals sharing common characteristics—typically, their disease state and course of action. The primary distinction lies in how modelers handle the flow between these compartments: while some works focus on the influence of behavior solely within

the Susceptible layer [21, 50, 78], others implement a full double-layer model [51, 76, 77]. Another key difference is whether the change in behavior dynamics is unidirectional, as in [77], or bidirectional, as seen in [21, 50, 76, 78], where individuals can adjust their actions in both directions.

Notably, some of the most influential aspects drawn from the literature for this thesis include the "double fear" structure developed by [21] and presented in 4.3.2, and the awareness element that influences behavior change, modeled through an external node $M(t)$ in [78], and seen in paragraph 4.3.2. Additionally, this thesis seeks to implement a fully coupled double-layer model for behavior and epidemic spread, incorporating elements such as memory waning and fatigue, which combine with conversational mechanisms to create bidirectional flows in the behavioral model. Unlike [76], which uses a simpler epidemic model, this work employs a more complex one to accurately reflect COVID-19 dynamics. Furthermore, the models developed in [51] and [81] share structural similarities with this thesis. However, [51] assumes faster information diffusion than disease transmission, decoupling the two layers, while [81] focuses on homophily and polarization of compartments—factors not considered here.

4.4.3 Final remarks

All the concepts presented in this chapter are useful for understanding the current state of epidemic behavior modeling and for explaining why the development of a new model was necessary for this thesis.

To summarize, the main features sought in a model are:

- Comparability to empirical data collected during a real epidemic, both for the disease and the behavioral layer.
- In a mean-field system, the ability to model disease incidence, peer pressure between individuals with different behaviors, fatigue in maintaining certain habits, and the possibility to modify these dynamics by introducing a mean-field intervention, such as government actions, to encourage the transition to more compliant behavior.
- Not using awareness as a factor in the model, as it is too abstract and difficult to observe or measure within a population; instead, focusing on behavior dynamics and peer-to-peer imitation based on which behavior appears more convincing.
- Exclusion of vaccination dynamics, as it is a well-known aspect and, in the case of COVID-19, vaccines were only available on a large scale after more than a year.

All these characteristics have been incorporated, and the following chapter explains how the model was developed and how these features were integrated.

Part II

Behavioral-Epidemiological Model

Chapter 5

Model development and justification

Because the main contribution of this thesis is the development of a new multi-system model, understanding the reasons that led to its development is crucial. Otherwise, the reader might question: "Why not use an already developed and analyzed model?"

The primary answer lies in the observation made while studying the literature: the connection between empirical data and epidemiological models is often missing. Most works relating social and epidemiological aspects are purely theoretical models based on ad-hoc assumptions; probably, because constructing a framework grounded in empirical data related to individual behavior is challenging [72], and, until the COVID-19 pandemic, data on this topic were scarce.

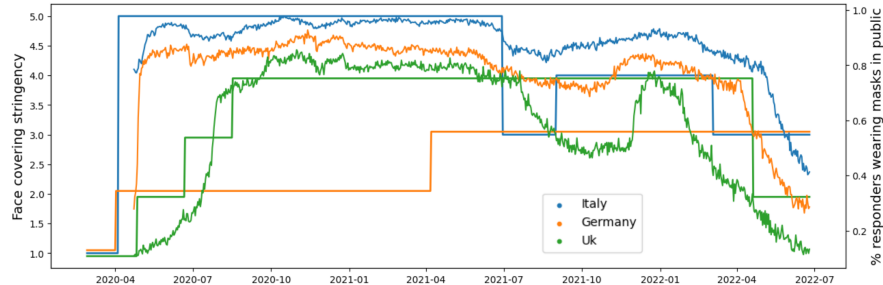


Figure 5.1: The evolution of mask wearing behaviors during the COVID-19 pandemic. Figure from [82].

The availability of research such as the one conducted by Meta during the COVID-19 pandemic [83] serves as a major source of inspiration and data. This research allows exploration of different behaviors related to how people react to and manage the necessity of living with an infectious disease. It also provides this valuable information as a dynamic time series.

Often, what emerges from this data is the non-linear dynamic evolution of behavior. While many models do not incorporate this characteristic [84], this feature is here addressed.

The behavioral-epidemic mean-field model we developed aims to interconnect these two features, linking the theoretical framework with empirical evidence. Often, in other works, this connection is realized using proxy models that attempt to reconstruct agent behavior, spatial motion, or opinion datasets extrapolated, for instance, from social networks, as done in [85, 86]. The problem with these approaches is that people's opinions do not always align with their actual behaviors, and the lack of a necessary and direct correlation between the two is another concept the model attempts to overcome.

For example, consider the evolution of mask-wearing behavior in different European countries during the COVID-19 pandemic, as shown in Figure 5.1. It is immediately evident that, at a certain point, there is a sharp increase in the use of this self-protective device, resembling a step function. This effect results from regulatory prescriptions introduced by authorities, and behaviors closely follow the evolution of these stringency measures.

Such phenomena have been incorporated into the model development using a coefficient parameter, ψ , to represent the effect of centralized interventions and modify the basic persuasion rate of different behaviors. Additional empirical evidence supporting the development of the model can be found in [82].

To introduce the model and begin its description, the next chapter first presents and analyzes the two layers that together form the complete model: a SIRS epidemic model and a behavioral model consisting of three compartments: Compliant, Against, and Heedless. Then, the full model is presented, described and analysed in Chapter 7. Then the full model is presented, described and analysed. The full model comprises seven compartments, as the heedless behavior is not possible for individuals that are infected or recovered. This assumption stems from the reasoning that it is highly improbable for an individual to act heedlessly when infected (unless, potentially, when completely asymptomatic).

Infection can be transmitted across all three behavioral groups, but the Compliant group is more cautious. A parameter, ρ , models their reduced probability of being infected, while another parameter, ϵ , accounts for their compliance with self-isolation while infectious. This reduces the number of infected Compliant individuals (I_C in the model equations that will be presented in the next chapter 7) contributing to new infections in the epidemic layer.

Behavior is "transmitted" through peer-to-peer influence with strength parameters ($k_i, i = 1, \dots, 6$), with i the number of compartments either Compliant or Against, and fatigue parameters (λ_i) are included to model the dropout rate caused by the difficulty of maintaining a certain behavior over time.

For the epidemic components of the model, classical coefficients are used: β (transmission rate), γ (recovery rate), and δ (immunity waning rate).

Chapter 6

Epidemic model and Behavioral model alone

To develop a multi-system model that combines an epidemiological layer with a behavioral one, we first present the dynamics of each layer independently. We briefly introduce the SIRS model, focusing primarily on the reasons for its selection. Then, the Heedless, Compliant, Against behavioral model is introduced, simulated, and analyzed. Understanding the underlying dynamics of this model is crucial for gaining insight into the complex interactions that emerge within the multi-system model.

6.1 SIRS model

To describe the epidemic evolution, a SIRS model is implemented. It is an extension of the most famous SIR discussed in Section 3.3.1. Its main addition is the possibility for individuals to become again susceptible after a certain period of time beyond the end of the infection due to waning immunity. There are four main characteristic parameters in this model:

- β is the transmission rate parameter for person-to-person contact.
- γ is the recovery rate.
- δ is the rate at which immunity wanes following recovery.
- \mathcal{R}_0 is the reproduction number, similar conceptually to the one presented in SIR model, but function of β , γ , and also δ .

A SIR-like model is chosen because of its ability to describe diseases like COVID-19; the literature provides numerous examples that use this model [28, 87]. The SEIR model could also be a viable choice due to the relevance of the "Exposed" compartment, which effectively captures the disease progression for infections such as COVID-19. In these cases, an incubation period occurs after exposure before symptoms appear and the individual becomes contagious. However, this compartment was excluded because it has been

shown [28] that a simpler SIR model can still accurately represent the disease dynamics. When comparing model simulations with real data, a delay can be incorporated to account for the lag between symptom onset, testing, and reporting. This delay reflects the time needed for symptoms to manifest, conduct testing, and report cases to relevant authorities. The differential system of equations describing the model are

$$\begin{cases} \frac{ds}{dt} = -\beta si + \delta r \\ \frac{di}{dt} = \beta si - \gamma i \\ \frac{dr}{dt} = \gamma i - \delta r \end{cases} \quad (6.1)$$

with $s(0) = s_0 > 0$, $i(0) \geq 0$ and $r(0) = 0$. The mass conservation assumption holds so $s(t) + i(t) + r(t) = 1$. The model includes the possibility of reinfection, which is important when studying long-term scenarios. Considering the effect of individual behavior on disease progression, two critical phases are hypothesized to influence this evolution: the initial stages of the epidemic and the period following the first peak.

In the initial stages, the SIRS model behaves similarly to a typical SIR model, because reinfection is unlikely to occur in a short time frame. However, over time, as reinfections become possible, individual attitudes and behaviors increasingly impact the disease spread.

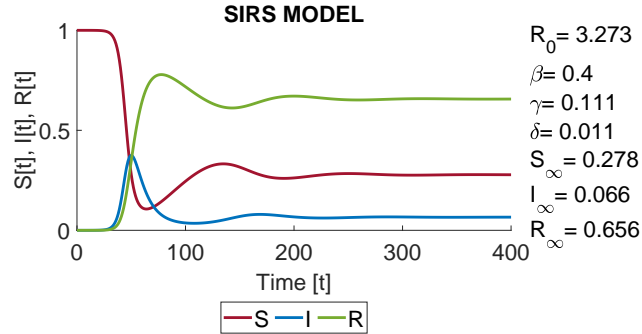


Figure 6.1: Simulation of the SIRS model. The parameters of the model, which meaning is presented in section 3.3.1, are chosen to resemble those of the initial stages of the COVID-19 pandemic [88] and are the same as those used for simulations with the full epi-behavioral model.

6.2 Behavioural model

The development of the behavioral model builds on several works already presented in the literature. In particular, the following mechanisms are considered to be the most relevant:

- The competition between two opposing behaviors/opinions, driven by peer pressure [21]. The implementation is inspired by the Unaware-Aware-Unaware opinion model

class [64, 78] (refer to Section 4.3.1 and 3.3.2), for how the compartments are linked together and for the idea of social pressure between individuals.

- Non-compliance viewed as a form of social contagion [77].
- The fatigue mechanism, due to which maintaining a certain behavior for long leads to a spontaneous loss of compliance [21].

To integrate all these aspects into a mean-field model, the first step is to define the compartments used to segment the population. The population is divided into three compartments: Heedless, Compliant, and Against, denoted respectively as H, C, and A. The meaning of each compartment is as follows:

H: Individuals who behave without much regard for guidelines and are careless about the risks associated with the infection.

C: Individuals who actively seek to avoid becoming infected or spreading the virus by following guidelines and taking precautions.

A: Individuals who do not consider the infection a risk to their safety and do not use protection or modify their behavior during the epidemic. They disregard risk-mitigating guidelines and do not align with safer behaviors as the epidemic unfolds.

Initial conditions

As an initial condition, the hypothesis is that most of the population is in the Heedless compartment. This assumption is based on the idea that when a new disease emerges, it is poorly understood, and the population has limited information about it. The hypothesis is that people in the Heedless compartment may be clueless about the risks of becoming infected. This lack of knowledge causes them to maintain their usual behavior, making them susceptible to infection. This assumption is also supported by data and literature [89]. As an example of this initial configuration, the case of COVID-19 in Italy is considered. In the early stages of its spread, when the disease was primarily affecting China, it was not viewed as a significant threat by most of the population in Western countries. It was perceived as a distant issue affecting a faraway nation. Therefore, when the epidemic reached Europe and Italy, both the population and the government were caught off guard. There was an initial delay in the implementation of countermeasures, as well as in the dissemination of reliable information about the disease progression to the general public.

In addition, there are two opposing behavioral groups, which in the initial phase of the dynamic comprise a small fraction of the population: Compliant and Against.

The Compliant group actively seeks to reduce their chances of becoming infected or infecting others. They adopt self-protection measures such as wearing face masks, sanitizing their hands, and voluntarily limiting their presence in public spaces to reduce contact with others.

In contrast, the Against group consists of individuals who, for personal reasons—such as anti-scientific beliefs, low trust in policymakers, or other concerns—do not take action to minimize their chances of infection or the possibility of infecting others. This category encompasses phenomena such as:

- vaccine denial;
- misinformation spread;
- denial of the existence of the disease;
- distrust of doctors and government policies.

The inclusion of the Against compartment stems from the fact that, especially in the early stages of a new disease outbreak, there is often a lack of reliable knowledge. As documented by [90], this can lead to the spread of false beliefs in the population. It has also been demonstrated [91] that misinformation, especially when associated with fear, can have lasting effects. A notable example is the belief that the measles, mumps, and rubella (MMR) vaccine can cause developmental disorders in children. Despite the fact that the original publication making this claim has been scientifically discredited [55], this idea remains popular and has contributed to a rise in vaccine skepticism [91].

Social contagion dynamic

The evolution of the model is governed by two principal mechanisms:

- Heedless individuals transition to either Compliant or Against compartments.
- Compliant and Against individuals return to the Heedless compartment.

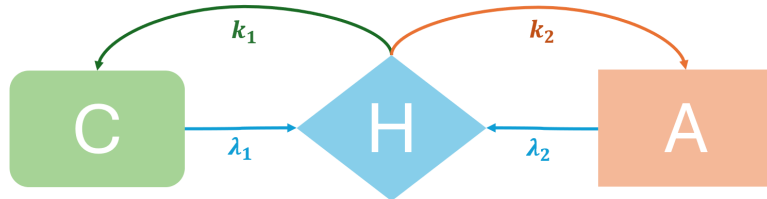


Figure 6.2: The figure visualizes the developed behavioral model, featuring three compartments: Heedless, Compliant, and Against, abbreviated as H , C , and A . The arrows indicate the inflows and outflows between these compartments.

The first mechanism is driven by peer pressure: the size of each group and its level of persuasiveness are the parameters that govern this process. It is mathematically modeled similarly to person-to-person disease transmission, as seen in the SIR-like mean-field model described in Section 3.3.1. Instead, the return to the Heedless compartment is modeled as a spontaneous decay process: individuals naturally leave the Compliant and Against compartments and return to Heedless, transitioning spontaneously depending on the level of fatigue associated with maintaining the behavior. The flow between an intermediate compartment, represented by H , rather than a direct transition between A and C (and vice versa), is a modeling choice stemming from the idea that heedlessly can, when a new disease appears, signify lack of awareness about it. Over time, it can represent

instead the state of people after a period of coexistence with the disease, where the fatigue of maintaining compliance increases, or when indifference toward the disease grows. To describe these transitions, different coefficients are introduced. The k_1 and k_2 are persuasion rates, while λ_1 and λ_2 represent fatigue rates. Their meanings are as follows:

- k_1 : persuasion rate from Heedless to Compliant;
- k_2 : persuasion rate from Heedless to Against;
- λ_1 : rate at which the Compliant behavior is abandoned due to fatigue;
- λ_2 : rate at which the Against behavior is abandoned due to fatigue.

The resulting differential equations describing the model dynamic are:

$$\begin{cases} \dot{H} = -k_1 HC - k_2 HA + \lambda_1 C + \lambda_2 A \\ \dot{C} = k_1 HC - \lambda_1 C \\ \dot{A} = k_2 HA - \lambda_2 A \end{cases} \quad (6.2)$$

We assume population conservation, meaning that the relationship $H + C + A = 1$ holds. Additionally, the initial conditions described in the previous section are translated as follows:

$$\begin{cases} H(0) = 1 - C_0 - A_0 \\ C(0) = C_0 > 0 \\ A(0) = A_0 > 0 \end{cases} \quad (6.3)$$

Behavior conversion number

To simplify the understanding of the system underlying dynamics, an analogy can be drawn with the reproduction number in epidemic models. By examining the system equations (6.2), a relationship can be identified. From both the second and third equations, we can isolate the two coefficients (specifically k_1, λ_1 , and k_2, λ_2) and derive a new parameter, called "Behavior Conversion Rate", \mathcal{B} . This rate is the result of the ratio between the persuasion rate and the fatigue decay rate, and can be viewed as a measure of the transmission potential of social contagion. The general formula to calculate it is:

$$\mathcal{B}_i = \frac{k_i}{\lambda_i} \quad \text{with } i = 1, \text{ or } 2. \quad (6.4)$$

In the model presented here, \mathcal{B}_1 represents the Behavior Conversion Rate associated with the Compliant compartment, while \mathcal{B}_2 , is associated with the Against compartment. The results of different numerical simulations are now displayed to demonstrate how the relationship between these two values influences the evolution of social contagion.

6.2.1 Model simulation

To represent different dynamics, four main cases are now presented. The coefficient values have been set appropriately to highlight different interesting situations in which the system can evolve.

I case: $\mathcal{B}_1, \mathcal{B}_2 < 1$, $\mathcal{B}_1 > \mathcal{B}_2$, and $\lambda_1 > \lambda_2$.

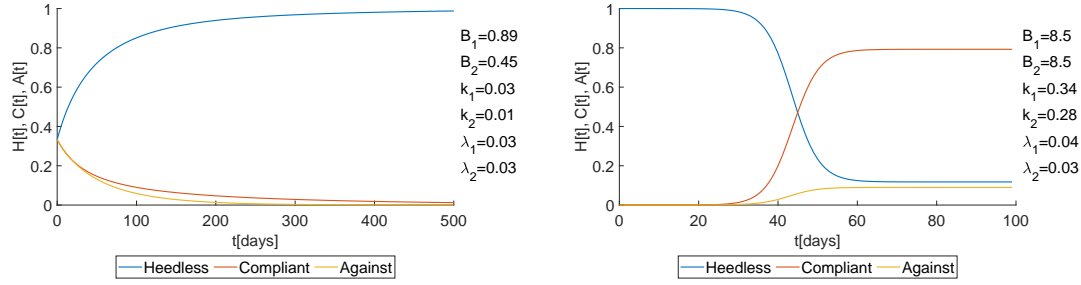
II case: $\mathcal{B}_1, \mathcal{B}_2 > 1$, $\mathcal{B}_1 = \mathcal{B}_2$, and $\lambda_1 < \lambda_2$.

III case: $\mathcal{B}_1, \mathcal{B}_2 > 1$, $\mathcal{B}_1 > \mathcal{B}_2$, and $\lambda_1 = \lambda_2$.

IV case: $\mathcal{B}_1, \mathcal{B}_2 > 1$ and $\mathcal{B}_1 > \mathcal{B}_2$, and $\lambda_1 < \lambda_2$.

The values k_1 and k_2 can be calculated from the formula of \mathcal{B}_1 and \mathcal{B}_2 .

Figure 6.3a shows that, when both Behavior conversion numbers are less than one, social contagion does not spread: even though, in this case, the Compliant and Against compartments together represent 60% of the total population at the beginning of the simulation, they clearly tend to zero over time. In contrast, Figure 6.3b shows the case where the two \mathcal{B} values are equal and greater than one. To emphasize the importance of the relations between fatigue and persuasion rate, it is shown that, even if the conversion numbers are equal, (i.e. k_2 is lower than k_1), the Compliant compartment becomes the majority group by the end of the simulation. Here the Against do not tend to zero, but there is a rather constant flow between the Compliant and Against compartments, through the Heedless state, such that none of the compartments becomes empty.



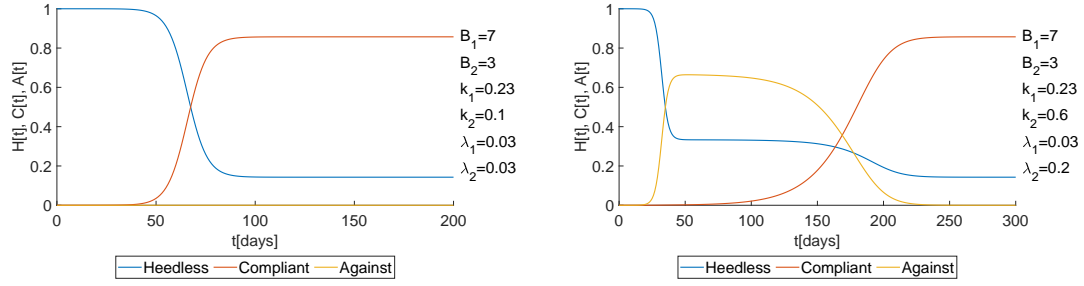
(a) $\mathcal{B}_1, \mathcal{B}_2 < 1$, $\mathcal{B}_1 > \mathcal{B}_2$, and $\lambda_1 > \lambda_2$.

(b) $\mathcal{B}_1, \mathcal{B}_2 > 1$, $\mathcal{B}_1 = \mathcal{B}_2$, and $\lambda_1 < \lambda_2$.

Figure 6.3: Behavioral system dynamics first two cases (I and II). In the left panel there is the case in which both $\mathcal{B}_1, \mathcal{B}_2$ are less than one. The system tends to an equilibrium in which all individuals tends to the H state. In the right panel, instead the case in which the conversion number are equal, but because $k_1 > k_2$ the Compliant variable becomes greater than the Against one.

Figure 6.4 illustrates two other interesting scenarios. On the left, we observe the dynamics when one of the \mathcal{B} values is greater than the other, and both λ values are the same: the variable with the largest \mathcal{B} becomes dominant. It is straightforward to

understand that this dynamic would also occur if, with the same values of \mathcal{B} , the λ of the dominant behavior were greater than the other, as a larger λ would be compensated by a higher k (persuasion rate). The right panel, however, presents a particularly intriguing situation. Here, $\lambda_1 < \lambda_2$, combined with $k_2 > k_1$, leads to an initial rapid spread of the Against group, even though $\mathcal{B}_2 < \mathcal{B}_1$! It is only after some time that the system evolves to the final equilibrium, which is the same as in the left scenario, as the \mathcal{B} values are the same in both simulations.



(a) $\mathcal{B}_1, \mathcal{B}_2 > 1$, $\mathcal{B}_1 > \mathcal{B}_2$, and $\lambda_1 = \lambda_2$. (b) $\mathcal{B}_1, \mathcal{B}_2 > 1$ and $\mathcal{B}_1 > \mathcal{B}_2$, and $\lambda_1 < \lambda_2$.

Figure 6.4: Behavioral system dynamics: the second two cases (III and IV). In the left panel, the scenario depicts Compliant becoming the dominant group, while Against gradually tends toward zero. In the right panel, with the same value for the conversion number but a higher persuasion rate for Against compared to Compliant, the system converges to the same equilibrium as in the left figure. However, it first goes through a phase where the Against group becomes dominant.

6.2.2 Equilibrium and stability analysis

To enhance our understanding of the system, equilibria are computed and their stability is studied. As observed, the system equilibrium values vary according to parameter values. Specifically, the coefficients were combined to produce two Behavior conversion numbers, \mathcal{B}_1 and \mathcal{B}_2 . One way to identify and visualize the system equilibria for a specific parameter set is through nullclines, used in an autonomous system of differential equations (DE) to sketch the phase plane of the system. In a system of two DE:

$$\frac{dx}{dt} = f(x, y) \quad (6.5)$$

$$\frac{dy}{dt} = g(x, y) \quad (6.6)$$

there are two types of nullclines: x -nullcline, and y -nullcline. The x -nullcline is the set of points in the phase plane so that $\frac{dx}{dt} = 0$, and graphically can be represented as a set of vectors that go either straight up or down. Instead, the y -nullcline is the set of points

for which $\frac{dy}{dt} = 0$. In these points the vectors are horizontal, going either to the left or to the right.

The original system of three equations, (6.2), has been reduced, to better visualize nullclines in a two-dimensional graph, by using the population conservation assumption: $1 = H + C + A$. By substituting the A term as $A = 1 - H - C$, it is obtained a system of two equations with two unknowns:

$$\begin{cases} \dot{H} = -k_1 HC - k_2(1 - H - C)H + \lambda_1 C + \lambda_2(1 - H - C) \\ \dot{C} = k_1 HC - \lambda_1 C \end{cases}$$

To simplify the readability and use a notation more familiar for plotting, H, C have been substituted with respectively x, y . So, the equations become:

$$\begin{cases} \dot{x} = -k_1 yx - k_2(1 - y - x)x + \lambda_1 y + \lambda_2(1 - y - x) \\ \dot{y} = k_1 yx - \lambda_1 y \end{cases} \quad (6.7)$$

The nullclines can be calculated by imposing $\dot{x} = 0$ and $\dot{y} = 0$. For the first nullcline, with $\dot{x} = 0$,

$$y = \frac{x(k_2 - k_2 x + \lambda_2) - \lambda_2}{x(k_2 - k_1) + \lambda_1 - \lambda_2} \quad (6.8)$$

and for the second, with $\dot{y} = 0$,

$$x = \frac{\lambda_1}{k_1} = 1/\mathcal{B}_1 \quad \text{or } y = 0.$$

The existence condition for the first nullcline can be calculated, imposing that the denominator must not be equal to zero:

$$x \neq \frac{\lambda_2 - \lambda_1}{k_2 - k_1}$$

This value can be in the interval $[0,1]$ only if $\lambda_2 > \lambda_1$ and $k_2 > k_1$, or $\lambda_2 < \lambda_1$ and $k_2 < k_1$. The second nullcline instead, always exists if $k_1 \neq 0$.

Equilibria of the system

The equilibrium value can be computed as the intersection point of the two nullclines, from equation (6.8). In fact if $x = \frac{\lambda_1}{k_1}$, then $y = 1 - \frac{\lambda_1}{k_1}$. Instead if $y = 0$, two values are found: $x = 1$, and $x = \frac{\lambda_2}{k_2}$. The three equilibria, indicated as Eq_1, Eq_2 , and Eq_3 , are then:

- $Eq_1 = (\frac{\lambda_1}{k_1}, 1 - \frac{\lambda_1}{k_1})$
- $Eq_2 = (1, 0)$
- $Eq_3 = (\frac{\lambda_2}{k_2}, 0)$

Equilibria stability analysis

To assess the local stability of the equilibrium points, the Routh-Hurwitz criterion is applied, requiring the Jacobian matrix of the system evaluated at each equilibrium. The equilibrium is locally stable if:

- the trace of the Jacobian is negative: $\text{tr}(J) < 0$
- the determinant of the Jacobian is positive: $\det(J) > 0$

The Jacobian of the system (6.7) is

$$J = \begin{bmatrix} -k_1y - k_2 + k_2y + 2k_2x - \lambda_2 & -k_1x + k_2x + \lambda_1 - \lambda_2 \\ k_1y & k_1x - \lambda_1 \end{bmatrix} \quad (6.9)$$

The trace of J is

$$\text{tr}(J) = -k_1y - k_2 + k_2y + 2k_2x - \lambda_2 - \lambda_1 + k_1x \quad (6.10)$$

Its determinant is instead

$$\det(J) = k_2\lambda_1 + \lambda_1\lambda_2 + 2k_1k_2x^2 - k_1k_2x - k_1\lambda_2x - 2 \cdot k_2\lambda_1x + k_1\lambda_2y - k_2\lambda_1y \quad (6.11)$$

For each equilibrium point, stability conditions can be expressed as relationship between the coefficients k_1 , k_2 , and λ_1 , λ_2 .

Stability of equilibrium $Eq_1 = (\frac{\lambda_1}{k_1}, 1 - \frac{\lambda_1}{k_1})$. The trace $\text{tr}(J(Eq_1)) = -k_1 + \frac{\lambda_1}{k_1}(k_1 + k_2) - \lambda_2$ is less than zero, if $-k_1 + \frac{\lambda_1}{k_1}(k_1 + k_2) - \lambda_2 < 0$. From this we obtained the relation:

$$\frac{\lambda_1}{k_1} < \frac{k_1 + \lambda_2}{k_1 + k_2}$$

Some algebraic manipulations allow us to rewrite this inequality as $k_1(k_1 - \lambda_1) > \lambda_1k_2 - k_1\lambda_2$. Instead, the determinant is $\det(J(Eq_1)) = k_1\lambda_2 - \lambda_1\lambda_2 - k_2\lambda_1 + k_2\frac{\lambda_1^2}{k_1}$. The determinant is greater than zero if

$$k_1^2\lambda_2 + k_2\lambda_1^2 - k_1k_2\lambda_1 - k_1\lambda_1\lambda_2 > 0.$$

Namely, $k_1\lambda_2(k_1 - \lambda_1) - k_2\lambda_1(k_1 - \lambda_1) > 0$, or equivalently $(k_1 - \lambda_1)(k_1\lambda_2 - k_2\lambda_1) > 0$. However, when both factors are negative, the condition on the trace cannot be verified; in fact, the expression $k_1(k_1 - \lambda_1) > k_2\lambda_1 - k_1\lambda_2$, would require a negative term to be greater than a positive one, which is never possible. Conversely, both factors being positive is equivalent to the two conditions $B_1 > 1$ and $B_1 > B_2$. These two conditions satisfy both the inequality for the determinant and the inequality for the trace.

In conclusion, equilibrium Eq_1 is locally stable if $B_1 > 1$, and $B_1 > B_2$.

Stability of equilibrium $Eq_2 = (1, 0)$. Calculating the Jacobian determinant at this point yields the expression $\det(J(Eq_2)) = -k_2\lambda_1 + \lambda_1\lambda_2 + k_1k_2 - k_1\lambda_2$. By grouping terms and analyzing the inequality necessary to satisfy the Routh-Hurwitz criterion, this simplifies to $k_1(k_2 - \lambda_2) - \lambda_1(k_2 - \lambda_2) > 0$, which further reduces to $(k_1 - \lambda_1)(k_2 - \lambda_2) > 0$. This inequality is satisfied if both terms in the product are either positive or negative:

- Case I : $k_1 > \lambda_1$, and $k_2 > \lambda_2$
- Case II : $k_1 < \lambda_1$, and $k_2 < \lambda_2$

Evaluating the trace at this point, the result is $\text{tr}(J(Eq_2)) = k_2 - \lambda_2 - \lambda_1 + k_1 < 0$. Rearranging terms gives the condition $k_1 + k_2 < \lambda_1 + \lambda_2$, which is true only under Case II identified above. Thus, it can be concluded that equilibrium point B is locally stable only if $\frac{k_1}{\lambda_1} < 1$, and $\frac{k_2}{\lambda_2} < 1$, which correspond to $\mathcal{B}_1 < 1$, and $\mathcal{B}_2 < 1$.

Stability of equilibrium Eq_3 $Eq_3 = (\frac{\lambda_2}{k_2}, 0)$. The determinant at this point is given by $\det(J(Eq_3)) = k_2\lambda_1 - \lambda_1\lambda_2 + k_1\frac{\lambda_2^2}{k_2} - k_1\lambda_2 > 0$. Also here, rearranging terms simplifies the inequality to: $k_2[\lambda_1 - \lambda_1\frac{\lambda_2}{k_2} + k_1\frac{\lambda_2^2}{k_2} - k_1\frac{\lambda_2^2}{k_2}] > 0$, $k_2[\lambda_1(1 - \frac{\lambda_2}{k_2}) - k_1\frac{\lambda_2}{k_2}(1 - \frac{\lambda_2}{k_2})] > 0$, which further reduces to:

$$k_2 \left[\left(\lambda_1 - k_1 \frac{\lambda_2}{k_2} \right) \left(1 - \frac{\lambda_2}{k_2} \right) \right] > 0$$

To satisfy the inequality both terms inside the parenthesis must have the same sign, as in the previous point Eq_2 :

- Case I : $\frac{k_2}{\lambda_2} > \frac{k_1}{\lambda_1}$, and $k_2 > \lambda_2$
- Case II : $\frac{k_2}{\lambda_2} < \frac{k_1}{\lambda_1}$, and $k_2 < \lambda_2$

The trace value is given by:

$$\text{tr}(J(Eq_3)) = -k_2 + k_2 \frac{\lambda_2}{k_2} + k_1 \frac{\lambda_2}{k_2} - \lambda_1 < 0,$$

leading to the inequality:

$$\frac{\lambda_2}{k_2}(k_1 + k_2) < k_2 + \lambda_1,$$

which simplifies to:

$$\frac{\lambda_2}{k_2} < \frac{k_2 + \lambda_1}{k_1 + k_2}.$$

Only by choosing Case I, we ensure that the trace inequality is satisfied, otherwise we obtain a condition impossible to verify such as in the Eq_1 case.

Therefore, it can be concluded that equilibrium Eq_3 is stable if $\mathcal{B}_2 > \mathcal{B}_1$ and $\mathcal{B}_2 > 1$.

6.2.3 Equilibrium simulations

Based on the equilibrium analysis, we now understand how the model behaves with various parameter values. To confirm these results, nullcline plots for the four previously simulated cases are generated, and the different scenarios are examined. First, it is important to describe what can be visualized in the nullcline plot. The blue curve is the expression found solving the x-nullcline, and the vertical line in the plot correspond to the point of discontinuity of this expression, as discussed before. The green line is instead the

y-nullcline, composed of a vertical and a horizontal line, representing the two possible solutions. In purple the three equilibria points are visualized. If stable, they are marked with a diamond, will unstable with a circle. The values of coefficients used in the five cases are:

	B_1	$\lambda_1 [d^{-1}]$	B_2	$\lambda_2 [d^{-1}]$
case I	0.89	1/30	0.45	1/40
case II	8.5	1/25	8.5	1/30
case III	7	1/30	3	1/30
case IV	7	1/30	3	1/5
case V	0.6	1/20	4	1/30

Variables k_1 and k_2 are derived using the expression $\mathcal{B}_i = k_i/\lambda_i$, where $i = 1, 2$.

I case: $\mathcal{B}_1, \mathcal{B}_2 < 1$, $\mathcal{B}_1 > \mathcal{B}_2$, and $\lambda_1 > \lambda_2$.

If both the Conversion numbers are less than one, there is only one equilibrium in the phase plane, where both Compliant and Against are zero.

In the Figure 6.5a, the nullcline plot shows an intersection between the two nullclines only at the point (1,0). Under this condition, the only equilibrium is at $H = 1$, with both A and C equal to zero. Using the notation from the system equation (6.7), this corresponds to $x = 1$ and $y = 0$. Calculating the trace and determinant of the Jacobian at this point yields $\text{tr}J(1,0) = -\frac{209}{12000}$ and $\det J = \frac{121}{2400000}$. Thus, the equilibrium is locally asymptotically stable, as it satisfies the Routh-Hurwitz condition.

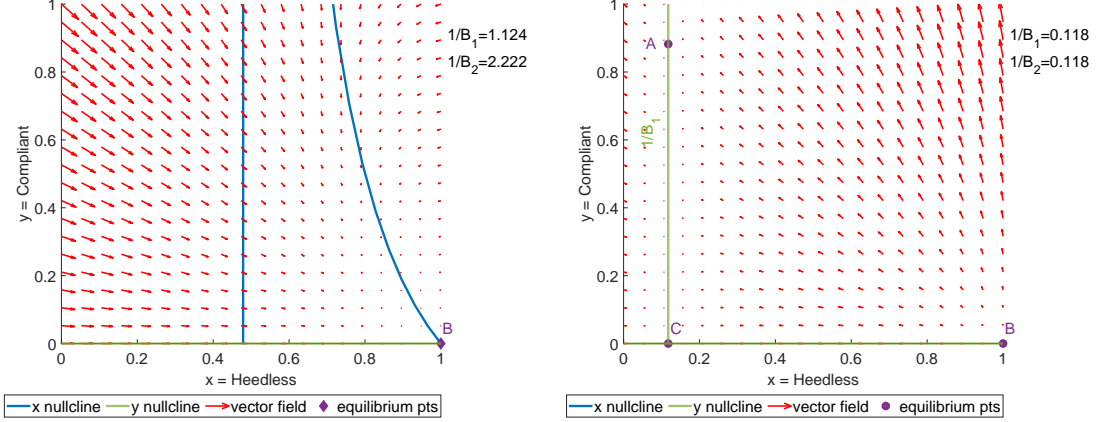
II case: $\mathcal{B}_1, \mathcal{B}_2 > 1$, $\mathcal{B}_1 = \mathcal{B}_2$, and $\lambda_1 < \lambda_2$.

This second situation is the most complex to analyze. Due to the equal value of the two influence processes, the asymptotic value of the state variables cannot be determined solely by the previously established relations but also depends on the initial conditions.

The Heedless density at the equilibrium can still be determined as previously discussed, and the same value is obtained for both $x = \lambda_1/k_1$ and $x = \lambda_2/k_2$. Thus, the final equilibrium value of x is $\bar{x} = 0.12$. Also the equilibrium (1,0) is possible, but is certainly unstable with the parameter value considered in this case. As it can be seen from the system evolution in Figure 6.3, and nullcline plots of Figure 6.5, at the equilibrium \bar{x} , the Against and Compliant sums up to $y+z = 1-\bar{x}$ part, where y represent Compliant and z Against. The ratio between A and C depends on the initial conditions. Applying the Routh-Hurwitz criterion does not yield information on this equilibrium because the Jacobian determinant equals zero. An explanation for this is that, given the equilibrium alignment of points A and C and the equality of their conversion numbers, the influxes and outfluxes between the Compliant and Against compartments balance. Consequently, the system evolution is influenced by the initial numbers of Compliant and Against individuals, and once the system reaches the equilibrium value of Heedless, it remains in this configuration.

III case: $\mathcal{B}_1, \mathcal{B}_2 > 1$, $\mathcal{B}_1 > \mathcal{B}_2$, and $\lambda_1 = \lambda_2$.

In this scenario, as shown in Figure 6.6, there is an intersection between the two nullclines, at the point 0. The equilibrium has coordinates $x_{Eq_1} = \lambda_1/k_1$ and $y_{Eq_1} = 1 - \lambda_1/k_1$, derived by solving the nullcline expressions as previously described. $\text{tr}J(\bar{x}, \bar{y}) = -23/105$,



(a) $\mathcal{B}_1, \mathcal{B}_2 < 1$, $\mathcal{B}_1 > \mathcal{B}_2$, and $\lambda_1 > \lambda_2$. Point B , corresponding to Eq_2 is the stable equilibrium

(b) $\mathcal{B}_1, \mathcal{B}_2 > 1$, $\mathcal{B}_1 = \mathcal{B}_2$, and $\lambda_1 < \lambda_2$. There is not a stable equilibrium in this case.

Figure 6.5: Nullclines plots of the first two situations analyzed: In (a) the case in which both $\mathcal{B}_1, \mathcal{B}_2 < 1$. (b) is the phase plane representation when $\mathcal{B}_1 = \mathcal{B}_2 < 1$.

and $\det J(\bar{x}, \bar{y}) = 2/525$, so the equilibrium is locally asymptotically stable and the solution converges to it regardless of the initial conditions.

IV case: $\mathcal{B}_1, \mathcal{B}_2 > 1$ and $\mathcal{B}_1 > \mathcal{B}_2$, and $\lambda_1 < \lambda_2$.

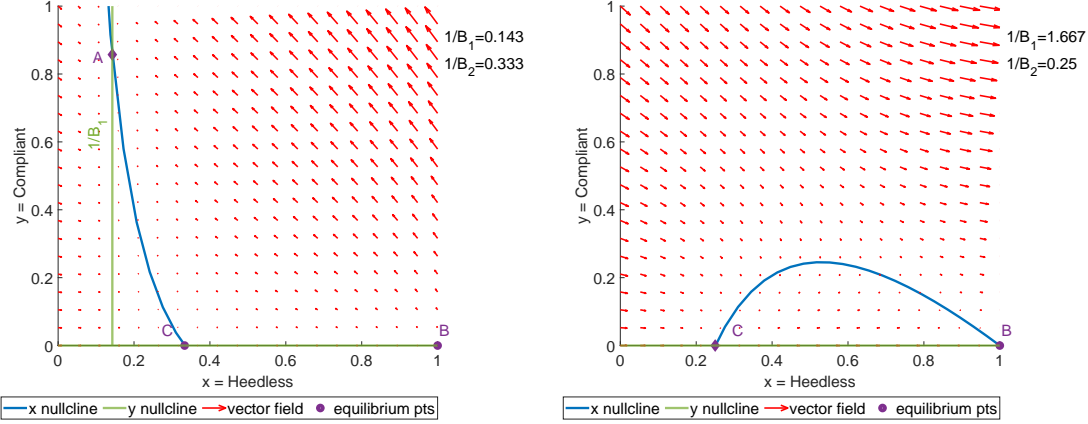
In this situation, the equilibrium has the same value, as in III case, and also the stability condition are verified. However, the nullcline plot is very different as shown in Figure 6.7. In fact, looking at the model simulation in Figure 6.4, the system initially evolves to what seems as a first equilibrium, corresponding to $x_{Eq_3} = \lambda_2/k_2$, $y_{Eq_3} = 0$. However, this equilibrium is unstable (as verified with the Routh-Hurwitz criterion), and so the model continues its evolution until it reaches the locally stable equilibrium.

V case: $\mathcal{B}_1 < 1$ $\mathcal{B}_2 > 1$, $\mathcal{B}_1 < \mathcal{B}_2$.

The system's evolution shows opposite behavior compared to the third case, with the Compliant, tending to zero at equilibrium. The right panel of Figure 6.6, shows two intersections in the phase plane at points Eq_2 and Eq_3 . At both points, $y = 0$, but only point Eq_3 is locally stable, as it satisfies the Routh-Hurwitz conditions. The equilibrium point is calculated as $x_{Eq_3} = \lambda_2/k_2$ and $y_{Eq_3} = 0$.

6.2.4 Behavioural model: numerical experiments

To better understand all possible scenarios emerging from the behavioral model, a set of simulations is conducted. Four vectors are defined, one for each model parameter,



(a) $B_1, B_2 > 1$, $B_1 > B_2$, and $\lambda_1 = \lambda_2$. The point A, (E_{q1}) is the stable equilibrium.

(b) $B_1 < 1, B_2 > 1$ and $B_2 > B_1$. Point C, corresponding to E_{q3} is the stable equilibrium.

Figure 6.6: Nullclines plots of the third and fifth cases: in (a) $B_1 > B_2$ and the phase plane arrows point to A equilibrium. In (b), where $B_1 < B_2$, the stable equilibrium is in point B, where there is no Compliant.

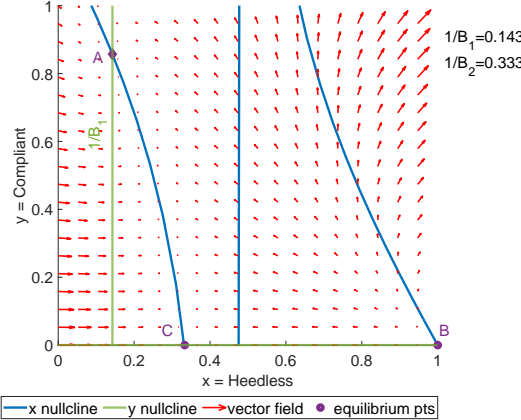


Figure 6.7: IV case of nullcline simulation. A point (corresponding to E_{q1}) is the locally stable equilibrium.

and a separate simulation is performed for each parameter combination. During each simulation, the parameter values remain constant. The variation range for each parameter is as follows:

- k_1 between 0.1 and 0.99
- k_2 between 0.1 and 0.99
- λ_1 between $1/2$ and $1/40 d^{-1}$
- k_1 between $1/2$ and $1/40 d^{-1}$

varied with twenty equally spaced steps. The resulting $\mathcal{B}_1, \mathcal{B}_2$ have a range spanning between 0.5, and 29.7. These ranges are chosen based on the assumption that the "fatigue" rate realistically spans between two and forty days, a range supported by prior research, such as the study in [92]. For the behavior persuasion rate (k_1, k_2), both low and high values for transition rates are included. We observe the dynamics across all states, recording key metrics for each simulation, such as the final compartment values, peak values, and the time of peak occurrence. Additionally, for generating the sensitivity plots, the Conversion number derived from the coefficient combinations in equation (6.4) are applied.

Heat map: asymptotic state values

Figure 6.8 shows heat maps of the final value reached by the various variables, for varying \mathcal{B}_1 and \mathcal{B}_2 . The threshold effect observed in the stability analysis performed earlier is clearly visible. While one of the reproduction ratios becomes larger than the other, the population is composed of the dominant group from either C and A and plus a number of Heedless individuals. The larger are \mathcal{B}_1 and \mathcal{B}_2 , and the more distant from 1 is their ratio, the smaller is the equilibrium fraction of the Heedless. Considering Figure 6.8a, until $\mathcal{B}_1 > \mathcal{B}_2$ Compliant behavior is dominant. Then, in the area of the heat map where the conversion number $\mathcal{B}_1, \mathcal{B}_2$ are similar (which correspond to the diagonal clearly visible) the two groups have similar density. Finally, when \mathcal{B}_1 becomes smaller than \mathcal{B}_2 , the Compliant abruptly tend to zero. This threshold effect can also be observed in Figure 6.9.

The plots show how, for a fixed values of λ_1, λ_2 and k_2 , the equilibrium value of the variables changes when varying the k_1 coefficient. To highlight the threshold effect due to the comparison of reproduction rates, the x-axis reports \mathcal{B}_1 , which can be calculated knowing the value of λ_1 and k_1 . For the same reason, different \mathcal{B}_2 are considered.

The threshold effect is clearly visible here as well. When examining the final values for the Compliant and Against variables, it is evident that once the \mathcal{B}_1 reproductive coefficient becomes dominant, the increase in the final size observed in the Compliant variable results from a decrease in the Against variable.

Heat map of peak values

We consider the peak values reached by the Compliant and Against variables. Figure 6.10 illustrates the maximum value reached by the Against variable. Instead, Figure 6.11 shows the evolution of Against, in different simulations where k_1, k_2, λ_1 are kept constant, and different λ_2 are considered. In both Figures, two situations are compared: in the first, $k_1 \sim k_2$, while in the other the difference between the two parameters is higher. Figure 6.10 shows three possible situations:

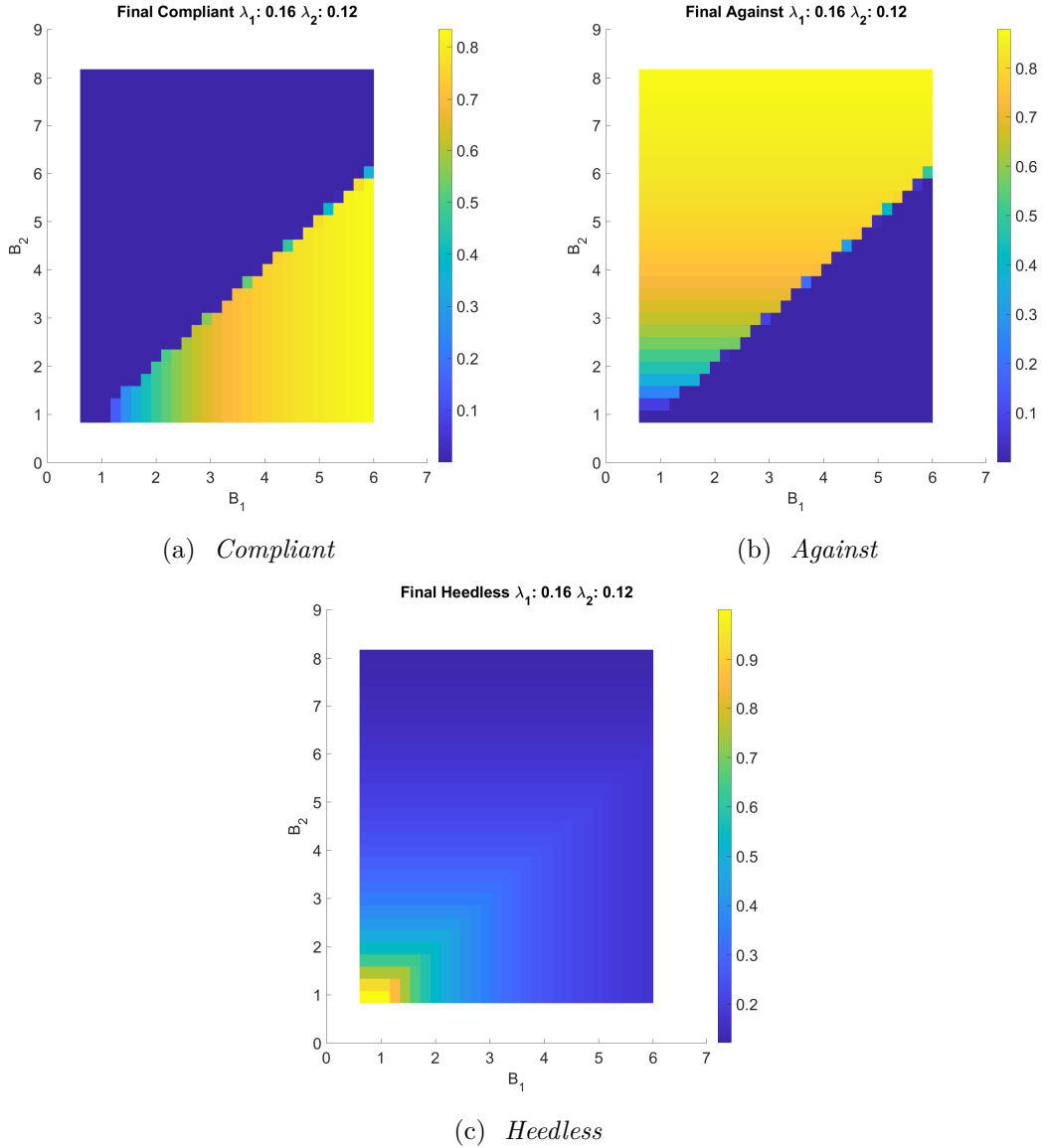


Figure 6.8: The asymptotic value reached at the equilibrium by the variables in the behavioral model.

- $B_2 > B_1$, and the maximum value corresponds to the value at the Equilibrium. It is the bottom right part of the picture.
- $B_2 < B_1$, but $\lambda_2 > \lambda_1$. These cases are located on the diagonal threshold of the heat map, and are the situations in which there is first a peak of A , but then C is the dominant group at the equilibrium.
- $B_2 < B_1$ and also $\lambda_2 < \lambda_1$. Here there is no peak, and A tends always to zero, or

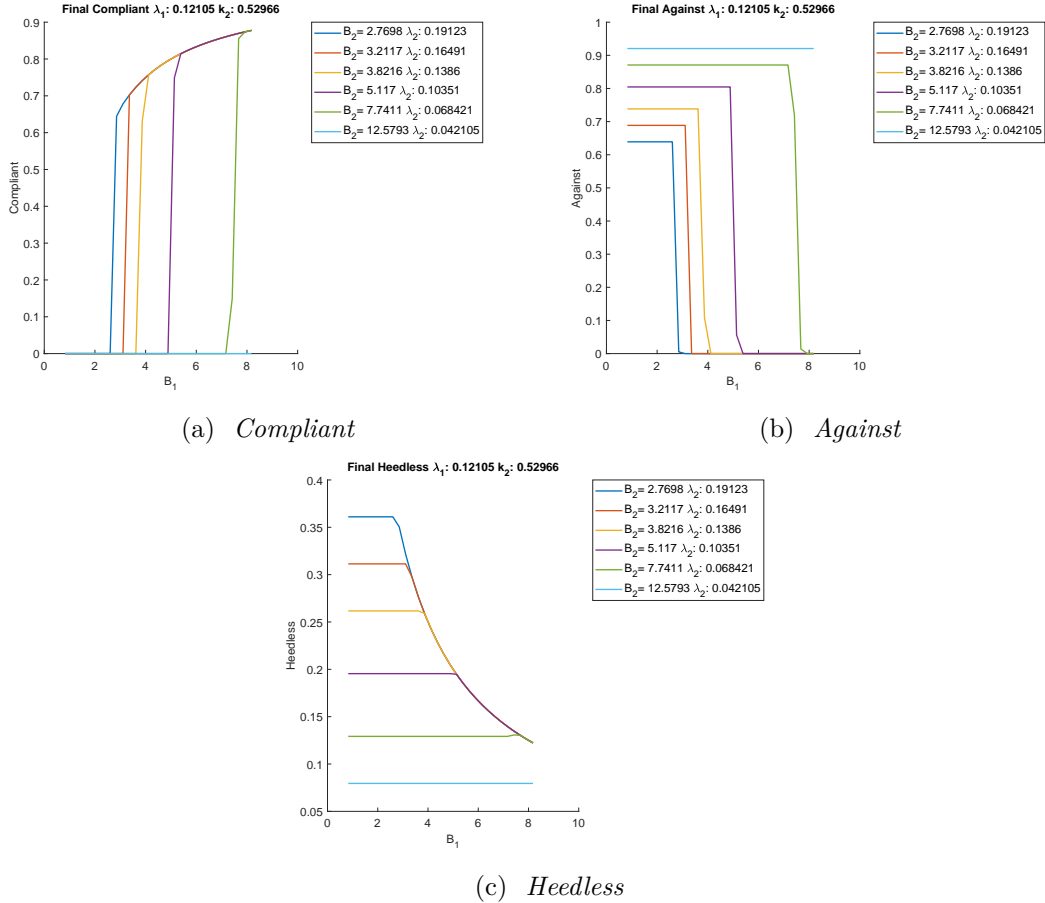
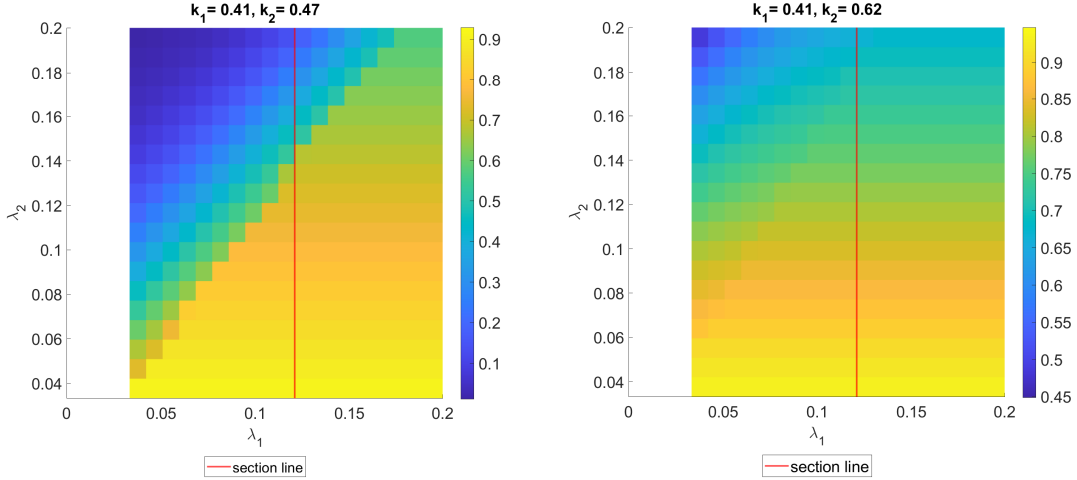


Figure 6.9: The asymptotic value reached at the equilibrium by every variable in the behavioural model as a function of B_1 for different B_2 values.

remain approximately zero, depending on the initial conditions. It is the top left part of pictures.

In Figure 6.10a, $k_1 \sim k_2$, and the heatmap clearly shows the threshold effect when B_1 becomes larger than B_2 . The transition of the peak value is not as abrupt as the one shown in Figure 6.8, as it reflects scenarios where there is a peak of A before reaching the asymptotic value. These scenarios are similar to those presented in Case IV of the simulation discussed earlier in Section 6.2.3. Figure 6.11a illustrates examples of scenarios that follows this change in the dynamics: depending on the considered value of λ_2 , the evolution of A varies. In certain scenarios, A becomes dominant, while in others, it shows a peak and then tends toward zero.

Figures 6.10b, 6.11b represent the situation with $k_2 \gg k_1$. Here the Against is always dominant for every combination of λ_1, λ_2 . The red vertical line, called "section line" in Figure 6.10, represents the part of the heat map, with the same parameters values used in the simulation in Figure 6.11.



(a) Maximum value of the Against variable with $k_1 \sim k_2$ (b) Maximum value of the Against variable with $k_1 < k_2$

Figure 6.10: The peak value of Against variable varying the λ_1, λ_2 .

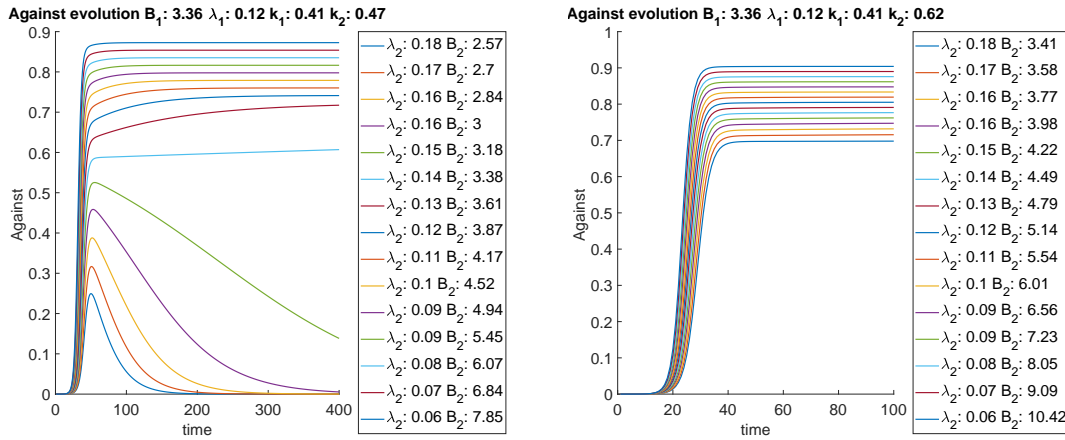


Figure 6.11: The evolution of the Against variable, fixing k_1, λ_1 , and k_2 and varying only λ_2 .

Conclusions

In this chapter, we have introduced the SIRS model and conducted an in-depth study of the behavioral model. We have outlined the modeling choices underlying its design and analyzed the system's possible evolutions both analytically and through simulations.

The key findings from the behavioral model analysis are as follows:

- For a behavior to spread within the population, its transmission rates, k_i , must exceed the fatigue associated with maintaining it, λ_i , (with $i = 1, 2$). This condition translates into requiring the reproduction conversion number to be greater than one, $\mathcal{B}_i > 1$.
- When two opposing behaviors coexist in the same system, if both have $\mathcal{B}_i > 1$, the behavior with the higher \mathcal{B}_i value becomes dominant asymptotically, while the other behavior diminishes to negligible levels.
- If the two behaviors have the same \mathcal{B}_i value, the initial proportions of Compliant and Against individuals in the population determine the final distribution, as the influxes and outfluxes between the compartments tend to balance each other.
- A behavior may have a lower reproduction conversion number, \mathcal{B}_i , than the other, yet exhibit a higher k_i and λ_i . For example, consider the case where $k_1 = 0.1$, $\lambda_1 = 0.01$, and $k_2 = 0.3$, $\lambda_2 = 0.15$. The corresponding conversion numbers are $\mathcal{B}_1 = \frac{k_1}{\lambda_1} = 10$ and $\mathcal{B}_2 = 2$. In this scenario, the system does not immediately converge to the behavior associated with \mathcal{B}_1 . Instead, due to the higher transmission rate k_2 , behavior 2 initially spreads at the expense of behavior 1. Over time, however, behavior 2's high fatigue cost (λ_2) leads individuals to abandon it in favor of behavior 1, which is less attractive but also much less hard to sustain. This situation can be interpreted as a transitory popular trend, where a rapidly adopted behavior eventually gives way to a more stable alternative.

The insights gained here form the foundational toolkit required to accurately interpret the results arising from coupling the SIRS model with the behavioral model. In the next chapter (7), we present the design and the results of this coupling.

Chapter 7

Behavioral-epidemic model

7.1 Model description

The newly developed model in this thesis, the Susceptible-Against-Heedless-Compliant-Infected-Recovered (SAHCIR) model, combines both epidemic and behavioral components, establishing an innovative approach to disease modeling. This model aims to bridge the epidemiological and social dynamics of an outbreak, integrating empirical observations to compare model outcomes with real-world data, as discussed in the article [82]. While some existing models combine these aspects, such as the one presented in [51], they often rely on predefined assumptions about specific behaviors rather than direct empirical basis.

The SAHCIR model incorporates a variety of behavioral stances towards safety measures, reflecting both proactive (pro-precaution) and non-compliant (anti-precaution) attitudes. The model also recognizes that, particularly during an epidemic's initial phase, a significant portion of the population may not follow safety measures—not out of skepticism, but due to a lack of awareness about the severity of the outbreak. Additionally, the model allows for government intervention through parameters that influence the spontaneous transition rate from the "Against" to the "Compliant" group, mirroring real-world public health policies aimed at promoting preventive behaviors.

This model thus provides a more empirically grounded framework for understanding the interplay between public health dynamics and social behaviors, filling a gap in the literature by providing a model designed for direct confrontation with real-world data rather than solely hypothetical scenarios.

The model is composed of two layers coupled together: a disease layer, describing the evolution of an epidemic, and a behaviour layer describing the transition among different behaviours during the epidemic development. The behavioral layer has three possible compartments, as seen in Chapter 6.2: Heedless, Compliant, and Against.

H: Heedless, people careless of the risk associated with the infection;

C: Compliant, people that want to avoid becoming infected or infecting others

A: Against, people who not see the epidemic as a risk and do not use protections or change their behaviour during the epidemic.

In the model, behavioral dynamics are combined with a SIRS epidemic model to create seven distinct, mutually exclusive compartments that capture both disease states and behavioral responses. The Heedless behavior can only be adopted by individuals who are susceptible to infection. This reflects the assumption that when a new disease emerges, individuals lack sufficient information and, consequently, they behave "normally," without adopting safety measures.

As people transition through stages of infection and recovery, the model assumes they can gain awareness of the disease's risks and recognize the importance of infection prevention. Thus, after infection or recovery, it is considered unrealistic for them to remain Heedless. Non-heedless individuals are divided into two categories: Compliant, those who adopt behaviors to minimize further spread, and Against, who are aware but do not actively prevent transmission, possibly due to personal beliefs or low risk perception.

Overall, we can recognize the following compartments:

S_H : Susceptible Heedless, the group where there is the majority of the population at the beginning of an epidemic. There is not much information about disease-associated risk and therefore the people in this compartment have no fear of becoming infected and do not modify their behaviors.

S_C : Susceptible Compliant, the group composed of those who actively avoid becoming infected and use non-pharmaceutical interventions to limit the possibility of getting sick and of spreading the contagion.

S_A : Susceptible Against, the people that do not comply with the recommendations provided by media or authority. They do not consider the threat represented by the disease and do not respect the safety rules or recommended behavior to avoid getting sick or infecting others.

I_C : Infected Compliant, people infected by the virus. This group receives infections coming from both S_C and S_H compartments, because it is considered that even those who have a "neutral" opinion about the risk associated with the infection change their minds when they become infected. The main behavior associated with this group is that safety measures such as quarantine are respected, which limits disease spread.

I_A : Infected Against, compartment composed of the Against Susceptibles who became sick. They do not respect self-isolation, and spread the disease.

R_C : Recovered Compliant, compliant people that are healed from the infection and contribute to raising awareness about the risk associated with the disease.

R_A : Recovered Against, against people that are healed from the infection. The most radicalized can be in this group. They are protected by immunity from a disease from which they do not believe of needing protection.

The resulting system is described by the following system of differential equations:

$$\begin{cases} \dot{S}_H = -\psi k_1 S_H \cdot C - k_2 S_H \cdot A + \lambda_1 S_C + \lambda_2 S_A + \delta(1 - \phi) R_C - \beta S_H \cdot I \\ \dot{S}_C = \psi k_1 S_H \cdot C + \delta \phi R_C - \lambda_1 S_C - \beta \rho S_C \cdot I \\ \dot{S}_A = k_2 S_H \cdot A - \lambda_2 S_A - \beta S_A \cdot I + \delta R_A \\ \dot{I}_C = \beta \rho S_C \cdot I + \beta S_H \cdot I + \psi k_3 I_A \cdot C - \lambda_3 I_C - k_4 I_C \cdot A + \lambda_4 I_A - \gamma I_C \\ \dot{I}_A = \beta S_A \cdot I - \psi k_3 I_A \cdot C + \lambda_3 I_C + k_4 I_C \cdot A - \lambda_4 I_A - \gamma I_A \\ \dot{R}_C = \gamma I_C - k_6 R_C \cdot A + \lambda_6 R_A + \psi k_5 R_A \cdot C - \lambda_5 R_C - \delta R_C \\ \dot{R}_A = \gamma I_A + k_6 R_C \cdot A - \lambda_6 R_A - \psi k_5 R_A \cdot C + \lambda_5 R_C - \delta R_A \end{cases} \quad (7.1)$$

where

- $A = S_A + I_A + R_A$ is the total fraction of Against individuals.
- $C = S_C + I_C + R_C$ is the total fraction of Compliant individuals.
- $I = \epsilon \cdot I_C + I_A$ is the fraction of infected people contributing to spreading the infection.
- ψ is a parameter that represents an increased (if its value is larger than 1) incentive to transition to the Compliant group. It can be regarded as an intervention from an external mean-field global agent.
- ϕ is a normalized parameter, used to split the population while re-entering in the susceptible class in the Headless or Compliant group.
- ρ is the protection factor of Compliant people that reduces their risk of becoming infected.
- β is the infectivity rate associated with the disease.
- γ is the recovery rate.
- δ is the rate at which immunity wanes (so that recovered people become susceptible again).
- ϵ specifies the fraction of compliant infected that participate in the infection process.

7.2 Basic reproduction number calculation

The first analysis that can be performed on the Behavioral Disease model is to compute its basic reproduction number. It is defined as the spectral radius of the next-generation matrix. Using the method outlined in [93] and now briefly described, this quantity is calculated. To distinguish between this value, that is related to the whole model, and is thus influenced by both the social and epidemic layer, and the classic epidemic only Reproduction number, described in Section 3.3.1, we denote this quantity with the symbol E_0 . It is the "Epidemic reproduction number". Consider $x = (x_1, x_2, \dots, x_n)^T$ a vector

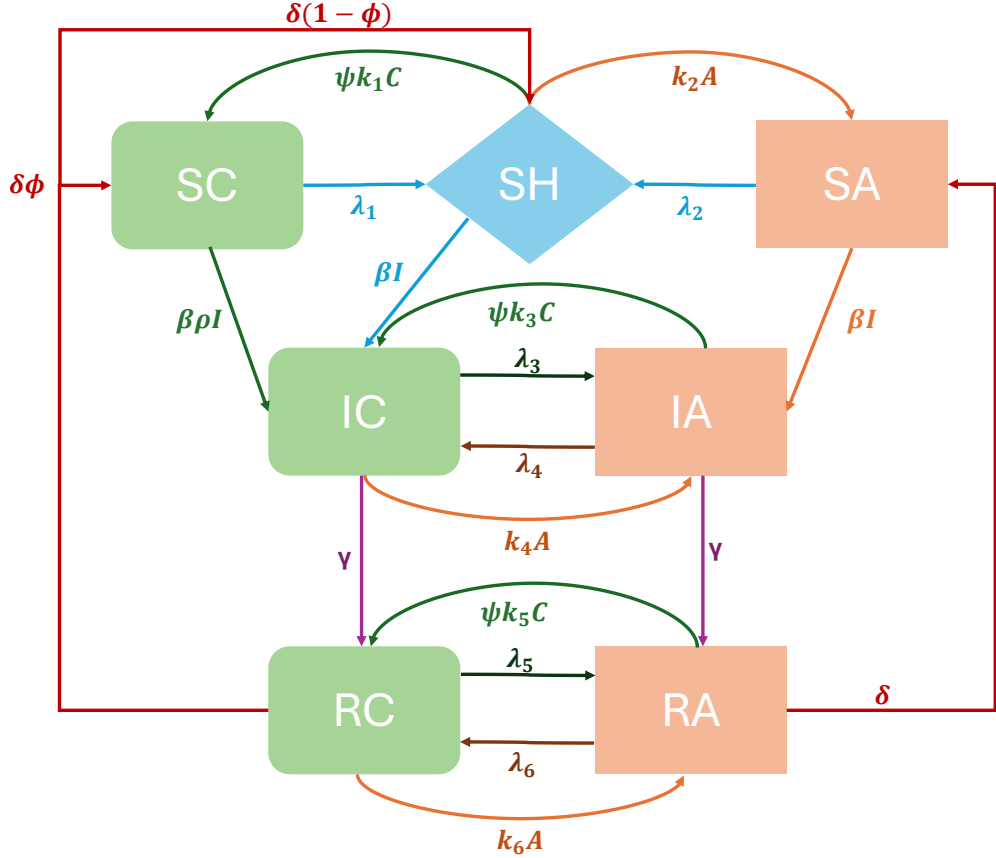


Figure 7.1: Epidemic behavioral model with compartments and fluxes.

describing the number of individuals in each compartment. The compartments of infected are m , and the relation $m < n$ holds. Assume that the system has a disease free equilibrium (DFE), denoted as x_0 : x_0 exist and is stable in the absence of the disease, so when the infected compartments have value equal to zero. Furthermore, in the DFE, the linearized equations for x_1, x_2, \dots, x_m decouple from the other equations. Thanks to these assumptions, it is possible to write the m infected equations in the form:

$$\frac{dx_i}{dt} = \mathcal{F}_i(x) - \mathcal{V}_i(x), \text{ for } i = 1, 2, \dots, m \quad (7.2)$$

The two terms appearing in equation (7.2), are $\mathcal{F}_i(x)$, the rate of appearance of new infected in the compartments i , and $\mathcal{V}_i(x)$ the rate of other transitions between compartment i and other infected compartments. It is assumed that each function is continuously differentiable at least twice in each variable.

To describe the evolution of the system, the following matrix notations is adopted:

- $F = \left[\frac{d\mathcal{F}_i}{dx_j} (x_0) \right]$ with $1 \leq i, j \leq m$.

- $V = \left[\frac{d\mathcal{V}_i}{dx_j} (x_0) \right]$ with $1 \leq i, j \leq m$.

The matrices are both evaluated at the disease free equilibrium, where $x = x_0$, and have dimension $m \times m$, with m being the number of infected compartments in the model. Using the defined matrices, according to [93, 94], the Epidemic reproduction number E_0 for the model (7.1) at a disease free equilibrium, where all infected densities are zero, is given by:

$$E_0 = \text{spec}(FV^{-1}) \quad (7.3)$$

The disease-free equilibrium is defined as a locally stable equilibrium of the system in which there is no disease. The matrix FV^{-1} is called next generation matrix, while $\text{spec}(M)$ is the spectral radius of a matrix M.

To understand the entries of the matrix, consider perturbing a population at the DFE by introducing one infected individual in compartment k . The (j, k) entry of V^{-1} is the average time that the individual spends in the compartment j . Instead, the (i, j) entry of F is the rate at which infected in compartment j produce new infections in i . In F only individuals that become infected for the first time must be inserted, while other influxes in the i -th compartment, must be considered in the V matrix. Finally the entry (i, k) in FV^{-1} is the expected number of new infections in i produced by the infected individual originally introduced in k .

Considering the system dynamics presented in (7.1), matrices F and V are

$$\begin{aligned} F &= \begin{bmatrix} \beta\epsilon(\rho S_C + S_H) & \beta(\rho S_C + S_H) \\ \beta\epsilon S_A & \beta S_A \end{bmatrix} \\ V &= \begin{bmatrix} \lambda_3 + k_4(S_A + I_A + R_A) + \gamma - \psi k_3 I_A & k_4 I_C - \lambda_4 - \psi k_3 (S_C + I_C + R_C) \\ \psi k_3 I_A - \lambda_3 - k_4(S_A + I_A + R_A) & \psi k_3 (S_C + I_C + R_C) - k_4 I_C + \lambda_4 + \gamma \end{bmatrix} \end{aligned}$$

Once the matrices composing the next-generation matrix are defined, the value of the epidemic reproduction number is calculated, resulting in:

$$\begin{aligned} E_0 &= \frac{\beta}{\gamma} \cdot \frac{\text{num}}{\text{den}} \\ \text{num} &= S_A(\gamma + \lambda_3 + \epsilon\lambda_4) + (S_H + \rho S_C)(\lambda_3 + \epsilon\gamma + \epsilon\lambda_4) + \dots \\ &\quad (S_A + S_H + \rho S_C)[(I_A - \epsilon I_C)(k_4 - \psi k_3) + k_4(R_A + S_A) + \psi\epsilon k_3(R_C + S_C)] \\ \text{den} &= \lambda_3 + \lambda_4 + \gamma + k_4(A - I_C) + \psi k_3(C - I_A) \end{aligned} \quad (7.4)$$

To compute the value of E_0 , the above expression must be evaluated at the DFE equilibria. Now it is determined how to compute them.

7.2.1 DFE calculation

To calculate the value of the DFE points of the system, consider the equations in system (7.1), referring to them as $\dot{x}_i = f_i(x)$, with $i = 1, \dots, 7$, corresponding to the seven different compartments that form the model. With j is instead defined the compartments

of infected in the model, and the condition that $j < 7$ holds. Disease-free equilibria are solutions of the system in which no infection is present, so $x_j = 0$, and the differential expressions are equal to zero. Imposing these conditions, along with mass conservation, leads to the following system to solve:

$$\begin{cases} \dot{x}_i = 0 & i = 1, \dots, 7 \\ x_j = 0 & j \geq 1, j < 7 \\ \sum_{i=1}^7 x_i = 1 & i = 1, \dots, 7 \end{cases}$$

Solving the system of equations symbolically using Matlab, three disease free equilibria are found which yield the corresponding E_0 after inserting their values in equation (7.4):

	S_C	S_H	S_A	E_0
type-A	0	1	0	$\frac{\beta}{\gamma} \frac{\lambda_3 + \epsilon\gamma + \epsilon\lambda_4}{\lambda_3 + \lambda_4 + \gamma}$
type-B	0	$\frac{\lambda_2}{k_2}$	$1 - \frac{\lambda_2}{k_2}$	$\frac{\beta}{\gamma} \frac{\gamma + \lambda_3 + \epsilon\lambda_4 + S_H\gamma(\epsilon - 1) + k_4 S_A}{\gamma + \lambda_3 + \lambda_4 + k_4 S_A}$
type-C	$1 - \frac{\lambda_1}{k_1}$	$\frac{\lambda_1}{k_1}$	0	$\frac{\beta}{\gamma} \frac{(S_H + \rho S_C)(\lambda_3 + \epsilon\gamma + \epsilon\lambda_4 + \psi\epsilon k_3 S_C)}{\lambda_3 + \lambda_4 + \gamma + \psi k_3 S_C}$

For all equilibria, the corresponding values of R_C and R_A are equal to zero.

7.3 Model simulations

We now present an analysis of the model through a set of numerical simulations to observe how the system reacts and evolve with different sets of parameters is performed. Performing an analysis similar to the one conducted for the behavior model alone is in fact too complex, as it involves numerous equations and parameters. Even though models similar to the one presented here have been analyzed in other works, such as [51], those analyses often rely on strong assumptions. E.g. in [51] the hypothesis is the existence of different time scales between the epidemic and behavioral layers, enabling the simplification of the analysis. However, this assumption was deemed unreliable during the development of this model. Models intended to use empirical data, such as those related to epidemic evolution, typically rely on data collected on a daily basis. For this reason, it is assumed that the time scales of the epidemic and behavioral layers comparable. Although adopting the time-separation hypothesis might simplify the analysis, it would essentially yield the same results found in the behavior model alone. Thus, extensive simulations become crucial to enhance understanding of the model.

A first evaluation of E_0 is performed to assess its capability to provide indications about the stability of the equilibrium. As stated in [93, 94], the DFE is locally asymptotically stable if $E_0 < 1$. Conversely, if $E_0 > 1$, a fully susceptible population, when perturbed by the introduction of infectious individuals, will progress toward an epidemic.

The same four cases of parameter configurations used in the previous chapter for the behavioral layer are employed here. For the epidemic layer, the value of R_0 is fixed

at 3.2727, based on the assumption of an average recovery period lasting 9 days and a transmission rate similar to that estimated for diseases like COVID-19 at the early stages of its spread [88]. An additional V case is introduced, in which the magnitudes of \mathcal{B}_1 and \mathcal{B}_2 are inverted relative to those in case IV.

To represent a wide range of scenarios, the epidemiological framework is kept constant, maintaining the same values for β , γ , and δ across all five cases. What varies is the intensity and relationship between the conversion numbers \mathcal{B}_1 and \mathcal{B}_2 .

All computations are performed using the following fixed set of parameters:

$$\begin{array}{llll} \beta = 0.40 & \gamma = 0.35 & \delta = 1/9 & \epsilon = 0.15 \\ \epsilon = 0.15 & \rho = 0.65 & \psi = 1 & \phi = 0.5 \end{array}$$

With these coefficient values, considering separately the epidemic and behavioral layers the basic epidemiological-only reproduction number of the SIRS model is:

$$R_0 = \frac{\beta}{\gamma + \delta} = 3.2727$$

For the other behavioral coefficients it is assumed $k_3 = k_5 = k_1$, and $k_4 = k_6 = k_2$. Also $\lambda_3 = \lambda_5 = \lambda_1$, and $\lambda_4 = \lambda_6 = \lambda_2$. The values of these coefficients change across the five cases.

	B_1	$\lambda_1 [d^{-1}]$	B_2	$\lambda_2 [d^{-1}]$
case I	0.89	1/30	0.45	1/40
case II	8.5	1/40	8.5	1/20
case III	7	1/30	3	1/30
case IV	7	1/30	3	1/5
case V	3	1/30	7	1/2

The values of the variables k_1 and k_2 are derived using the expression $\mathcal{B}_i = k_i/\lambda_i$, where $i = 1, 2$. The results of all simulations and the corresponding E_0 values are summarized in Table 7.2.

It is immediately noticeable how the value of E_0 changes and is influenced by both the behavioral parameters and the considered DFE. The initial distribution of the population across compartments is chosen by perturbing the computed DFE, through the insertion of some infected. The DFE type-C, where the population is divided between the Compliant and Heedless Susceptible compartments, is always locally asymptotically stable. In contrast, the type-B equilibrium is always unstable, with $E_0 > 1$. A possible explanation for this observation lies in the effects of the parameters ρ and ϵ , which respectively reduce the likelihood of S_C becoming infected and the ability of I_C to infect others. In the next paragraphs, the plots of the most relevant simulations for each of the five cases defined by these parameters are shown. In the simulations conducted using the Runge-Kutta second-order method, the number of infected individuals at time zero is slightly greater than zero: $I_{C0} = I_{A0} = 10/60e6$.

Case #	DFE type	SC	SH	SA	E_0
1	A	0	1	0	1.142
2	A	0	1	0	0.951
2	C	0.8824	0.1176	0	0.5148
3	A	0	1	0	1.1138
3	B	0	0.3333	0.6667	2.7191
3	C	0.8571	0.1429	0	0.567
4	A	0	1	0	0.8361
4	B	0	0.3333	0.6667	2.6257
4	C	0.8571	0.1429	0	0.5091
5	A	0	1	0	0.6983
5	B	0.6667	0.3333	0	0.524
5	C	0	0.1429	0.8571	3.1669

Figure 7.2: The results of the simulations illustrate how E_0 , the Epidemic Reproduction Number, varies across different possible scenarios.

7.3.1 I case: $\mathcal{B}_1, \mathcal{B}_2 < 1$, $\mathcal{B}_1 > \mathcal{B}_2$, and $\lambda_1 > \lambda_2$

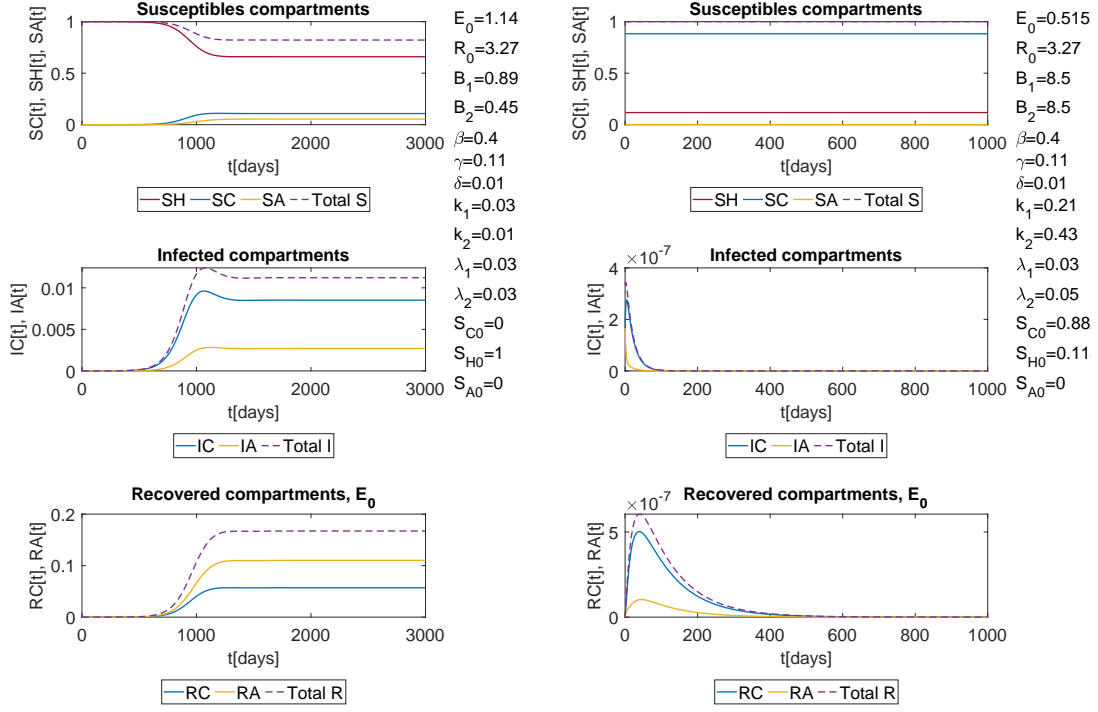
When calculating the Disease-Free Equilibrium (DFE), only one solution is found. It corresponds to the state $S_{C_0} = 0$, $S_{A_0} = 0$, and $S_{H_0} = 1$. In this equilibrium, the value of $E_0 = 1.142$, is greater than one. Therefore, as stated in the theorem presented in [93], the DFE is unstable, and a disease can evolve into an epidemic from this initial condition.

Observing the behavior layer, since both Conversion numbers \mathcal{B}_1 and \mathcal{B}_2 are less than one, the majority of the population remains in the Heedless compartment in this scenario. This facilitates disease propagation because only a small portion of individuals are in the Susceptible-Compliant (S_C) category, reducing their likelihood of infection, governed by $\rho\beta$ with $\rho < 1$. Meanwhile, S_A and S_H share the same probability of contracting the disease, β .

In the left panel of Figure 7.3, it is evident that the dynamics are dominated by the Heedless compartment. Furthermore, an infection peak is observed, and the final equilibrium reached by the system is not disease-free: a relatively small portion of the population remains infected.

7.3.2 II case: $\mathcal{B}_1, \mathcal{B}_2 > 1$, $\mathcal{B}_1 = \mathcal{B}_2$, and $\lambda_1 < \lambda_2$

If both behavioral layers have the same behavior conversion number, $\mathcal{B}_1 = \mathcal{B}_2$, as shown in the right panel of Figure 7.3, the epidemic evolution is heavily influenced by the initial compartment values. This property holds even when the balance of the Behavior reproduction number is achieved with different coefficient values. Recall that k_1 and k_2 determine which behavior becomes dominant, while λ_1 and λ_2 impact the persistence of a certain behavior. In this case, the Compliant course of action is more dominant and slightly less persistent. However, the initial conditions play a critical role in shaping the model evolution. When perturbing the type-C equilibrium, where the majority of the population is in the Compliant compartments, the population remains largely Compliant. Even when some infected individuals are introduced to perturb the disease-free state, the infection is rapidly suppressed. The equilibrium DFE, with a value of $E_0 = 0.515$, is



(a) I case: Both \mathcal{B}_1 and \mathcal{B}_2 are less than one. None of the possible behaviors become dominant.

(b) II case: \mathcal{B}_1 is equal to \mathcal{B}_2 . Starting from a type-C DFE, we have an E_0 that confirms the local asymptotic stability of the equilibrium. No epidemic develops in the system, as shown in the simulation.

Figure 7.3: Cases I and II of the simulations performed. In the left panel, there is an epidemic outbreak leading to an endemic equilibrium, while in the right panel, the disease dies out, and the population remains in the Susceptible compartment at equilibrium.

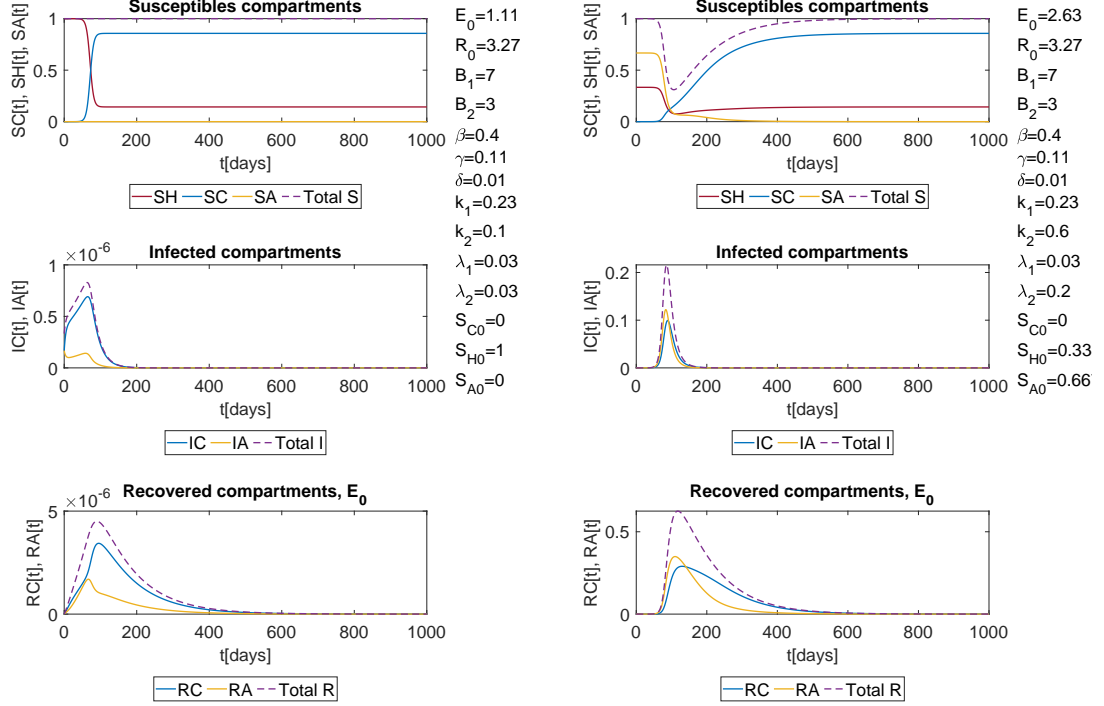
locally asymptotically stable.

7.3.3 III case: $\mathcal{B}_1, \mathcal{B}_2 > 1$, $\mathcal{B}_1 < \mathcal{B}_2$, and $\lambda_1 = \lambda_2$

Figure 7.4, explores the impact of compliance with rules and the adoption of self-precautions on the diffusion of an epidemic. Starting from the disease-free equilibrium type-A, where $S_{C0} = 1$ and all other compartments are equal to zero, the introduction of infected individuals triggers the spread of an infection. The value of $E_0 = 1.11$ indicates that the DFE is in fact unstable.

Although the disease can spread in a fully susceptible population, the protection provided by compliant behavior significantly reduces its spread. With \mathcal{B}_1 larger than \mathcal{B}_2 , compliant behavior quickly spreads throughout the population and persists longer than the infection duration. As a result, the majority of the population transitions to the S_C

compartment, while S_A tends toward zero. The epidemic fades after reaching a small peak and infecting only a minor fraction of the population.



(a) III case: $\mathcal{B}_1 > \mathcal{B}_2$, the Compliant behavior becomes dominant. This dominance significantly mitigates the effects of the epidemic, both in terms of the number of infected individuals and the duration of the outbreak.

(b) IV case: $\mathcal{B}_1 > \mathcal{B}_2$, starting from a type-B Disease-Free Equilibrium (DFE), and with k_2, λ_2 larger than k_1, λ_1 , a high peak in infections occurs. This is due to the initial phase, during which the Against group constitutes the majority, allowing the disease to spread freely.

Figure 7.4: In Case III, illustrated in panel (a), there is a small epidemic outbreak, which is eventually contained as the disease tends to disappear. This outcome occurs due to the high proportion of the population that becomes compliant, thereby significantly reducing the spread of the infection. In Case IV, shown in panel (b), we observe a scenario in which an outbreak occurs, and the disease rapidly spreads within a population predominantly composed of individuals who are Against. This lack of compliance exacerbates the diffusion of the infection.

7.3.4 IV case: $\mathcal{B}_1, \mathcal{B}_2 > 1$ and $\mathcal{B}_1 > \mathcal{B}_2$, and $\lambda_1 < \lambda_2$

The fourth case highlights and describes the negative effects of non-compliant behavior. Even though $\mathcal{B}_2 < \mathcal{B}_1$, the condition $k_2 \gg k_1$ allows the Against behavior to initially

spread more rapidly. As observed previously with the behavior model alone in Section 6.2.3, this dynamic results in significant early non-compliance. The simulation begins close to the DFE corresponding to type-B, where the majority of the population is in S_A . These initial conditions lead to a higher epidemic reproduction number, with $E_0 = 2.63$. Consequently, the number of infected individuals reaches a much higher peak compared to the third case. However, as the simulation progresses, the Compliant group gradually gains prevalence due to $\mathcal{B}_1 > \mathcal{B}_2$. The population tends to shift toward compliance, and after the peak, the disease diminishes toward zero.

7.3.5 V case: $\mathcal{B}_1, \mathcal{B}_2 > 1$ and $\mathcal{B}_1 < \mathcal{B}_2$

The final case represents the worst scenario for epidemic spread. The majority of the population adopts the Against behavior, which prevents the epidemic from being mitigated by NPIs or self-isolation. These measures are only adopted by an increasingly smaller portion of individuals. As a result, the epidemic trajectory closely resembles that of an SIRS-only model. With $E_0 = 3.17$, the highest value among all the cases presented, the infection peak is large, and the disease does not disappear. Instead, the system reaches an endemic equilibrium.

7.3.6 Influence of the ψ parameter

To model how government policies can influence the behavior of the population and create a distinction between spontaneous behavior and reactions to regulations, the parameter ψ was introduced. It acts as a central mean-field intervention, multiplying the coefficients k_1 , k_3 , and k_5 .

The value of ψ is greater than one ($\psi > 1$) when the simulations consider enforced policies that individuals must follow, and equal to one ($\psi = 1$) when no such regulations are in place.

In Figure 7.6, the evolution of S_C and the total number of infected individuals as ψ varies is represented. It is evident that increasing the value of ψ changes the timescale of compliance, causing S_C to reach its maximum more quickly, while also increasing the final number of S_C . Furthermore, it significantly reduces the peak value of infected individuals.

This effect is very pronounced when comparing cases: with $\psi = 1$, the peak value of I is around 2%, whereas in other cases, it drops to approximately 0.0007%.

Discussion

Overall, the implemented multi-system model demonstrates its ability to adapt effectively to a variety of scenarios. Specifically, it captures both situations: one where Compliant behavior significantly mitigates the disease's impact, and the opposite scenario, where the dominant presence of the Against group triggers a disease outbreak. These outcomes arise under the same disease parameter values, β, γ, δ . The estimated value of E_0 proves to be a valuable indicator of the stability of the system's Disease-Free Equilibrium (DFE). On the other hand, the parameter ψ has a significant impact on the evolution of the epidemic. This parameter can be particularly useful in scenarios where the reproduction conversion

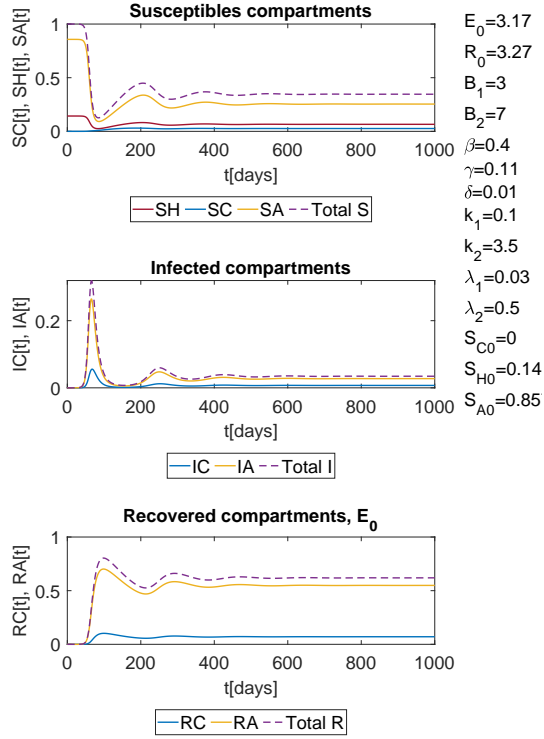


Figure 7.5: V case: where $B_1 < B_2$, the simulation starts from a type-B Disease-Free Equilibrium (DFE). The Against group is dominant from the beginning, allowing the disease to spread almost freely. This results in several peaks of infection, and, at equilibrium, the disease becomes endemic within the population.

number for the compliant group is close to one (but still greater than one), as it can accelerate the population's transition toward compliance.

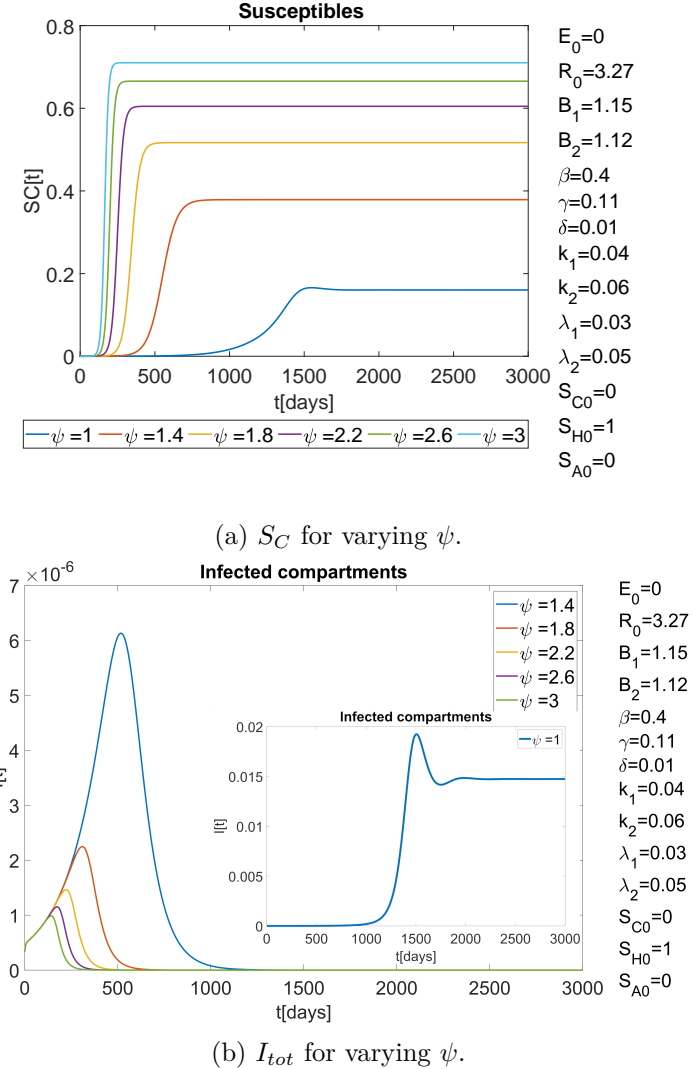


Figure 7.6: Simulations of the epidemic-behavioral model with varying parameter ψ . In the first figure, the changes in the S_C curve are shown. The maximum is reached more quickly when $\psi > 1$. In the second figure, the corresponding $I = I_C + I_A$ curves are presented. The small panel represents the case with $\psi = 1$. For $\psi > 1$, the infection peak becomes significantly smaller.

Chapter 8

Conclusions

The work conducted during this thesis has led to the development of a novel epidemiological-behavioral model that couples an SIRS model with a behavioral mean-field model. Both opinion and behavioral modeling have been studied, and the most significant contributions in this field from recent years have been presented to provide a comprehensive perspective on how social dynamics can be integrated into disease progression models.

The main contributions of this study are summarized as follows:

- **Behavioral-Epidemic Interactions:** The work highlights the complex dynamics that emerge when a disease interacts with human behavior. A behavioral model with three possible behavioral states during the onset and progression of an epidemic is implemented. From its coupling with the disease model, the role of social dynamics in shaping epidemic outcomes becomes apparent.
- **Insights from Simulations:** Through analyses of individual model components and subsequent simulations, key parameters such as the Epidemic Reproduction Number (E_0) were identified. The evolution of E_0 and its effectiveness as an indicator to predict whether an epidemic will evolve were explored. Furthermore, the model demonstrates various dynamics: while compliance diffusion can mitigate the epidemic impact, the spread of misinformation, which alters individual behavior, can lead to more severe outcomes. The interplay of behavioral parameters, in particular, creates intriguing influences on epidemic evolution, which are explained in this work.
- **Framework Flexibility:** Developed with empirical data in mind, the resulting model is a versatile tool that can be adapted to different scenarios and reflects a wide range of behavioral and epidemiological dynamics.

8.1 Limitations

The proposed multi-system epidemiological-behavioral model is based on certain assumptions that may pose limitations; for instance, the homogeneous mixing assumption assumes

that individuals interact with equal probability with anyone in the population. Incorporating features like clustering or homophily—the tendency of individuals to associate with those who are similar to themselves—could add depth and realism to the model.

Another limitation is the presence of the Heedless compartment only in the Susceptible layer. This restriction can limit the model’s accuracy for the infected and recovered compartments since all individuals in S_H transition to I_C . Exploring alternative subdivisions of S_H could address this aspect, but it would require a thorough and detailed analysis to ensure consistency and reliability.

8.2 Future perspective

Possible improvements and refinements include:

- Conducting an analysis based on empirical data to evaluate the model’s ability to replicate real behavioral patterns observed during the COVID-19 pandemic.
- Developing a more complex ψ parameter that incorporates information about the disease state (such as incidence or prevalence) or accounts for aspects like the economic costs associated with the disease, to better model the stringency of policies implemented by governments.
- Extending the investigation by exploring different values for the behavior transmission rates, k_i , and fatigue to maintain a behavior, λ_i .

To conclude, the present work is significant because it introduces a novel multi-system model that effectively integrates epidemiological and behavioral dynamics, providing insights into how individual and collective behaviors influence the spread of diseases. The model’s flexibility allows it to adapt to various scenarios, offering a valuable framework for understanding complex interactions between disease transmission and human behavior. Moreover, the potential to incorporate empirical data and compute the parameter values in this way allows for interesting future possible developments for the model.

Bibliography

- [1] Guenter B Risse. “Epidemics and history: ecological perspectives and social responses”. In: *AIDS: The burdens of history* 33 (1988).
- [2] William F Keegan. “Destruction of the Taino.” In: *Archaeology* 45.1 (1992), pp. 51–56.
- [3] B. de Sahagun, A.J.O. Anderson, and C.E. Dibble. *Florentine Codex: Book 12: Book 12: The Conquest of Mexico Volume 12*. Florentine Codex, A General History of the Things of New Spain. University of Utah Press, 1965. ISBN: 9780874800968. URL: https://books.google.it/books?id=R_qAMgAACAAJ.
- [4] Roy M. Anderson. *The Population Dynamics of Infectious Diseases*. Population and Community Biology Ser. Description based on publisher supplied metadata and other sources. New York, NY: Springer, 1982. 1380 pp. ISBN: 9781489929013.
- [5] Stein Emil Vollset et al. “Burden of disease scenarios for 204 countries and territories, 2022–2050: a forecasting analysis for the Global Burden of Disease Study 2021”. In: *The Lancet* 403.10440 (2024), pp. 2204–2256. ISSN: 0140-6736. DOI: 10.1016/s0140-6736(24)00685-8.
- [6] Europe. *Causes of death statistics*. URL: https://ec.europa.eu/eurostat/statistics-explained/index.php?title=Causes_of_death_statistics#Major causes of death in the EU in 2021.
- [7] Saloni Dattani. “What were the death tolls from pandemics in history?” In: *Our World in Data* (2023). <https://ourworldindata.org/historical-pandemics>.
- [8] *List of epidemics and pandemics*. URL: https://en.wikipedia.org/wiki/List_of_epidemics_and_pandemics.
- [9] Haiyang Yang and Jingjing Ma. “How an Epidemic Outbreak Impacts Happiness: Factors that Worsen (vs. Protect) Emotional Well-being during the Coronavirus Pandemic”. In: *Psychiatry Research* 289 (July 2020), p. 113045. ISSN: 0165-1781. DOI: 10.1016/j.psychres.2020.113045.
- [10] Esteban Ortiz-Ospina and Max Roser. “Healthcare Spending”. In: *Our World in Data* (2017). <https://ourworldindata.org/financing-healthcare>.
- [11] M. T. Barlow, N. D. Marshall, and R. C. Tyson. “Optimal shutdown strategies for COVID-19 with economic and mortality costs: British Columbia as a case study”. In: *Royal Society Open Science* 8.9 (2021), p. 202255. DOI: 10.1098/rsos.202255.

- [12] Esteban A. Hernandez-Vargas et al. “Modelling and Control of Epidemics Across Scales”. In: *2022 IEEE 61st Conference on Decision and Control (CDC)*. IEEE, 2022. DOI: 10.1109/cdc51059.2022.9992380.
- [13] Matt J Keeling and Ken T.D Eames. “Networks and epidemic models”. In: *Journal of The Royal Society Interface* 2.4 (June 2005), pp. 295–307. ISSN: 1742-5662. DOI: 10.1098/rsif.2005.0051.
- [14] O. Diekmann and Hans Jap Heesterbeek. *Mathematical epidemiology of infectious diseases. Model buildign, analysis and interpretation*. Vol. 5. Originally published: 1999. Chichester: Wiley, 2000. 320 pp. ISBN: 0471492418.
- [15] Fred Brauer, Carlos Castillo-Chavez, and Carlos Castillo-Chavez. *Mathematical models in population biology and epidemiology*. Vol. 2. 40. Springer, 2012. DOI: 10.1007/978-1-4614-1686-9.
- [16] Glenn Ledder. *Mathematical Modeling for Epidemiology and Ecology*. Springer International Publishing, 2023. ISBN: 9783031094545. DOI: 10.1007/978-3-031-09454-5.
- [17] Ottar N. Bjørnstad and Cecile Viboud. “Timing and periodicity of influenza epidemics”. In: *Proceedings of the National Academy of Sciences* 113.46 (2016), pp. 12899–12901. ISSN: 1091-6490. DOI: 10.1073/pnas.1616052113.
- [18] Zhen Wang et al. “Coupled disease–behavior dynamics on complex networks: A review”. In: *Physics of Life Reviews* 15.China. (2015), pp. 1–29. ISSN: 1571-0645. DOI: 10.1016/j.plrev.2015.07.006.
- [19] Manlio De Domenico et al. “The physics of spreading processes in multilayer networks”. In: *Nature Physics* 12.10 (2016), pp. 901–906. ISSN: 1745-2481. DOI: 10.1038/nphys3865.
- [20] Alexandra Teslya et al. “The effect of competition between health opinions on epidemic dynamics”. In: ed. by Sergey Gavrilets. Vol. 1. 5. Oxford University Press (OUP), 2022. DOI: <https://doi.org/10.1093/pnasnexus/pgac260>.
- [21] Joshua M. Epstein, Erez Hatna, and Jennifer Crodelle. “Triple contagion: a two-fears epidemic model”. In: *Journal of The Royal Society Interface* 18.181 (2021), p. 20210186. DOI: 10.1098/rsif.2021.0186.
- [22] Angélica S. Mata. “Mathematical modeling applied to epidemics: an overview”. In: 2021. DOI: [.org/10.1007/s40863-021-00268-7](https://doi.org/10.1007/s40863-021-00268-7).
- [23] Rafael Capurro and Birger Hjørland. “The concept of information”. In: *Annual Review of Information Science and Technology* 37.1 (2003), pp. 343–411. ISSN: 1550-8382. DOI: 10.1002/aris.1440370109.
- [24] Carlos Andres Devia and Giulia Giordano. “A framework to analyze opinion formation models”. In: *Scientific Reports* 12.1 (2022). DOI: 10.1038/s41598-022-17348-z.
- [25] Mark Granovetter. “Threshold Models of Collective Behavior”. In: *American Journal of Sociology* 83.6 (1978), pp. 1420–1443. ISSN: 1537-5390. DOI: 10.1086/226707.

- [26] William Ogilvy Kermack and Anderson G McKendrick. “A contribution to the mathematical theory of epidemics”. In: *Proceedings of the Royal Society of London. Series A, Containing Papers of a Mathematical and Physical Character* 115.772 (1927), pp. 700–721. ISSN: 2053-9150. DOI: 10.1098/rspa.1927.0118.
- [27] Roy M. Anderson and Robert M. May. *Infectious diseases of humans. Dynamics and control*. Reprinted. Literaturverz. S. [697] - 735. Oxford [u.a.]: Oxford Univ. Press, 2010. 757 pp. ISBN: 9780198540403. URL: <https://books.google.it/books?id=HT0--xBguQC&lpg=PA1&hl=it&pg=PA1#v=onepage&q&f=false>.
- [28] Jonas Dehning et al. “Inferring change points in the spread of COVID-19 reveals the effectiveness of interventions”. In: *Science* 369.6500 (2020). ISSN: 1095-9203. DOI: 10.1126/science.abb9789.
- [29] Daniele Proverbio et al. “Dynamical SPQEIR model assesses the effectiveness of non-pharmaceutical interventions against COVID-19 epidemic outbreaks”. In: *PLOS ONE* 16.5 (2021). Ed. by Michele Tizzoni, e0252019. ISSN: 1932-6203. DOI: 10.1371/journal.pone.0252019.
- [30] D. Breda et al. “On the formulation of epidemic models (an appraisal of Kermack and McKendrick)”. In: *Journal of Biological Dynamics* 6.sup2 (2012), pp. 103–117. ISSN: 1751-3766. DOI: 10.1080/17513758.2012.716454.
- [31] FS Akinboro, S Alao, and FO Akinpelu. “Numerical solution of SIR model using differential transformation method and variational iteration method”. In: *General Mathematics Notes* 22.2 (2014), pp. 82–92.
- [32] Hildeberto Jardón-Kojakhmetov et al. “A geometric analysis of the SIR, SIRS and SIRWS epidemiological models”. In: *Nonlinear Analysis: Real World Applications* 58 (2021), p. 103220. ISSN: 1468-1218. DOI: 10.1016/j.nonrwa.2020.103220.
- [33] Yutaka Okabe and Akira Shudo. “A Mathematical Model of Epidemics A Tutorial for Students”. In: *Mathematics* 8.7 (July 2020), p. 1174. DOI: 10.3390/math8071174.
- [34] Dimiter Prodanov. “Analytical solutions and parameter estimation of the SIR epidemic model”. In: *Mathematical Analysis of Infectious Diseases*. Elsevier, 2022, pp. 163–189. DOI: 10.1016/b978-0-32-390504-6.00015-2.
- [35] Zhiting Xu. “Traveling waves in a Kermack–Mckendrick epidemic model with diffusion and latent period”. In: *Nonlinear Analysis: Theory, Methods and Applications* 111 (Dec. 2014), pp. 66–81. DOI: 10.1016/j.na.2014.08.012.
- [36] Mustafa Turkyilmazoglu. “Explicit formulae for the peak time of an epidemic from the SIR model”. In: *Physica D: Nonlinear Phenomena* 422 (Aug. 2021), p. 132902. DOI: 10.1016/j.physd.2021.132902.
- [37] Herbert W. Hethcote. “The Mathematics of Infectious Diseases”. In: *SIAM Review* 42.4 (2000), pp. 599–653. ISSN: 1095-7200. DOI: 10.1137/s0036144500371907.
- [38] Linda J.S. Allen. “A primer on stochastic epidemic models: Formulation, numerical simulation, and analysis”. In: *Infectious Disease Modelling* 2.2 (Mar. 11, 2017), pp. 128–142. ISSN: 2468-0427. DOI: 10.1016/j.idm.2017.03.001.

- [39] M. E. J. Newman. “Spread of epidemic disease on networks”. In: *Physical Review E* 66.1 (2002), p. 016128. ISSN: 1095-3787. DOI: 10.1103/physreve.66.016128.
- [40] P. Van Mieghem, J. Omic, and R. Kooij. “Virus Spread in Networks”. In: *IEEE/ACM Transactions on Networking* 17.1 (2009), pp. 1–14. ISSN: 1558-2566. DOI: 10.1109/tnt.2008.925623.
- [41] Michele Tizzoni et al. “On the Use of Human Mobility Proxies for Modeling Epidemics”. In: *PLoS Computational Biology* 10.7 (July 10, 2014). Ed. by Marcel Salathe, e1003716. ISSN: 1553-7358. DOI: 10.1371/journal.pcbi.1003716.
- [42] Clara Granell, Sergio Gómez, and Alex Arenas. “Dynamical Interplay between Awareness and Epidemic Spreading in Multiplex Networks”. In: *Physical Review Letters* 111.12 (Sept. 2013), p. 128701. ISSN: 1079-7114. DOI: 10.1103/physrevlett.111.128701. URL: <https://github.com/sergio-gomez/Radalib>.
- [43] Beate Krickel, Leon de Bruin, and Linda Douw. “How and when are topological explanations complete mechanistic explanations? The case of multilayer network models”. In: *Synthese* 202.1 (2023). ISSN: 1573-0964. DOI: 10.1007/s11229-023-04241-z.
- [44] Wei Wang et al. “Coevolution spreading in complex networks”. In: *Physics Reports* 820 (2019), pp. 1–51. DOI: 10.1016/j.physrep.2019.07.001.
- [45] Chris Bauch, Alberto d’Onofrio, and Piero Manfredi. “Behavioral Epidemiology of Infectious Diseases: An Overview”. In: *Modeling the Interplay Between Human Behavior and the Spread of Infectious Diseases*. Springer New York, 2012, pp. 1–19. ISBN: 9781461454748. DOI: 10.1007/978-1-4614-5474-8_1.
- [46] Giulia Giordano et al. “Modelling the COVID-19 epidemic and implementation of population-wide interventions in Italy”. In: *Nature Medicine* 26.6 (Apr. 2020), pp. 855–860. DOI: 10.1038/s41591-020-0883-7.
- [47] Sebastian Funk, Marcel Salathé, and Vincent A. A. Jansen. “Modelling the influence of human behaviour on the spread of infectious diseases: a review”. In: *Journal of The Royal Society Interface* 7.50 (2010), pp. 1247–1256. DOI: 10.1098/rsif.2010.0142.
- [48] George Vogiatzis, Ian Macgillivray, and Maria Chli. “A Probabilistic Model for Trust and Reputation”. In: 2010. DOI: ng.
- [49] Collinson Shannon and Heffernan Jane. “Modelling the effects of media during an influenza epidemic”. In: *BMC Public Health* 14.1 (2014). ISSN: 1471-2458. DOI: 10.1186/1471-2458-14-376.
- [50] Rebecca C. Tyson et al. “The Timing and Nature of Behavioural Responses Affect the Course of an Epidemic”. In: *Bulletin of Mathematical Biology* 82.1 (2020). DOI: 10.1007/s11538-019-00684-z.
- [51] Iulia Bulai, Mattia Sensi, and Sara Sottile. “A geometric analysis of the SIRS compartmental model with fast information and misinformation spreading”. In: Nov. 10, 2023. DOI: 10.1016/j.chaos.2024.115104.

- [52] Andrei Sontag, Tim Rogers, and Christian A. Yates. “Misinformation can prevent the suppression of epidemics”. In: *Journal of The Royal Society Interface* 19.188 (2022). ISSN: 1742-5662. DOI: 10.1098/rsif.2021.0668.
- [53] Dan M. Kahan. “A Risky Science Communication Environment for Vaccines”. In: *Science* 342.6154 (2013), pp. 53–54. ISSN: 1095-9203. DOI: 10.1126/science.1245724.
- [54] Chris T. Bauch and Samit Bhattacharyya. “Evolutionary Game Theory and Social Learning Can Determine How Vaccine Scares Unfold”. In: *PLoS Computational Biology* 8.4 (2012). Ed. by Marcel Salathé, e1002452. ISSN: 1553-7358. DOI: 10.1371/journal.pcbi.1002452.
- [55] Andrew J Wakefield et al. “RETRACTED: Ileal-lymphoid-nodular hyperplasia, non-specific colitis, and pervasive developmental disorder in children”. In: *The lancet* 351.9103 (1998), pp. 637–641. DOI: 10.1016/s0140-6736(97)11096-0.
- [56] A.K. Misra, Anupama Sharma, and J.B. Shukla. “Modeling and analysis of effects of awareness programs by media on the spread of infectious diseases”. In: *Mathematical and Computer Modelling* 53.5–6 (2011), pp. 1221–1228. ISSN: 0895-7177. DOI: 10.1016/j.mcm.2010.12.005.
- [57] Sebastian Funk et al. “The spread of awareness and its impact on epidemic outbreaks”. In: *Proceedings of the National Academy of Sciences* 106.16 (2009), pp. 6872–6877. ISSN: 1091-6490. DOI: 10.1073/pnas.0810762106.
- [58] Paulo Cesar Ventura da Silva et al. “Epidemic spreading with awareness and different timescales in multiplex networks”. In: *Physical Review E* 100.3 (2019), p. 032313. ISSN: 2470-0053. DOI: 10.1103/physreve.100.032313.
- [59] Clara Granell, Sergio Gómez, and Alex Arenas. “Competing spreading processes on multiplex networks: Awareness and epidemics”. In: *Physical Review E* 90.1 (2014), p. 012808. DOI: 10.1103/physreve.90.012808.
- [60] K.M. Ariful Kabir, Kazuki Kuga, and Jun Tanimoto. “Analysis of SIR epidemic model with information spreading of awareness”. In: *Chaos, Solitons Fractals* 119 (Feb. 2019), pp. 118–125. DOI: 10.1016/j.chaos.2018.12.017.
- [61] Chao Zuo et al. “A New Coupled Awareness-Epidemic Spreading Model with Neighbor Behavior on Multiplex Networks”. In: *Complexity* 2021 (2021). Ed. by xiaoke xu xiaoke, pp. 1–14. ISSN: 1076-2787. DOI: 10.1155/2021/6680135.
- [62] Carlos Andres Devia and Giulia Giordano. “Classification-Based Opinion Formation Model Embedding Agents’ Psychological Traits”. In: *Journal of Artificial Societies and Social Simulation* 26.3 (2023). DOI: 10.18564/jasss.5058.
- [63] Jamie Bedson et al. “A review and agenda for integrated disease models including social and behavioural factors”. In: *Nature Human Behaviour* 5.7 (June 2021), pp. 834–846. DOI: 10.1038/s41562-021-01136-2.
- [64] Kaiyan Peng et al. “A multilayer network model of the coevolution of the spread of a disease and competing opinions”. In: *Mathematical Models and Methods in Applied Sciences* 31.12 (2021), pp. 2455–2494. DOI: 10.1142/s0218202521500536.

- [65] Alejandro Carballosa, Mariamo Mussa-Juane, and Alberto P. Munuzuri. “Incorporating social opinion in the evolution of an epidemic spread”. In: *Scientific Reports* 11.1 (Jan. 2021). DOI: 10.1038/s41598-021-81149-z.
- [66] Meliksah Turker and Haluk O. Bingol. “Multi-layer network approach in modeling epidemics in an urban town”. In: *The European Physical Journal B* 96.2 (2023). ISSN: 1434-6036. DOI: 10.1140/epjb/s10051-023-00484-4. arXiv: 2109.02272 [cs.CY].
- [67] Faryad Darabi Sahneh, Caterina Scoglio, and Piet Van Mieghem. “Generalized Epidemic Mean-Field Model for Spreading Processes Over Multilayer Complex Networks”. In: *IEEE/ACM Transactions on Networking* 21.5 (2013). Matematicamente mi sembra complesso, ma molto interessante come lavoro, pp. 1609–1620. DOI: 10.1109/tnet.2013.2239658.
- [68] Kathinka Frieswijk et al. “A Mean-Field Analysis of a Network Behavioral-Epidemic Model”. In: *IEEE Control Systems Letters* 6 (2022), pp. 2533–2538. ISSN: 2475-1456. DOI: 10.1109/lcsys.2022.3168260.
- [69] M.Christopher Auld. “Choices, beliefs, and infectious disease dynamics”. In: *Journal of Health Economics* 22.3 (2003), pp. 361–377. DOI: 10.1016/s0167-6296(02)00103-0.
- [70] Wei Wang et al. “Dynamics of social contagions with memory of non redundant information”. In: *Physical Review E* 92.1 (2015), p. 012820. ISSN: 1550-2376. DOI: 10.1103/physreve.92.012820.
- [71] Marko Gosak et al. “Endogenous social distancing and its underappreciated impact on the epidemic curve”. In: *Scientific Reports* 11.1 (Feb. 2021). DOI: 10.1038/s41598-021-82770-8.
- [72] Hendrik Nunner. “A model for the co-evolution of dynamic social networks and infectious disease dynamics”. In: 2021. DOI: 10.1186/s40649-021-00098-9.
- [73] Michael A. Krassa. “Social groups, selective perception, and behavioral contagion in public opinion”. In: *Social Networks* 10.2 (1988), pp. 109–136. ISSN: 0378-8733. DOI: 10.1016/0378-8733(88)90018-4.
- [74] Duncan J. Watts. “A simple model of global cascades on random networks”. In: *Proceedings of the National Academy of Sciences* 99.9 (2002), pp. 5766–5771. ISSN: 1091-6490. DOI: 10.1073/pnas.082090499.
- [75] Lucila G. Alvarez-Zuzek et al. “Epidemic spreading in multiplex networks influenced by opinion exchanges on vaccination”. In: *PLOS ONE* 12.11 (2017). Ed. by Yamir Moreno, e0186492. DOI: 10.1371/journal.pone.0186492.
- [76] Mark M. Tanaka, Jochen Kumm, and Marcus W. Feldman. “Coevolution of Pathogens and Cultural Practices: A New Look at Behavioral Heterogeneity in Epidemics”. In: *Theoretical Population Biology* 62.2 (2002), pp. 111–119. ISSN: 0040-5809. DOI: 10.1006/tpbi.2002.1585.

- [77] Marcelo Bongarti et al. “Alternative SIAR models for infectious diseases and applications in the study of non-compliance”. In: *Mathematical Models and Methods in Applied Sciences* 32.10 (Sept. 2022), pp. 1987–2015. ISSN: 1793-6314. DOI: 10.1142/s0218202522500464.
- [78] Chao Zuo. “Analyzing COVID-19 Vaccination Behavior Using an SEIRM/V Epidemic Model With Awareness Decay”. In: 2022. DOI: 10.3389/fpubh.2022.817749.
- [79] Françoise Kemp et al. “Modelling COVID-19 dynamics and potential for herd immunity by vaccination in Austria, Luxembourg and Sweden”. In: *Journal of Theoretical Biology* 530 (Dec. 2021), p. 110874. ISSN: 0022-5193. DOI: 10.1016/j.jtbi.2021.110874.
- [80] Marko Gosak et al. “Community lockdowns in social networks hardly mitigate epidemic spreading”. In: *New Journal of Physics* 23.4 (Apr. 2021), p. 043039. DOI: 10.1088/1367-2630/abf459.
- [81] Paul E. Smaldino and James Holland Jones. “Coupled dynamics of behaviour and disease contagion among antagonistic groups”. In: *Evolutionary Human Sciences* 3 (2021). ISSN: 2513-843X. DOI: 10.1017/ehs.2021.22.
- [82] Daniele Proverbio, Riccardo Tessarin, and Giulia Giordano. “Data informed epidemiological-behavioural modelling”. In: (2024). DOI: 10.48550/ARXIV.2410.10472.
- [83] Christina M. Astley et al. “Global monitoring of the impact of the COVID-19 pandemic through online surveys sampled from the Facebook user base”. In: *Proceedings of the National Academy of Sciences* 118.51 (Dec. 2021), e2111455118. ISSN: 1091-6490. DOI: 10.1073/pnas.2111455118.
- [84] Raoul Huys and Viktor K Jirsa. *Nonlinear dynamics in human behavior*. Vol. 328. Springer, 2010.
- [85] Brian D. O. Anderson and Mengbin Ye. “Recent Advances in the Modelling and Analysis of Opinion Dynamics on Influence Networks”. In: *International Journal of Automation and Computing* 16.2 (Feb. 2019), pp. 129–149. ISSN: 1751-8520. DOI: 10.1007/s11633-019-1169-8.
- [86] Lorenzo Zino and Ming Cao. “Analysis, Prediction, and Control of Epidemics: A Survey from Scalar to Dynamic Network Models”. In: *IEEE Circuits and Systems Magazine* 21.4 (2021), pp. 4–23. ISSN: 1558-0830. DOI: 10.1109/mcas.2021.3118100.
- [87] Xia Li et al. “A martingale formulation for stochastic compartmental susceptible-infected-recovered (SIR) models to analyze finite size effects in COVID-19 case studies”. In: *Networks and Heterogeneous Media* 17.3 (2022), p. 311. DOI: 10.3934/nhm.2022009.
- [88] Arroyo-Marioli F et al. *Estimate of the effective reproduction rate (R) of COVID-19*. URL: https://ourworldindata.org/explorers/covid?country=USA~BRA~JPN~DEU~ITA~OWID_EU27~OWID_WRL&Metric=Reproduction+rate&Interval=Cumulative&Relative+to+population=true.

BIBLIOGRAPHY

- [89] Kim Usher et al. “Pandemic-related behaviours and psychological outcomes; A rapid literature review to explain COVID-19 behaviours”. In: *International Journal of Mental Health Nursing* 29.6 (Oct. 2020), pp. 1018–1034. ISSN: 1447-0349. DOI: 10.1111/inm.12790.
- [90] Lauren A. McCormack et al. “Gaps in Knowledge About COVID-19 Among US Residents Early in the Outbreak”. In: *Public Health Reports®* 136.1 (Nov. 2020), pp. 107–116. ISSN: 1468-2877. DOI: 10.1177/0033354920970182.
- [91] Samantha Vanderslott. “Skepticism to vaccines and what to do about it”. In: *Our World in Data* (2019). <https://ourworldindata.org/vaccine-skepticism>.
- [92] Dominika Kwasnicka et al. “Theoretical explanations for maintenance of behaviour change: a systematic review of behaviour theories”. In: *Health Psychology Review* 10.3 (Mar. 2016), pp. 277–296. ISSN: 1743-7202. DOI: 10.1080/17437199.2016.1151372.
- [93] Pauline van den Driessche. “Reproduction numbers of infectious disease models”. In: *Infectious Disease Modelling* 2.3 (Aug. 2017), pp. 288–303. ISSN: 2468-0427. DOI: 10.1016/j.idm.2017.06.002.
- [94] P. van den Driessche and James Watmough. “Reproduction numbers and sub-threshold endemic equilibria for compartmental models of disease transmission”. In: *Mathematical Biosciences* 180.1–2 (Nov. 2002), pp. 29–48. ISSN: 0025-5564. DOI: 10.1016/s0025-5564(02)00108-6.

Acknowledgements

So long, and thanks for all the fish.